# An Integrated Real-Time Simulation/Optimization System for the Eastern Shore Highway Network: Research Methodology

**To**

**Office of Policy and Research**
**Maryland State Highway Administration**
**707 N. Calvert Street**
**Baltimore, MD 21202**

**by**


**Gang-Len Chang, Ying Liu**
**Ali Haghani, Abbas M. Asshar**
**gang@eng.umd.edu**

**Department of Civil Engineering**
**The University of Maryland**
**College Park, MD 20742**


June 2007

# TABLE OF CONTENTS

# Chapter 1

## Introduction

### 1.1 Research Background

The Eastern Shore of Maryland is composed of nine counties east of the Chesapeake Bay. The counties are Caroline County, Cecil County, Dorchester County, Kent County, Queen Anne's County, Somerset County, Talbot County, Wicomico County, and Worcester County.

Although the Eastern Shore comprises more than one third of Maryland's land area, it has a population of 420,000 (2004 census). That is about 8 percent of Maryland's population. The main activities on the Eastern Shore are farming, seafood, chicken breeding, and more importantly, services related to tourism. Ocean City is the most famous resort destination on the Eastern Shore.

The population of Ocean City in the summer peak season can reach 150,000 to 300,000, compared with 7,000 to 25,000 during the off-peak season[1].


Figure 1-1: Delmarva Peninsula and Evacuation routes

[1] Town of Ocean City, Maryland, Emergency Operations Plan, December 2002

This large population size in the summer season and the potential threat of hurricanes during the same period justify the need for design of hurricane evacuation plans. Figure 1-1 shows the Delmarva Peninsula and the major evacuation routes to the Bay Bridge and I-95.

This study was proposed in response to the need of evacuating a large volume of traffic in the Ocean City region prior to the threat of a hurricane. To safely evacuate all residents and tourists within an allowable "time window" during an emergency evacuation, responsible City and State officials will have to employ all available operational and control means, such as on-line route guidance, ramp or interchange closures, using shoulders as travel lanes, and special coordinated signal plans. The effectiveness of these strategies and their collective impacts on the network traffic conditions during the evacuation, however, cannot be reliably evaluated in advance with any existing analytical method and is certainly beyond the capacity of expert judgments.

One of the most effective methods for contending with such a complex and critical evacuation task is to replicate the actual regional transportation network and potential distribution of Eastern Shore populations in a computerized system. A well designed simulation system will offer a "simulated" evacuation environment for responsible planners/engineers to assess all candidate evacuation plans, and explore necessary supplemental strategies under all possible "what-if" scenarios.

More specifically, this study intends to extend the Phase-I research results and expand both the simulation and real-time routing algorithms from the Ocean City-Salisbury area all way to the Bay Bridge. The product of this study is *a decision-support tool* that enables City and State responsible staff to efficiently perform the following critical tasks during any emergency scenario that requires effective and reliable traffic management:

- Evaluate traffic conditions in Ocean City and its neighboring network via Salisbury to the Bay Bridge in real time and identify its current bottlenecks;
- Assess the effectiveness and potential traffic impacts of any pre-planned evacuation strategies in advance of an emergency evacuation;

- Project traffic conditions over a target time horizon for Ocean City and its neighboring highway networks during any emergency that necessitates the implementation of a network wide traffic management plan; and
- Provide a reliable evaluation of any implemented plan during the emergency evacuation, and allow responsible staff to take necessary strategic adjustments in a timely manner, as the actual traffic under emergency scenarios may not evolve to the expected patterns when encountering some incidents.

## 1.2 Research Objectives

In response to the above needs, this study has focused on the development of a simulation/optimization system that can exert the following principal components for traffic management:

- A set of optimal route algorithms that allow responsible staff to optimally direct evacuation populations under different allowable evacuation time windows and traffic conditions;
- A microscopic traffic simulator that covers the entire network from Ocean City to the Bay Bridge, including both arterial signals and all ramp access controls within Ocean City and Salisbury;
- A customized interface that allows target users to conveniently model all pre-planned traffic management strategies (such as using shoulders as traffic lanes) during any emergency evacuation; and
- A customized output module that can display the simulated traffic conditions based on the request of users and the proposed traffic management plan, such as the travel time and speed for a selected highway segment over a target time window.

Note that since the research results associated with the Eastern Shore simulator and its customized interface have been documented on the website ( ***http://oceancity.umd.edu)*** this report will mainly present the underlying methodology and mathematical models associated with the first project objective.

### 1.3 Report Organization

To detail the employed methodology and all embedded mathematical models for the optimal management of evacuation traffic, this report has classified all associated research results into six chapters. A brief description of information contained in each chapter is presented in sequence below.

Chapter 2 presents the review of state-of-the-art and state-of-the-practice studies associated with emergency evacuations, including the design of optimal traffic routing strategies so as to best utilize the available roadway capacity, assessing the needs of implementing reversed-lane operations, and maximizing the traffic throughput with specially designed signal control methods. The strengths and limitations of all available methods for contending with various types of evacuation operations constitute the core of this chapter. Also included in the literature review are the unique characteristics of evacuation traffic flows and the research needs to realistically capture such behavioral patterns in the system applications.

Chapter 3 reports an optimal traffic routing model developed from the network planning perspective. The developed model first employs dynamic assignment concept to generate the preliminary routing strategies for evacuation populations over the Eastern Shore network during a specified time window. It then executes the microscopic simulator to evaluate the time-varying network traffic performance, based on the recommended demands and their target distribution at each key control point. Depending on the allowable time window and resulting traffic conditions, the optimal model can revise its routing strategies and activate another round of evaluation. This chapter also presents the application results of the proposed optimal routing planning model and the analysis of its sensitivity.

Chapter 4 documents the second method for developing the set of optimal evacuation plans during emergency related operations. This set of models, developed for operational needs, has taken into account all network geometric and operational constraints. The entire set of models covers two levels of operations, one for directing the evacuation populations to different routes and the other for the design of signal timings at each key intersection for accommodating the evacuation traffic flows. This chapter mainly illustrates the modeling methodology and formulations of traffic flow characteristics at the network level, including how to capture the dynamic interactions between the capacity of available routes and the distribution of evacuation populations, and how to assess the need of implementing reversed-lane operations. The application results of the proposed network models and their performance effectiveness under different volumes are also documented in this chapter.

Chapter 5 highlights the signal control models designed especially for accommodating the oversaturated traffic flows during evacuation operations. The proposed models employ the cell-transmission methodology to capture the spatial and temporal interactions between traffic demands and intersection capacity, and allow the network to maximize the throughput during the evacuation period. To contend with the need of balancing the traffic flows among available evacuation routes, this chapter also presents an integrated corridor control model that can concurrently take into account traffic volumes on neighboring arterials and design a set of coordinated signal plans to maximize the total system throughput during the target period of evacuation operations. Extensive numerical results that compare the performance of the integrated control system with the individual signal optimized model under various traffic conditions are also discussed in this chapter.

Chapter 6 summarizes the key research findings from this project and potential issues associated with the application of the developed simulation/optimization system for Eastern Shore traffic networks. Future enhancement with respect to both traffic flow detection and real-time incident response during emergency evacuation operations are discussed in this chapter. Also included in this chapter are the key features of the website customized for on-line traffic monitoring and evaluation of the Eastern Shore traffic conditions, based on the developed microscopic traffic simulator and a customized system interface.

# Chapter 2

## Literature Review

### 2.1 Introduction

In view of the large body of literature on various aspects of evacuation operations, this chapter presents a comprehensive review of only those research efforts in design of the routing and control strategies for network evacuation. The purpose is to identify the special characteristics, strengths, and deficiencies of existing studies and thus to define the primary directions for this study.

To facilitate the presentation, this review has divided all related studies on network evacuation controls into the following four categories:

- Traffic Routing Strategies: to utilize the available network capacity more efficiently by guiding route selections of evacuees;
- Contraflow Design: to reverse the normal driving direction of some travel lanes in the evacuation network so as to increase the safety-bound capacity;
- Staged Evacuation: to reduce network congestion by evacuating those evacuation zones with different evacuation time windows in a proper sequence; and
- Arterial Signal Control: to maximize arterial traffic throughput with a set of specially designed signal plans.

The next four sections will review and discuss the available methodologies in the above four categories in sequence. Based on a review of the existing literature, the last section will present further research needs for this critical evacuation subject.

## 2.2 Traffic Routing Strategies for Emergency Evacuation

While route selection depends upon a number of driver and situation-specific characteristics, the most important question to be resolved by the modeler is the level of myopia versus preplanning that drivers put into their route selection process (Southworth, 1991). Traffic routing, as one of the main control efforts, aims to identify the best set of routing decisions so as to fully utilize the available capacity of an evacuation network.

Urbanik (2000) described the mechanism of traffic routing as load balancing, with evacuation traffic being diverted from routes of excess demand to those of excess capacity. Such a balancing state is mainly achieved by optimizing some predefined performance measurements for the entire evacuation operation with the approximated network traffic demand. Based on the methodology employed to approximate traffic evolution, this section divides related studies into the following three groups: network flow models, dynamic traffic assignment (DTA) models, and other models. Review of each model will emphasize the performance index for evaluating the evacuation operations, the type of routing decisions generated, and the operational constraints embedded in route generations.

Note that traffic routing is different from those route selection models widely used in most simulation-based software packages, which are for simulating the route selection behavior of drivers, based on the prevailing network conditions. Examples of such studies include NETVAC1 (Sheffi et al., 1982), which allows dynamic route selection in each interval at each intersection, based on traffic conditions directly ahead; MASSVAC (Hobeika, et al., 1994; 1998), that determines routes for evacuees departing from their origins with static traffic assignment algorithms; and CEMPS (Pidd et al., 1996; de Silva and Eglese, 2000), whose route selection mechanism has evolved from an immediate-congestion-based mechanism in its earlier versions to a shortest-path-based mechanism. Such route selection models are myopic in nature and will not be included in the following review.

### 2.2.1 Network Flow Models

By formulating evacuation routing as a minimal cost flow problem, Dunn (1992) proposed two algorithms to find the set of path flows that minimize the total travel distance through a capacity-constrained network.

Cova et al. (2003) proposed the concept of lane-based routing to reduce intersection delays by temporarily transforming intersections into uninterrupted flow facilities through proper turning restrictions. The output includes the allowable turning movements at each intersection or the mapping between approaching lanes and exiting lanes. As an extension of the minimal cost flow problem, the model minimizes the total travel distance while preventing flow conflicts and restricting merging points at intersections. Network flow is simplified with the flow conservation constraints at each node as shown in Equation 2.1, and the link capacity constraints.

$$\sum_{j \in \Gamma^{-1}(i)} x_{ij} - \sum_{j \in \Gamma(i)} x_{ji} = b_i \qquad (2.1)$$

where $x_{ij}$ is the vehicle flow from lane $i$ to lane $j$; $b_i$ is net flow generated at $i$; $\Gamma(i)$ denotes the set of predecessor nodes of node $i$; and $\Gamma^{-1}(i)$ denotes the set of successor nodes of node $i$.

To represent the evolution of a building evacuation process over time, Chalmet et al. (1982) constructed a dynamic network flow model by expanding it into a time-space network. The objective is to minimize the time to when the last evacuee exits, which is known as the quickest flow problem. Following the same line of inquiry, Hamacher and Tufekci (1987) extended the quickest flow problem to take into account different priority levels for different parts of the evacuation network. Choi et al. (1988) formulated three dynamic network flow problems for building evacuation (i.e., maximum flow, minimum cost and quickest flow problems), which introduced additional constraints to define link capacity as a function of the incoming flow rate.

Miller-Hooks and Patterson (2004) proposed the time-dependent quickest flow problem in time-varying capacitated evacuation networks, where link travel times and capacities vary with time. Network flow is modeled with flow conservation constraints at each node (Equation 2.2) as well as link capacity constraints (Equation 2.3).

$$\sum_{j\in\Gamma^{-1}(i)} x_{ij}(t) - \sum_{j\in\Gamma(i)} \sum_{t':t'+\tau_{ji}(t')=t} x_{ji}(t') = b_i(t) \tag{2.2}$$

$$0 \le x_{ij}(t) \le u_{ij}(t) \tag{2.3}$$

where $x_{ij}(t)$ is the flow on link (*i*,*j*) that leaves node *i* at *t* and arrives at node *j* after travel time $\tau_{ij}(t)$; $b_i(t)$ is the flow generated at node *i* during time *t*; and $u_{ij}(t)$ is the capacity of link (*i*,*j*) at time *t*.

As an extension of the time-dependent quickest flow problem, Opasanon (2004) addressed the stochastic nature of the evacuation network for a large building and formulated two network flow problems to generate the optimal path flows. The minimal cost problem seeks to minimize the total travel time when both link capacities and travel time are random variables with time-varying probability mass functions. In contrast, the safest escape problem aims to maximize the minimum path probability of successful arrivals at destinations (Equation 2.4) on a network with the deterministic travel time and stochastic time-varying link capacities. Network flows are modeled with the same conservation equations as Equation 2.3 and the modified capacity equations as Equation 2.5.

$$Max \quad [\min_{\sigma\in\Omega} \prod_{((i,j),t)\in\sigma} P_{ij}^{x_{ij}(t)}(t)] \tag{2.4}$$

$$0 \le x_{ij}(t) \le \max_{z}\{u_{ij}^{z}(t)\} \tag{2.5}$$

where $\Omega$ is the set of all possible paths; $P_{ij}^{n}(t)$ denotes the probability that the capacity of link (*i*,*j*) at time *t* is not less than *n*; and $\{u_{ij}^{z}(t)\}$ is the set of possible capacities for link (*i*,*j*) at time *t*.

In summary, these studies formulate the evacuation networks as facilities with limited capacity, where traffic can go through links with known travel times as long as they do not exceed link capacity. These problems typically involve two types of network flow constraints, namely, flow conservation constraints at every node and capacity constraints for each link. However, some traffic phenomena, such as congestion-caused delay and queue formation/dissipation, are not captured in such models.

### 2.2.2 Dynamic Traffic Assignment Models

Sattayhatewa and Ran (2000) applied an analytical DTA model to minimize the total evacuation time under a nuclear power plant failure. The output includes the optimal inflow rate into and exit flow rate from each link at each time interval. The constraints are the basic network flow constraints, which represent vehicle propagation over the network with link and node flow conservation equations (Equations 2.6 and 2.7) as well as propagation equations (Equation 2.8) with a travel time function $\tau_a(t) = f(u,v,x)$.

$$dx_a^{rs}(t)/dt = u_a^{rs}(t) - v_a^{rs}(t) \qquad (2.6)$$

$$\sum_{a \in B(j)} v_a^{rs}(t) = \sum_{a \in A(j)} u_a^{rs}(t) \qquad (2.7)$$

$$u_a^{rs}(t) = v_a^{rs}(t + \tau_a(t)) \qquad (2.8)$$

where $x_a^{rs}(t)$ is the number of vehicles on link *a* at time *t* traveling from origin *r* to destination *s*; $u_a^{rs}(t)$ is the inflow rate into link *a* at time *t* between OD pair *r* and *s*;

$v_a^{rs}(t)$ is the exit flow rate from link *a* at time *t* between OD pair *r* and *s*; and *A(j)* and *B(j)* are, respectively, the set of links whose upstream and downstream node is $j$.

Liu et al. (2006) also applied the DTA approach in a Model Reference Adaptive Control (MRAC) framework for real-time evacuation traffic management. The DTA model functions to generate the desired traffic states and associated control strategies with a rolling horizon, which will serve as a reference point for the adaptive control. With a discrete time frame, the evacuation traffic flow is captured in two aspects, namely, link dynamics (Equation 2.9) and node dynamics (Equation 2.10).

$$x_{as}(k+1) - x_{as}(k) = u_{as}(k) - v_{as}(k) \tag{2.9}$$

$$\sum_{a \in B(j)} v_{as}(t) = \sum_{a \in A(j)} u_{as}(t) - d^{js}(k) \tag{2.10}$$

where $x_{as}(k)$ is the number of vehicles on link *a* at interval *k* traveling to destination *s*; $u_{as}(k)$ is the inflow rate into link *a* during interval *k* heading to *s*; $v_{as}(k)$ is the exit flow rate from link *a* during interval *k* heading to *s*; and $d^{js}(k)$ is the demand generated at node *j* during interval *k* heading to destination *s*.

Yuan et al. (2006) formulated the evacuation routing problem with the simulation-DTA models embedded in the software package DYNASMART-P. Using mesoscopic simulation to capture vehicle movements over the network, the program can generate two types of routing plans for minimization of total travel cost: 1) static routing that dispatches vehicles to different routes only at their departures, and 2) dynamic routing where vehicles can be assigned to a new route based on the prevailing network conditions.

Some other evacuation studies have also applied DTA models to generate optimal traffic routing schemes concurrently with other control strategies, such as contraflow design (Tuydes and Ziliaskopoulos, 2004, 2006; Tuydes, 2005; Mahmassani and Sbayti, 2005), staged evacuation order (Tuydes and Ziliaskopoulos, 2005), and scheduling of the evacuation demand (Chiu, 2004; Chiu et al., 2006, Sbayti and Mahmassani, 2006). These studies will be reviewed in later sections.

### 2.2.3 Other Models

Focused mainly on the evacuation network, Campos et al. (2000) presented a heuristic algorithm to identify k-optimal independent routes for evacuating the areas surrounding a nuclear power plant. The objective was to maximize the sum of capacity/travel time ratios for those selected routes.

Talebi and Smith (1985) modeled the stochastic evacuation problem with analytical queuing network models. In the extension work, Smith (1991) proposed a state-dependent queuing model for building evacuation. Assuming that evacuees' arrivals follow a Poisson distribution, the model approximates the evacuation process with M/G/C/C state-dependent queues, which capture the nonlinear effects of increased traffic flows on the service rate along emergency evacuation routes with the following exponential function (Equation 2.11):

$$\mu_n = nr_n = n\frac{V_n}{L} = n\frac{A}{L}\exp[-(\frac{n-1}{\beta})^r] \quad (2.11)$$

where $\mu_n$ is the state-dependent service rate of the evacuation corridor, $n$ is the number of evacuees using the corridor, $r_n$ is the service rate for each of the $n$ evacuees (actually inverse of the average travel time), $V_n$ is the average speed for $n$ evacuees, $A$ is the free flow speed for $n$=1, $L$ is the corridor length, and $\beta$ and $r$ are model parameters.

## 2.3 Contraflow Design for Emergency Evacuation

Contraflow design, or lane-reversing operation, refers to the shift of normal driving directions of some or all danger-bound lanes for use by safety-bound evacuation traffic. Such control is based on the observation that danger-bound traffic is usually light, whereas evacuation traffic always oversaturates the safety-bound capacity.

Contraflow design can significantly increase the capacity of the evacuation network. In the Southeast U.S. Hurricane Evacuation Traffic Study, PBS&J (2000) examined several alternatives of contraflow operations for a four-lane freeway, including reversing both danger-bound lanes (one-way-out operation) or reversing only one lane. FEMA (2000) estimated that a full reversal would provide an increase in capacity of near 70 percent over the conventional two-outbound-lane configuration, while the single-inbound-lane reversals are estimated to increase the outbound capacity by about 30%. Several simulation studies have also proved the effectiveness of contraflow operations in improving evacuation efficiency (Zou et al. 2005; Kwon and Pitt, 2005).

Recognizing its effectiveness, responsible agencies in those nine states along the Atlantic and Gulf Coasts have widely applied contraflow design in developing hurricane evacuation plans (Urbina, 2002; Urbina and Wolshon, 2003). For example, Georgia and South Carolina implemented freeway contraflow plans for the 1999 Hurricane Floyd evacuation. Despite a wide acceptance of contraflow operations in practice, limited research has been published regarding which lanes should be reversed for contraflow operations for the maximal effectiveness if under resource limitations.

On this issue, Tuydes and Ziliaskopoulos (2004) proposed link-coupling techniques for contraflow design, which match network segments that can exchange capacity in case of reversing. Assuming the coupled pair of links $I$ and $I^*$ share a total flow capacity $Q^t_{I-I*}$ and storage capacity $N^t_{I-I*}$, this study formulated a system-optimal DTA problem to obtain the optimal capacity allocation. Network flows are captured with the cell transmission model, which moves vehicles among road segments based on flow conservation law (Equation 2.12) and segment traffic states (Equations 2.13 and 2.14).

$$x_I^t = x_I^{t-1} + \sum_{k\in\Gamma(I)} y_{kI}^{t-1} - \sum_{j\in\Gamma^{-1}(I)} y_{Ij}^{t-1} \tag{2.12}$$

$$y_{Ij}^t = \min\{x_I^t, \; r_I Q_{I-I*}^t, \; , r_j Q_{j-j*}^t, \; , \delta_j^t (r_j N_{j-j*}^t - x_j^t\} \tag{2.13}$$

$$r_I + r_{I*} = 1 \tag{2.14}$$

where $x_I^t$ is the number of vehicles on segment *I* during interval *t*; $y_{Ij}^t$ is the number of vehicles from segment *I* to segment *j* during interval *t*; $\Gamma(I)$ and $\Gamma^{-1}(I)$ denote, respectively, the set of predecessor or successor segments of segment *I*; $r_I$ is the proportion of capacity allocated to segment *I*; and $\delta_j^t$ is a traffic flow parameter.

In the extended work, Tuydes (2005) introduced the definitions of lane-based capacity reversibility (LCR) and total-or-no-capacity reversibility (TCR) to replace the continuous variable $r_I$. Moreover, to cope with the high computational cost associated with the analytical DTA formulations, Tuydes and Ziliaskopoulos (2006) proposed a heuristic algorithm using both simulation-assignment and Tabu Search methods for potential application in real-life large-scale evacuation networks.

With a similar simulation DTA procedure, Mahmassani and Sbayti (2005) proposed an optimization scheme for dynamic capacity reallocation. Using the simulation software package DYNASMART, this study showed how to generate a time-dependent contraflow control policy to be deployed at target links during a major evacuation.

Except for the selection of roadway segments for implementing lane reversals, contraflow design involves various other operational issues. Wolshon (2001, 2002) discussed such issues related to hurricane evacuation and emphasized the rerouting of traffic at the entrance and the end of the reversed segments. With the microscopic simulation program CORSIM, Theodoulou and Wolshon (2004) and Lim and Wolshon (2005) assessed, respectively, the alternative entrance and termination designs of contraflow segments in evaluating the hurricane evacuation plan for the city of New Orleans. Kwon and Pitt (2005) also underscored the critical design of contraflow entry points while using the simulation software DYNASMART-P to test alternative plans for evacuating downtown Minneapolis.

## 2.4 Staged Evacuation

Staged evacuation, also known as phased evacuation or zoned evacuation, is another widely used control strategy to guide evacuation flows. Without changing the network geometry like contraflow design or enforcing route choice restrictions, staged evacuation aims to achieve more efficient network utilization mainly through a better distribution of evacuation demand over the allowable time window.

In a staged evacuation, the entire area to be evacuated is typically divided into small zones, based on the predicted evolution of emergency impacts and other associated factors. Operators will then issue evacuation orders at an earlier time to those zones with higher levels of urgency (e.g., with a shorter safety time window or with higher concentrations of hazardous chemicals) and start evacuating the low-urgency zones some time later. By restricting unnecessarily early evacuation of low-urgency areas, staged evacuation can effectively limit the surge in evacuation demand, reduce overall network congestion and, more importantly, avoid or at least mitigate potential casualty and stress levels caused by evacuees being blocked in more dangerous areas.

To justify different priorities in the evacuation process, staged evacuation is generally proposed only for those evacuation scenarios during which the impacts of the emergency event will expand progressively before covering the entire network and/or causing different levels of impact severity. For example, staged evacuation strategies have been widely proposed in high-rise building evacuations during fires, where only those floors in the vicinity of the fire source are urged to evacuate immediately (Pauls and Jones, 1980; Teo, 2001; Harrington, 2005). Some other regional evacuations with moving hazards have also considered the use of staged evacuation (Chen and Zhan, 2004; Snyder, 2004; Farrell, 2005).

The critical operational decisions in a staged evacuation plan are when to issue evacuation orders for different evacuation zones. Once an evacuation order is announced, the demand generation process will be determined only by evacuees' responses and is beyond the control of any system operator or enforcement agency. However, effective approaches to obtaining such starting times during a staged evacuation have not been adequately addressed in the literature or in practice. Chen and Zhan (2004) investigated the effectiveness of simultaneous (concurrent) and staged evacuation strategies in three road network structures using the microscopic simulation program PARAMICS, where the staged evacuation times are determined intuitively. Mitchell and Radwan (2006) identified some zonal parameters that might influence the staging decisions, such as population density, roadway exit capacity, distance to safety/shelter, and distance to a major evacuation route. However, the staging strategies tested in their study were also intuitive in nature.

So far, the most relevant study on the optimal design of staged evacuation decisions was conducted by Tuydes and Ziliaskopoulos (2005). They formulated a mixed-integer linear programming model to concurrently optimize destination/route choice and zone scheduling with demand mobilization duration $\chi^o$. Here, $\chi^o$ refers to the time period during which all demands generated at origin *o* have to get onto the evacuation network. With network flow constraints similar to Equations 2.12 and 2.13, this study introduced Equations 2.15 to 2.18 to control the demand mobilization process with binary variables $a^{o,t}$ and auxiliary variables $s^{o,t}$.

$$\sum_{(o,j)}\sum_{k=t}^{t+\chi^o} y_{oj}^t + s^{o,t} = d^o \tag{2.15}$$

$$s^{o,t} \leq INF \times (1 - a^{o,t}) \tag{2.16}$$

$$1 - a^{o,t} \le s^{o,t} \tag{2.17}$$

$$\sum_t a^{o,t} = 1 \tag{2.18}$$

where binary variable $a^{o,t}$ equals 1 and auxiliary variable $s^{o,t}$ equals 0 only when demand at origin *o* is mobilized starting at time $t$; $y_{oj}^{t}$ is the flow getting out of origin *o* to its downstream link *j* during interval *t*; and $d^{o}$ is the total demand at origin *o*.

Although the above study provided a starting time for each origin, it did not model the evacuees' actual response behaviors to the evacuation order. The only requirement was that the total demand should enter the evacuation network within a given time window once the evacuation process started at an origin. Further along this direction is the so-called evacuation scheduling problem, where operators are assumed to be able to control the demand generated during each interval (or the evacuation departure time for each evacuee).

Chiu (2004) formulated the evacuation scheduling problem as a mathematical programming model to minimize the total travel time by controlling $r_{i,k}^{t}$, the demand generated during interval *t* at origin *i* to travel via path *k*. The DTA program DYNASMART was used to provide the solution. Chiu et al. (2006) applied the cell transmission model to formulate the optimal evacuation destination-route-flow-staging problem, where similar formulations are used to generate the demand getting out of original points. Trying to minimize the evacuation clearance time, Sbayti and Mahmassani (2006) proposed an iterative bi-level formulation framework to solve the evacuation scheduling problem, where a dynamic network assignment problem is solved in the upper level to determine the time-dependent route assignments, and a dynamic loading problem is solved with DYNASMART in the lower level to determine the corresponding route travel times.

## 2.5 Signal Control in Emergency Evacuation

Signal control has been widely accepted as an effective strategy to increase arterial capacity and to mitigate congestion during daily traffic scenarios. For evacuation operations, PBS&J (2000) noted that a good timing plan could increase the capacity of local streets that provide access to/from evacuation routes and prevent bottlenecks at their access points. Various other documents associated with evacuation planning have also proposed to include arterial signal control as an integrated part of the overall evacuation control strategy (ITE, 2004; Ballard and Borchardt, 2005; PBS&J, 2005).

Despite this wide recognition of the critical role of signal control in emergency evacuation, the development of evacuation signal-timing plans has received limited attention in the literature. The current studies in this regard are quite scarce and mostly along the following two lines: 1) to apply simplified controls based on experience, and 2) to apply standard signal optimization practices for normal traffic conditions, but with a high demand.

Among the first group, Chen (2005) applied the microscopic simulation software CORSIM for two evacuation corridors of Washington, D.C., and examined four different signal-timing plans: 1) Red Flash Plan, providing red flash phase to all approaches; 2) Yellow Flash Plan, providing a yellow flash phase to arterials and a red flash phase to side streets; 3) Minimal Green Plan, which uses the longest cycle length the controller allows while offering only minimal green phases to side streets; and 4) Ordinary Peak Hour Plan, which was designed based on normal afternoon peak hour traffic conditions. Although this study offered some insights into the effects of different timing plans, its analysis of plan selection under various evacuation scenarios is mostly qualitative.

Among the second group of practices, Sisiopiku et al. (2004) used the signal optimization software SYNCHRO to establish the optimal signal-timing plans for a small area in Birmingham, Alabama. They then used the CORSIM simulator to test different evacuation plans and evaluated the impacts of signal-timing optimization on the selected measurements of effectiveness. The results suggested that traffic signal optimization could significantly reduce average vehicle delays and improve evacuation time. McHale and Collura (2003) applied another signal optimization program, TRANSYT-7F, to generate the optimal signal-timing plan when assessing the impact of emergency vehicles preemption strategies in a CORSIM simulator.

One area in emergency signal control that has received extensive attention is the preemption of emergency response vehicles. When these vehicles have to use the same roads as evacuees, the emergency vehicle preemption (EVP) function will prioritize the movement of emergency vehicles at intersections and thus may positively affect evacuation traffic.

In this regard, Bullock et al. (1999) used the CORSIM traffic simulator to model the EVP systems for three intersections on a major commuting corridor in Virginia, and the results showed that EVP has statistically significant negative impacts on other network traffic under given signal-timing plans and preemption strategies. A similar impact analysis of EVP, using the CORSIM simulation model, can be found in McHale and Collura (2003). Among another series of studies to evaluate EVP impacts, Louisell et al. (2003) proposed a conflict point analysis approach to evaluate the potential safety benefits of EVP. Furthermore, Louisell et al. (2004) developed a worksheet method to assess the crash reduction benefits of EVP on a given intersection or corridor during a preemption signal phase. Based on extensive field observations in the Northern Virginia Region, Louisell and Collura (2005) adopted the traditional time-space diagrams to estimate the benefits of EVP in performance improvement for an intersection or an emergency response corridor.

## 2.6. Closure

In summary, this chapter has provided a comprehensive review of those existing research efforts in the design of various network control strategies for evacuation operations. Those strategies, if properly designed, can effectively improve evacuation efficiency via demand control (e.g., staged evacuation), capacity enhancement (contraflow design and arterial signal control), or a better match of the demand pattern and the available network capacity (e.g., traffic routing).

Although each of these four popular traffic control strategies for evacuation has been reported in the literature or, in some cases, even applied in actual operations, there exist some technical deficiencies that remain to be overcome. For example,

- There lacks an overall operational framework or guidelines that can effectively integrate all four types of control strategies. If implemented concurrently in an evacuation operation, different control strategies will apparently interact with each other and affect traffic flows in the same time-space network. A properly designed staged evacuation may reduce the need for contraflow operations, while an arterial with effective traffic signal-timing plans will certainly better accommodate evacuees assigned by responsible system operators.
- Some critical nature of the evacuation traffic is not fully represented in the analytical formulations. For example, most studies for contraflow design typically treat reversed lanes exactly the same as the normal lanes. In reality, the driving behavior in the reversed and normal lanes may differ significantly due to the fact that most traffic signs, markings, and safety devices are intended for use only in the designed driving direction (Theodoulou and Wolshon, 2004).
- Some unnecessary or unrealistic assumptions have been employed in the literature for design of optimal evacuation control strategies. For example, models for contraflow design should take into account the geometric features and their discrepancies among different arterial segments so as to avoid creating local bottlenecks. Also, staged evacuation decisions should account for realistic response patterns of evacuees to the evacuation orders, rather than assuming that operators can fully control the departure time of each evacuee.

# Chapter 3

# Evacuation planning with Dynamic Traffic assignment methods

## 3.1 Introduction

This chapter presents the set of evacuation planning models developed with the dynamic traffic assignment methods. These models have been applied primarily for guiding the evacuation scenario where travel times are constant or possibly time-dependent. In actual vehicular traffic networks, travel times are often flow dependent and increase nonlinearly with higher densities until traffic slows down to crawling speeds and incurs queues. This phenomenon is particularly true under evacuation where the transportation system degrades quickly after its demand overwhelms the supply. While recognizing this flow dependence is essential to realistic modeling of traffic system evacuation, compared to assuming constant link travel times, it makes the problem considerably more difficult to solve.

The current methods of evacuation planning can be divided into two general categories, namely, traffic simulation and route planning approaches. The former approaches use traffic simulation tools to conduct stochastic emulation of traffic movements based on the distribution of traffic demands and employ queuing methods to account for road capacity constraints. The route planning approaches use the network flow and routing algorithms to produce origin-destination routes and schedules of evacuees on each route. The advantage of such approaches is their ability to model large-scale networks and to achieve the computing efficiency which is essential for real-time operations and controls.

The models presented hereafter take advantages of both approaches and offers the potential for efficient use in practice. First of all, the problem is formulated as a mathematical program that solves for the optimal traffic assignment along with the best choice of destinations for evacuees. Then, this optimization problem quickly finds the optimal evacuation routes and link volumes that are being used in the second part of simulation evaluation. The simulation results are used mainly for fine tuning and evaluation of the optimal evacuation routes generated from the proposed mathematical models.

### 3.2 Model Formulations for Evacuation Operations

The objective of the optimization problem is to assign the traffic to the routes in order to maximize the utilization of the network. For a given fix demand, this translates to minimizing the total travel time of the system while satisfying the demands. This is equivalent to the well known system optimal traffic assignment problem but with explicit capacity constraints. It can be formulated as:

*Minimize* $$Z(X) = \sum_{(i,j)} x_{(i,j)} t_{(i,j)} \left( x_{(i,j)} \right)$$

Subject to:

$$\sum_i x_{(i,j)} - \sum_k x_{(j,k)} = D_j \qquad \forall j \in S \qquad (1)$$

$$\sum_i x_{(i,j)} - \sum_k x_{(j,k)} = 0 \qquad \forall j \in V - \{S \cup T\} \qquad (2)$$

$$x_{(i,j)} \le C_{(i,j)} \qquad \forall i, j \in V \qquad (3)$$

$$x_{(i,j)} \ge 0 \qquad \forall i, j \in V \qquad (4)$$

Where:

$x_{(i,j)}$ = Traffic volume on link (i,j) ( in vehicle per hour)

$t_{(i,j)}\left(x_{(i,j)}\right)$ = Travel time on link (i,j) ( in hour)

$C_{(i,j)}$ = Maximum capacity of the link (i,j) ( in vehicle per hour)

$D_j$ = Demand at Origin node j (total demand at j divided by evacuation duration)

V = Set of all nodes

S = Set of origin nodes

T = Set of destination nodes

The first set of constraints is forcing the demand to be loaded to the network. The second set of constraints is simply the conservation of the flow at intermediate nodes meaning that the flow entering each node must be equal to the flow that exits that node. The third set of constraints requires the flow on each link to satisfy the maximum capacity of that link. Finally, the fourth constraint is preserving the non-negativity requirement on decision variables.

The conservation of flow at destination nodes is not required in this formulation. As a result, the optimization model can find the best destination assignment for the overall system. If a maximum capacity for destinations is defined, the following constraint must be added to the model:

$$\sum_i x_{(i,j)} - \sum_k x_{(j,k)} \leq U_j \qquad \forall j \in T \tag{5}$$

**3.3 Solution Method**

The model presented in the previous section is a nonlinear optimization problem with linear constraints. Since the constraints are linear with respect to decision variables, the optimization is a convex problem if and only if the objective function is a convex function. In order to have a convex objective function, the travel time is calculated using the well-known BPR travel time function:

$$t(x) = t_0\left(1 + \alpha\left(\frac{x}{C}\right)^{\beta}\right) \tag{6}$$

Where,

$x$ = Traffic volume on the link

$t_0$ = Free flow travel time on the link

C = Parameter known as link capacity

$\alpha, \beta$ = calibration parameters, usually $\alpha$ =0.15 and $\beta$ =4 is used.

It is worth mentioning that using BPR formula for this study is not a necessity. Any other travel time function formulation can be formulated and used instead. However, the unique global optimal solution is guaranteed only if the travel time function is a (strictly) convex function.

Microsoft Excel Solver is used for solving this model. The next section introduces the Excel Solver and some of the application procedures to model the current problem in Excel and solving it with Excel Solver.

### 3.3.1 Microsoft Excel Solver

The Solver is an add-on in the Microsoft Excel program. It is part of a suite of commands sometimes called what-if analysis tools. With this Solver, one can find an optimal value for a formula in one cell -called the target cell- on a worksheet. The Solver works with a group of cells that are related, either directly or indirectly, to the formula in the target cell. The Solver adjusts the values in the specified changing cells -called the adjustable cells- to produce the result expected from the target cell formula. One can apply constraints to restrict the values the Solver can use in the model, and the constraints can refer to the other cells that affect the target cell formula. [MS EXCEL 2003 HELP]

The Microsoft Excel Solver tool uses the Generalized Reduced Gradient (GRG2) nonlinear optimization code developed by Leon Lasdon, University of Texas at Austin, and Allan Waren, Cleveland State University. Linear and integer problems use the simplex method with bounds on the variables, and the branch-and-bound method, implemented by John Watson and Dan Fylstra, Frontline Systems, Inc. [MS EXCEL 2003 HELP]

In the proposed model, the changing cells (decision variables) are the traffic volumes on the links. The target cell (objective function value) is the total travel time (sum of the traffic volumes times travel times, on all links of the network).

The travel time values are calculated on a separate worksheet knowing the length, number of lanes, free flow speed, and traffic volume of each link. As mentioned earlier, BPR formula is used to calculate travel times.

The first set of constraints which enforce demand values and conservation of flow on nodes, is formulated on a worksheet called Incidence Matrix. In this worksheet, the net traffic volume at each link is calculated as sum of the flow entering each node minus the sum of the flow exiting that node. This value is called the Left Hand Side (LHS). Then, as a set of constraint, this LHS vector is set equal to a RHS vector which is basically the demand vector.

The next set of constraints is the link capacity constraints. The capacity for links is calculated as saturation flow rate times the number of lanes for each link of the network. These constraints are enforced directly at the Solver worksheet.

By running the solver, the program solves for system optimal traffic assignment while it is pushing as much of the demand as possible through the network. The output is the traffic volume of each link, number of vehicles sent to each destination, and the number of vehicles that remain at each origin node (unsatisfied demand). Then this optimal solution can be used to identify the maximum throughput of the network. It also can be used to solve for the turning fractions at intersections in order to implement the plan on site or to generate the simulation file for evaluation and fine tuning. The running time is usually less than one minute, with about 30 seconds on average for a Pentium IV 2.4 MHz machine with 1 GB Ram.

### 3.3.2 Network Clearance Time

Network clearance time is the time required to evacuate the whole region. Minimizing network clearance time is one of the major objectives in emergency evacuation planning. This tool can provide a good estimate of number of vehicles evacuated at each time and number of vehicles that remain at the origins. To do so, a parameter named “evacuation duration” is defined. Then in the traffic assignment formulation, the right hand side demands are replaced with demand rates (total number of vehicles at that origin divided by the evacuation duration).

For a given evacuation duration, the Excel Solver finds the maximum flow that can be discharged through the network and also gives the amount of unsatisfied demand at each node. In this way, by setting different values of evacuation duration, one can test the performance of the network over time. Network clearance time can be found by increasing the evacuation duration up to the point that all demand is satisfied and no vehicle is left at any origin.

### 3.4 Phase 1 Evacuation Plan

As a pilot study, the proposed methodology was first applied to Phase-I of the project. Phase-I network contains only Ocean City area with three evacuation destinations of Salisbury, US113 North, and US113 South shown in Figure 3-1. There were six evacuation plans for this small network introduced in “Evaluation Tool for Hurricane Evacuation Plan of Ocean City Maryland” the interface of which is depicted in Figure 3-2.

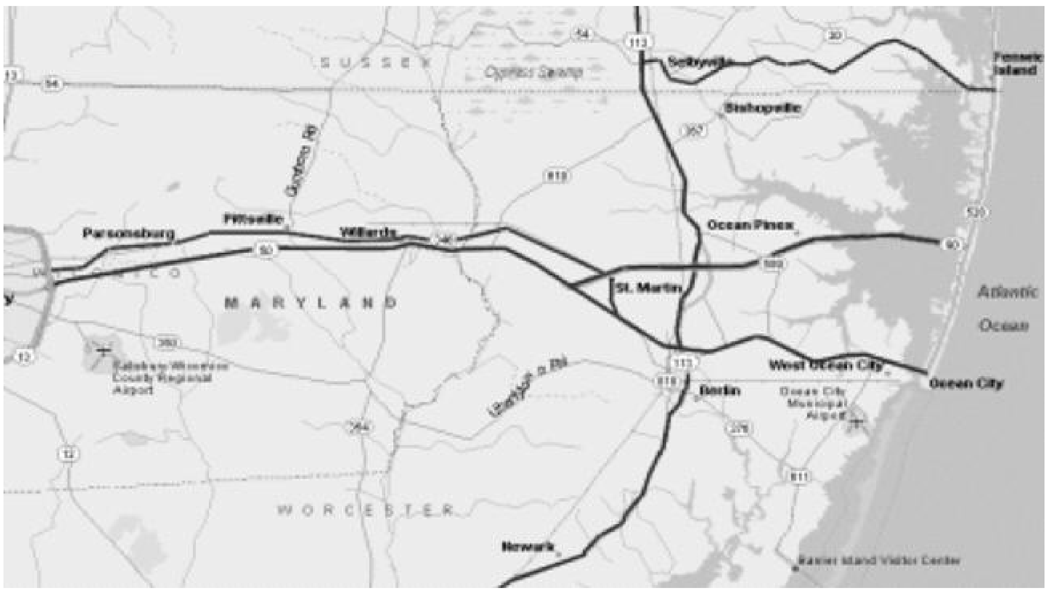


Figure 3-1: Phase 1 Network, Ocean City Maryland

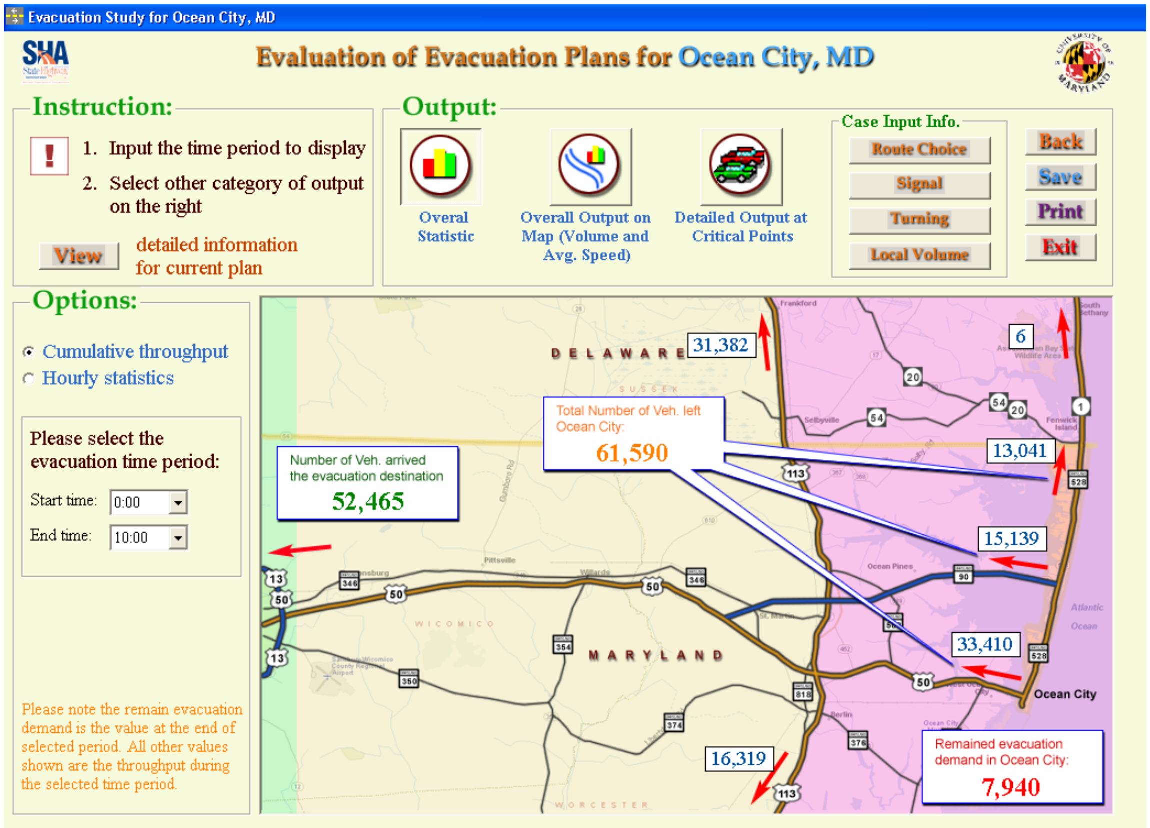


Figure 3-2: Evaluation Tool for Hurricane Evacuation Plan of Ocean City Maryland

The proposed method was applied to the small network. Then the optimal solutions from mathematical program were implemented in the Evaluation Tool. Table 3-1 demonstrates the simulation results for all six plans and also the simulation results from optimized plans. The first six rows of the table show the results from the current plans while the results of optimized plans are presented in the last two rows of the table.

While base Plan-I for 70,000 vehicles could evacuate 61,590 vehicles from the region, the optimized plan for the same 70,000 vehicles is able to evacuate 68,640 vehicles in the 10 hour evacuation duration. This is 7050 more vehicles and 11 percent better performance.

The optimized plan for 100,000 vehicles also performs better than its counterpart Plan-6 based with 100,000 vehicles' in 10 hours. The optimized plan can evacuate 2567 more vehicles and the number of vehicles left at Ocean City at the end of the 10 hours is only 1192 vehicles, compared to 3766 vehicles that could not evacuate in base Plan-6.

Table 3-1: Comparison of results for the phase 1 network

| | Reached Shelters | | | Aggregate Results | |
|---|---|---|---|---|---|
| | North | Salisbury | South | Evacuated | Remained |
| Plan 1 base 70,000 veh in 10 hours | 31382 | 52465 | 16319 | 61590 | 7940 |
| Plan 2 100,000 vehs in 10 hours | 36933 | 65158 | 31772 | 93390 | 5933 |
| Plan 2 uncontrolled 100,000 veh | 30086 | 56100 | 24844 | 75545 | 23784 |
| Plan 3 base 100,000 veh in 10 hours | 36761 | 62059 | 28060 | 82540 | 16794 |
| Plan 4 base 100,000 veh in 10 hours | 37329 | 67498 | 34298 | 95781 | 3550 |
| Plan 5 base 100,000 veh in 10 hours | 36705 | 67227 | 34100 | 95937 | 3392 |
| Plan 6 base 100,000 veh in 10 hours | 37466 | 73258 | 26788 | 95565 | 3766 |
| Optimized Plan 70,000 veh in 10 hours | 38799 | 45987 | 24798 | 68640 | 890 |
| Optimized Plan 100,000 veh in 10 hours | 38821 | 66200 | 35834 | 98134 | 1192 |

The pilot study was successful and the proposed methodology demonstrated a superior performance over the available plans. This provided the base for extending the approach and applying it to the large network containing the entire eastern shore of Maryland.

### 3.5 Entire Eastern Shore Network

In order to build the entire eastern shore network, two complementary sources are used: road map (Google Map) and the simulation file (CORSIM). The CORSIM file network is very detailed and loaded with minor roads which mainly act as feeders to the major roads and do not play a role when it comes to evacuation routing.

Thus, the map of the area (Google Map / Google Earth) is used to build the network structure and differentiate between major and minor roads. Some minor roads or the roads which are not in the general evacuation direction are eliminated from the network. The links are considered unidirectional unless there is a potential for two way operation. In that case, another link with the same characteristics but in the opposite direction is added to the network.

This network covers all major evacuation routes and it is checked to be consistent with the CORSIM file network (i.e. some links/nodes are omitted from the model since they didn't exist in CORSIM file). The level of details of this network do not consist the very specific turning moves at intersections; however, if geometry prevents certain types of movement at some junctions, a dummy node is added to take care of the movement requirements. Some of very close junctions are aggregated into a single node to reduce the network size and prevent very short links.

The resulting network is shown in Figure 3-3. The network consists of 50 nodes and 86 links. There are five evacuation destinations, node 32 at the Bay Bridge and nodes 41, 42, 43 and 44 which lead to interstate 95 in Delaware and northeast Maryland.

### 3.6 Data Acquisition

**- Demand**

The CORSIM simulation file is used as the reference for the amount and location of the demand generation points. Based on the data from the simulation file, there are 324 demand generation points, totaling 252,130 Vehicles in a 10 hour period. The approach has been to identify the major demand generation points and aggregate the single generation points neighboring each node of the network and impose the aggregated demand at that node. For example, Ocean City contains a total of 110,380 vehicles (43,830 vehicles, 45,850 vehicles and 20,700 vehicles at nodes 1, 2 and 3 respectively). Node-9 is Bethany Beach and contains 20,000 vehicles. The demand at Salisbury is 11,400 vehicles imposed at node 16. Other major demand generation points that are scattered all over the network have the total demand of 110,350 vehicles.

**- Link Characteristics**

-Link Labels

Instead of numbering the links, they are labeled by a four digit code. The first two digits stand for the number of the starting node and the last two digits stand for the ending node of any particular link. (e.g. link 0715 connects node 07 to node 15).

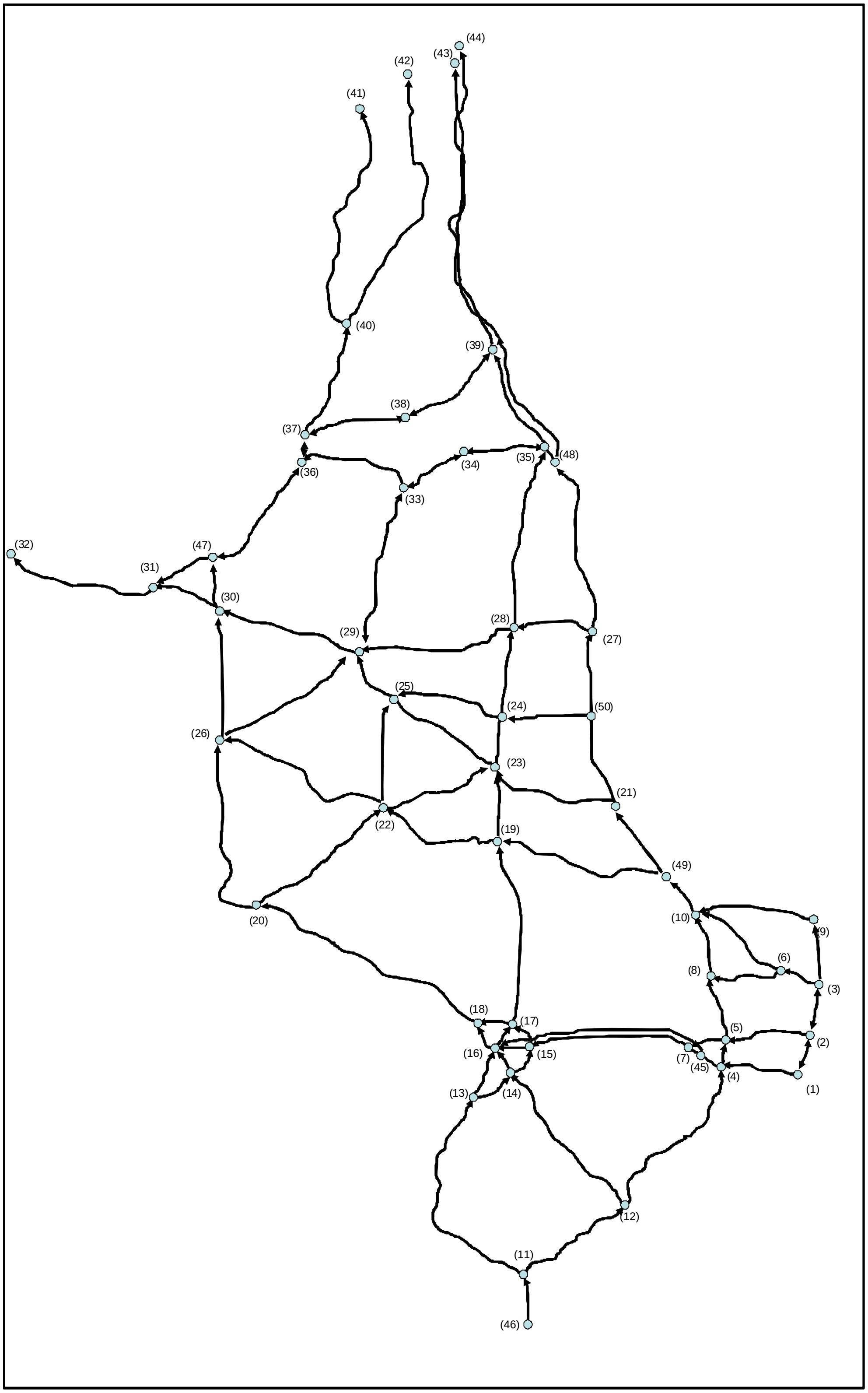


Figure3-3: The link-and-node representation of the Eastern Shore network

-Link Length: In order to find the length of the links, Google Earth software is used. Google Earth has a tool that can measure the length over the map even for curves and multiple segment paths.

-Number of Lanes: extracted from the simulation file. It is reconfirmed using Google Earth/Google Map in necessary cases.

-Free Flow Speed: a required component to calculate the travel times of the links. Major source for this set of data is in the simulation file. In some cases that different parts of a link have different free flow speeds in the simulation file, a weighted average of the speeds is used with more weight on the lower speed. For example if a link consists of five segments with one mile length each, and having the free flow speeds of 55, 55, 55, 45, and 35 miles per hour respectively. The free flow speed for entire link can be approximated by 45 mile per hour.

**3.7. Optimization results**

As discussed earlier, the problem is formulated as a mathematical program which solves for optimal assignment of vehicles to routes and destinations. This nonlinear constrained optimization problem is formulated in Microsoft Excel and solved with the Solver add-on. The program is solved for a range of evacuation durations. Table 3-2 shows the total number of vehicles evacuated and the total number of vehicles left at their origins for each time interval. Figure 3-4 presents the same results graphically.

Table 3-2 – Optimization results for the range of evacuation durations

| Entire East-Shore Evacuation | | | |
|---|---|---|---|
| Hour | Total Demand (veh) | Demand Satisfied (veh) | Demand Remained (veh) |
| 8 | 252130 | 149200 | 102930 |
| 9 | 252130 | 164400 | 87730 |
| 10 | 252130 | 178800 | 73330 |
| 11 | 252130 | 194499 | 57631 |
| 12 | 252130 | 207000 | 45130 |
| 13 | 252130 | 217800 | 34330 |
| 14 | 252130 | 228600 | 23530 |
| 15 | 252130 | 239400 | 12730 |
| 16 | 252130 | 250200 | 1930 |
| 17 | 252130 | 252130 | 0 |
| 18 | 252130 | 252130 | 0 |

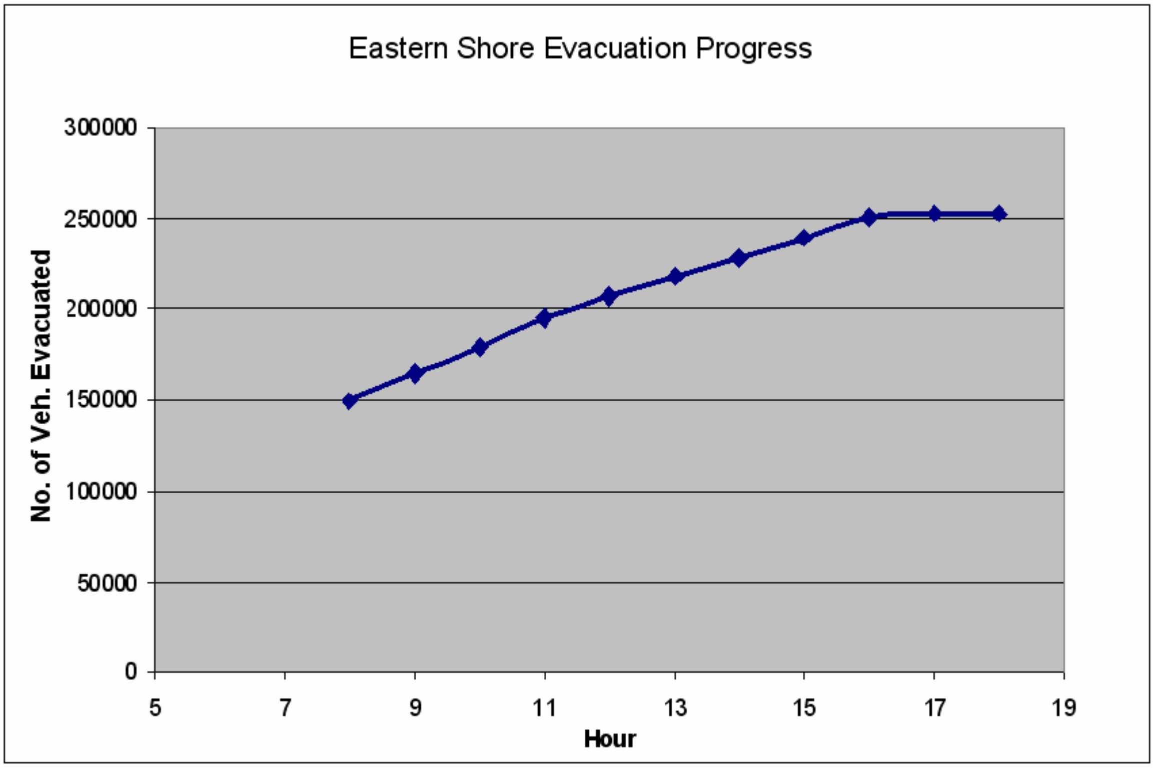


Figure 3-4: A graphical illustration of the evacuation throughput evolution

The results shown in Table 3-2 suggest that 17 hours are required to evacuate the entire eastern shore. However it is worth mentioning that this is a quick estimate, not considering signal timings, stochasticity, or human behavior. So it is optimistic and can serve as a lower bound on the required evacuation duration in real world cases. The microscopic simulation results presented in the Section eight of this report show the applicability of these results

### 3.7.1 Bottleneck analysis

The infrastructure and network topology along with high concentration of demands at Ocean City and Bethany Beach, form a bottleneck at the southeast section of the network. As introduced earlier, the shore strip involving Ocean City and Bethany Beach contains a total of 130,380 vehicles. This accounts for 52 percent of total demand. Major routes that exit in this area are US-113, US-50 and MD-346. These routes provide only five lanes of outgoing traffic if no contra-flow lane is employed.

To demonstrate the effect of these bottlenecks on the performance of the system and the evacuation time, two scenarios are defined. First, the traffic assignment is solved considering only the demand of Ocean City and Bethany Beach and all other demand are ignored. In the second scenario, the rest of the demand is loaded while the demand at shore strip is neglected.

Tables 3-3 and 3-4 present the evacuation progress for two scenarios. Table 3 shows that if there were not any other region needing evacuation except the tourist areas of the shore strip, it would still take about 15 hours to complete the evacuation. However, as can be seen in Table 4, if only the rest of demand is considered (which still counts for 121,750 vehicle or 48 percent of total), the evacuation would take only seven hours to complete.

This analysis proves the existence of a bottleneck for evacuation of Ocean City and Bethany Beach and shows the effect of this bottleneck on the evacuation duration required for clearing the entire Eastern Shore network. This analysis also demonstrates the immediate need for capacity expansion of the routes that exit in the bottleneck area. Using contra flow is suggested for dealing with this capacity shortage.

Table 3-3: Summary of Optimal results for the entire Eastern Shore

| Scenario1- Only Shore Strip Demand | | | |
|---|---|---|---|
| Hour | Total Deman d | Demand Satisfied | Demand Remained |
| 5 | 130380 | 43500 | 86880 |
| 6 | 130380 | 52200 | 78180 |
| 7 | 130380 | 60900 | 69480 |
| 8 | 130380 | 69600 | 60780 |
| 9 | 130380 | 78300 | 52080 |
| 10 | 130380 | 87000 | 43380 |
| 11 | 130380 | 95700 | 34680 |
| 12 | 130380 | 104400 | 25980 |
| 13 | 130380 | 113100 | 17280 |
| 14 | 130380 | 121800 | 8580 |
| 15 | 130380 | 130380 | 0 |
| 16 | 130380 | 130380 | 0 |

Table 3-4: Summary of Optimal results excluding Shore strip demand

| Scenario 2- Excluding Shore Strip Demand | | | |
|---|---|---|---|
| Hour | Total Demand | Demand Satisfied | Demand Remained |
| 2 | 121750 | 52000 | 69750 |
| 3 | 121750 | 68200 | 53550 |
| 4 | 121750 | 84400 | 37350 |
| 5 | 121750 | 100310 | 21440 |
| 6 | 121750 | 116800 | 4950 |
| 7 | 121750 | 121750 | 0 |
| 8 | 121750 | 121750 | 0 |

### 3.8 Model Evaluation

Based on the results from the optimization model, the traffic volume on each evacuation route is calculated. In order to simulate the obtained solution with CORSIM, turning fractions at intersections and ramps are calculated. The original simulation input file is modified to reflect the optimal traffic patterns. Some signal timings and traffic signs are modified to give the priority to the major traffic routes.

Table 3-5 shows the evacuation progression during the time. The number of evacuees who reach each destination and the total number and percentage of evacuees who reach their destinations are presented in the table. These results are the average values from four simulation runs with different random seeds. Each run takes about six hours on a 3.4 GHz processor with 2 GB RAM.

Table 3-5: Evacuation Progress from the Simulation Results

| HOUR | 10 | 11 | 12 | 13 | 14 | 15 | 16 | 17 | 18 |
|---|---|---|---|---|---|---|---|---|---|
| Exit 32 | 59120 | 65570 | 71990 | 78344 | 83699 | 86862 | 89071 | 90088 | 90438 |
| Exit 41 | 13036 | 14516 | 15752 | 16528 | 17346 | 18127 | 18930 | 19722 | 20477 |
| Exit 42 | 8427 | 9385 | 10160 | 10892 | 11601 | 12333 | 13043 | 13773 | 14428 |
| Exit 43 | 26617 | 30288 | 34027 | 37667 | 41333 | 45008 | 48727 | 52399 | 56114 |
| Exit 44 | 27161 | 30583 | 33987 | 37421 | 40671 | 43805 | 46794 | 49853 | 52733 |
| Others | 17800 | 17800 | 17800 | 17800 | 17800 | 17800 | 17800 | 17800 | 17800 |
| SUM | 152160 | 168142 | 183716 | 198651 | 212449 | 223936 | 234365 | 243634 | 251989 |
| % | 60.35 | 66.69 | 72.87 | 78.79 | 84.26 | 88.82 | 92.95 | 96.63 | 99.94 |

The last row in Table 3-5 shows the percentage of the total demand that reached a safe destination by the time given in the first row. It can be seen that for 18 hours of operation, 99.94 percent of the original 252,130 vehicles reached a safe destination. However, if we are planning for example for 90 percent of vehicles, 15.5 hours of evacuation time is enough.

As mentioned in the results of optimization model, 17 hours was suggested as the network clearance time. The evaluation results from microsimulation indicate that around 97 percent of vehicles will be able to complete the evacuation by the end of hour 17.

Exit nodes 32, 41, 42, 43 and 44 in Table 5 are shown in Figure 3. Others refer to those demand generation points in the simulation file that are located very close to interstate I-95. They are far from the coast danger zone and have their own local roads that discharge their evacuees to I-95 directly. Since they do not use major evacuation routes of our network and they do not face any congestion at local roads, it is assumed that they can be evacuated during the first 10 hours. The simulation results confirm this idea.

Figures 3-5 and 3-6 show the results given in Table 3-5 graphically. As it can be seen from both graphs, the evacuation operations continues linearly up to approximately hour 14, and after that the rate of arrival at destinations decreases indicating that the network is clearing and finally at hours 17 and 18 it converges to its ultimate values and evacuation is concluded.

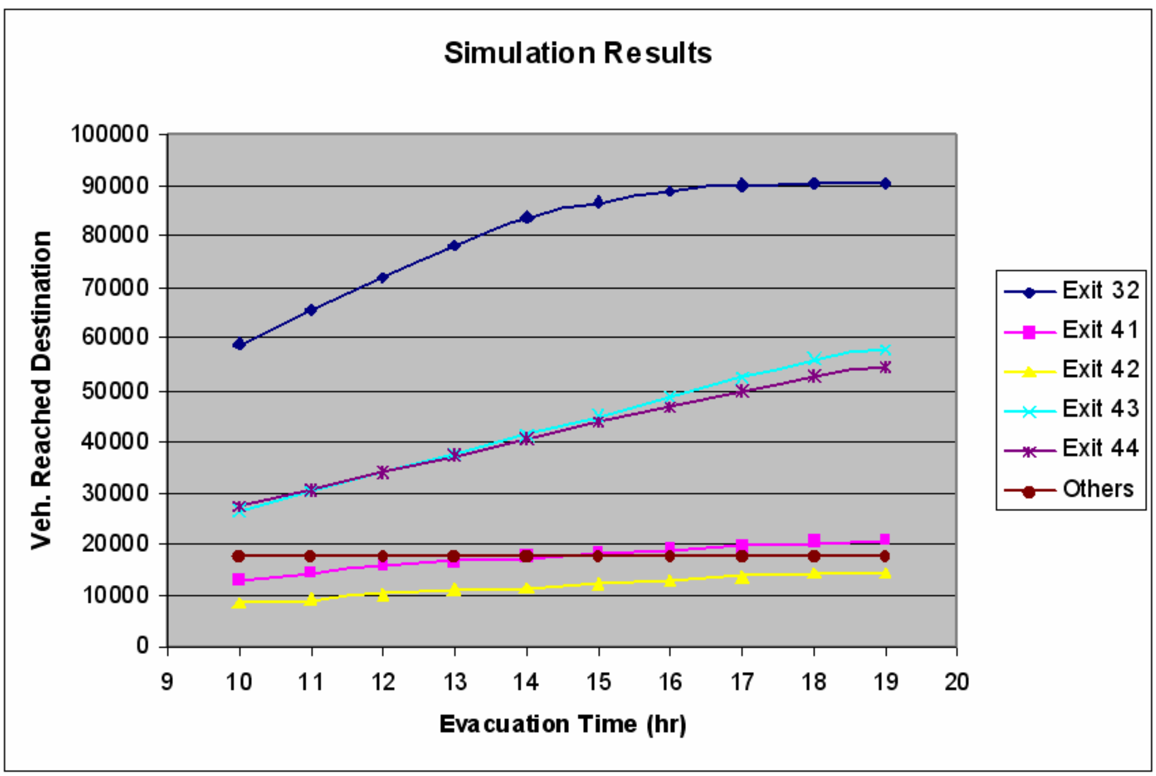


Figure 3-5: A graphical illustration of throughput evolution for different exits

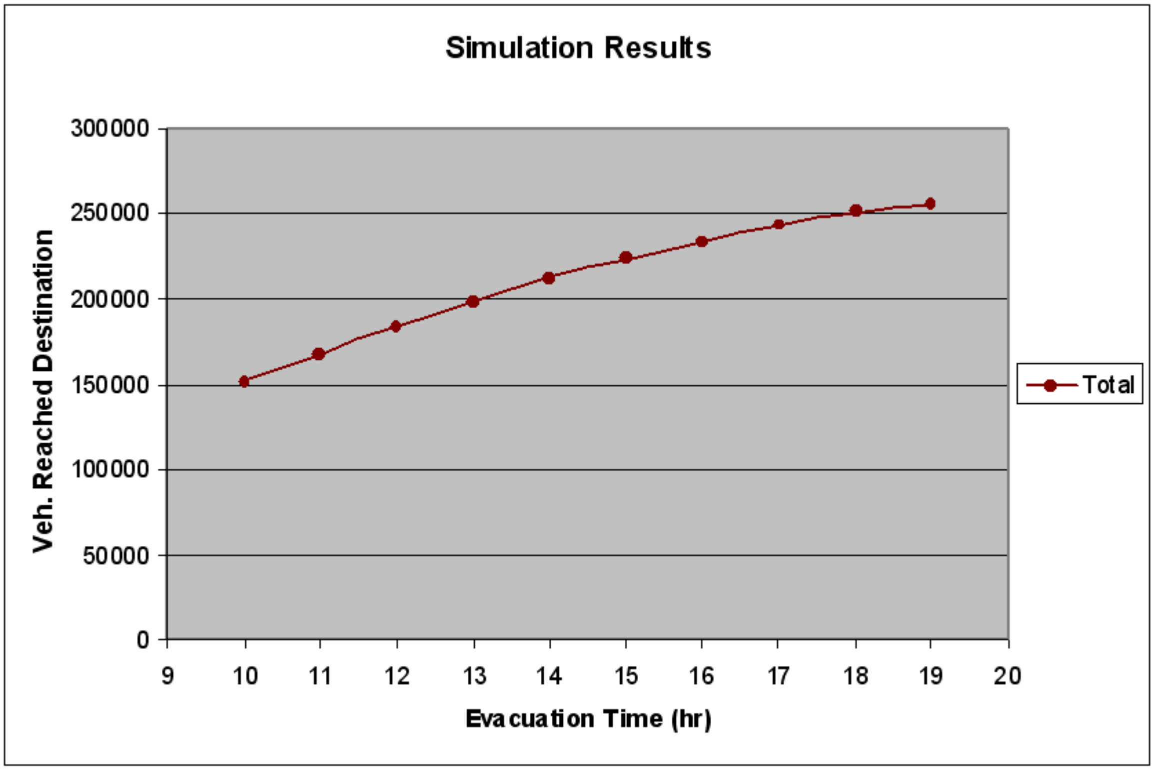


Figure 3-6: A graphical illustration of the total network throughput evolution

Table 3-6: Simulation results for the OC-Plan

| HOUR | 10 | 11 | 12 | 13 | 14 | 15 | 16 | 17 | 18 | 19 |
|---|---|---|---|---|---|---|---|---|---|---|
| Exit 32 | 44947 | 49137 | 53032 | 56921 | 60801 | 64674 | 68534 | 72469 | 76381 | 80308 |
| Exit 41 | 1039 | 1054 | 1058 | 1058 | 1058 | 1058 | 1058 | 1058 | 1058 | 1058 |
| Exit 42 | 13697 | 14955 | 15533 | 15933 | 16376 | 16811 | 17240 | 17698 | 18208 | 18645 |
| Exit 43 | 6497 | 7111 | 7532 | 8017 | 8406 | 8818 | 9070 | 9221 | 9414 | 9629 |
| Exit 44 | 23315 | 26224 | 29164 | 32086 | 34931 | 37825 | 40636 | 43537 | 46476 | 49393 |
| Others | 17800 | 17800 | 17800 | 17800 | 17800 | 17800 | 17800 | 17800 | 17800 | 17800 |
| SUM | 107295 | 116281 | 124119 | 131815 | 139372 | 146986 | 154338 | 161783 | 169337 | 176833 |
| % | 42.56 | 46.12 | 49.23 | 52.28 | 55.28 | 58.30 | 61.21 | 64.17 | 67.16 | 70.14 |

### 3.9 Comparison

Table 3-6 presents the results of simulation for the evacuation plan of Ocean City posted on Ocean City web site at http://oceancity.umd.edu/, referred to as OC-Plan in this section. It can be seen that in 10 hours only 42.5 percent of the total vehicles are evacuated and by the end of 19$^{th}$ hour 176,833 vehicles can evacuate which accounts for only 70 percent of the total.

Table 3-7 and Figure 3-7 compare the results from simulation of OC-Plan with the results from optimum solution presented in this report. After only 10 hours, the proposed solution shows huge improvement of 41.8 percent over the OC-Plan. At the end of hour 19, the proposed plan can evacuate 79,172 more vehicles than the OC-Plan which is about 44.8 percent more.

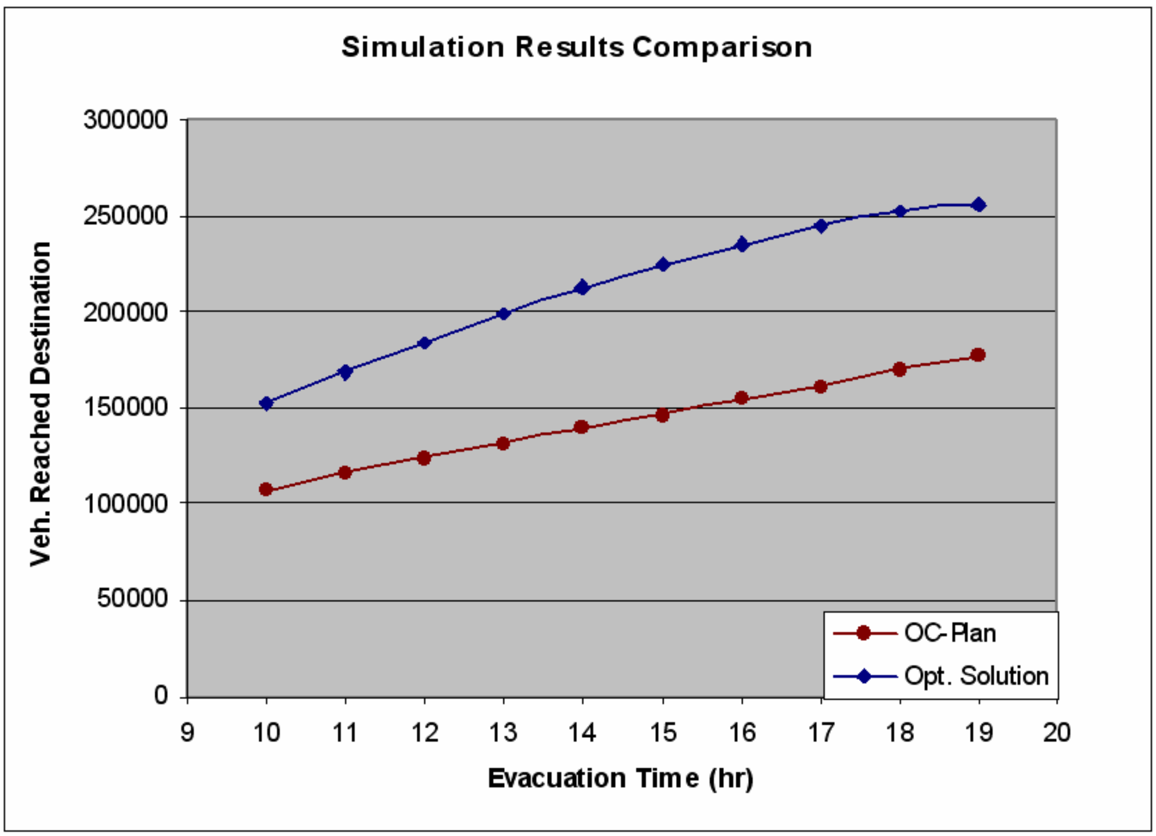


Figure 3-7: Comparison between state of the practice and the optimal solution

Table 3-7 Comparison of simulation results

| HOUR | 10 | 11 | 12 | 13 | 14 | 15 | 16 | 17 | 18 | 19 |
|---|---|---|---|---|---|---|---|---|---|---|
| OC-Plan | 107295 | 116281 | 124119 | 131815 | 139372 | 146986 | 154338 | 161783 | 169337 | 176833 |
| Optimal Plan | 152160 | 168142 | 183716 | 198651 | 212449 | 223936 | 234365 | 243634 | 251989 | 256005 |
| Difference | 44865 | 51861 | 59597 | 66836 | 73077 | 76950 | 80027 | 81851 | 82652 | 79172 |
| % Improve | 41.81 | 44.60 | 48.02 | 50.70 | 52.43 | 52.35 | 51.85 | 50.59 | 48.81 | 44.77 |

### 3.10 Conclusions

This chapter presents an optimization model and a solution approach for developing the evacuation plan for Eastern Shore of Maryland. The proposed mathematical program is a nonlinear and constrained optimization problem that minimizes the total travel time of the system while trying to discharge as many vehicles as the network capacity allows. The optimal solution from the model shows that for a total of 252,130 vehicles, it may take 17 hours to clear evacuation traffic in the network. Initially, this can be considered as a lower bound for the required evacuation duration because the planning formulation does not account for delays at signals, or discrepancies in driver behavior.

The results of simulation evaluation presented in Table 4 show the number of vehicles that can be evacuated during each hour of evacuation. The simulation results also indicate that approximately 252,000 vehicles can be evacuated over the period of 18 hours. About 97 percent of the total evacuees are able to exit the network in the first 17 hours.

The results of bottleneck analysis emphasize the need for capacity expansion at the south east part of the network connecting Ocean City and Bethany Beach to the rest of the network. The results show that it takes more than twice the time (15 hours) to evacuate Ocean City and Bethany Beach than it takes to evacuate the rest of the network (7 hours) while the two areas have approximately an equal number of evacuees. This means that increasing the capacity of roads heading out of Ocean City can dramatically benefit the system and reduce the total evacuation duration needed to clear the network.

The comparison of the simulation results from the original OC-Plan with the results after implementing the proposed optimized plan shows the potential improvements with respect to the number of evacuees who could each destination and the total number of vehicles that could exit the danger zone safely.

# Chapter 4

# Evacuation Control model at the Network Level

## 4.1. Introduction

Chapter 4 presents the formulations for design of evacuation control strategies at the network level, which include traffic routing, and contraflow. To ensure that the proposed formulations for network flow relations can realistically capture the temporal/spatial interactions of evacuation traffic over the network, Section 4.2 introduces a revised cell transmission concept. The revised modeling concept preserves the capability of the original methodology in capturing traffic dynamics, but allowing the use of cells of different sizes to improve the computing efficiency. This chapter will present the application of this concept in formulating traffic routing, and contraflow design.

Section 4.3 discusses the modeling issues regarding the design of traffic routing strategies. The proposed basic model is based on the following two assumptions: 1) the evacuation network is predetermined, although it can be either constant or time-varying during the evacuation operations; and 2) the time for activating an evacuation order is predetermined for each origin, i.e., the evacuation demand generated during each interval is known. With these assumptions, presentations of the proposed base model will emphasize the selection of objective functions and the modeling of network traffic interactions.

Section 4.4 discusses the modeling issues regarding the contraflow design. As an extension of the base model, the proposed model will relax the assumption regarding the network conditions, and intend to reallocate capacities by reversing some travel lanes. This extended model features a network enhancement that expands the network with dummy segments and modifies the objective functions and network traffic formulations shown in Section 4.3.

.

The last section summarizes research efforts that have been completed in this chapter. Figure 4.1 has demonstrated the logical relations between different sections in this Chapter.

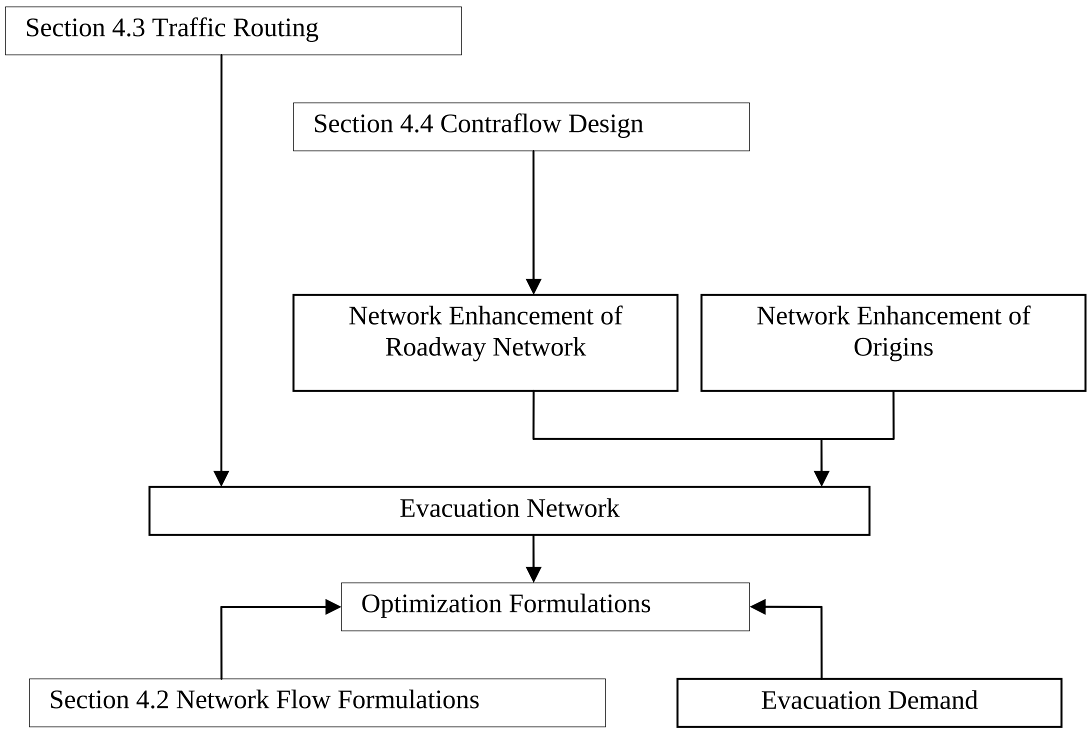


Figure 4-1: Interrelations between main sections in Chapter 4

## 4.2 Network Flow Formulations

To ensure the effectiveness of the proposed optimization models, one has to choose an approach to mathematically represent traffic flow evolution in an evacuation network. To accommodate the complexity associated with large-scale network applications and to improve the computational efficiency, this study proposes a revised cell transmission formulation for use as the underlying network flow model.

The basic idea of the cell transmission concept proposed by Daganzo (1994; 1995) is to convert roadway links into equal-sized segments, or named cells, that could be traversed in a unit time interval at the free-flow speed. Then, the movements of vehicles among these cells are defined with two types of relations, namely, flow propagation relations to decide flows between two cells based on upstream/downstream traffic conditions and flow conservation equations to depict the evolution of the cell status (i.e., the number of vehicles in each cell) over time.

To reduce the size of formulations in large-scale network applications, Ziliaskopoulos and Lee (1996) have proposed the use of cells of an adjustable size. Their idea is to update those longer cells with a lower frequency, and use the averaged parameters for those intermediate intervals. Such a formulation requires the size of a long cell to be an integral multiple of its connected short cells, and may cause the propagated flows deviated from those homogenous cells.

To offer the flexibility and also to improve the accuracy in large-scale network applications, the revised cell transmission formulation proposed in this study will allow cells of different sizes to be connected as needed. Its core concept is presented below.

### 4.2.1 Network Conversion

To successfully apply the revised cell transmission formulation, one needs to convert the road network into a set of connected cells, based on the following principal steps:

- *Identify homogenous road segments*: homogeneity is defined by the same free flow speed, same number of lanes, same jam density, same saturation flow rate, and no ramps within a segment.
- *Define unit time interval*: the maximal unit interval $\tau$ is constrained by the shortest time to traverse a homogenous segment, as in Equation 4.1. Other unit intervals can also be used, provided $\tau$ is the integral multiple of it.

$$\tau = \min\{\frac{length \quad of \quad a \quad segment}{corresponding \quad free \quad flow \quad speed}\} \qquad (4.1)$$

- <u>*Convert road segments to cells*</u>: basically, every homogenous segment is converted to a cell, and the cell size $l$ is defined by Equation 4.2.

$$l = INT\{\frac{length \quad of \quad segment}{corresponding \quad free \quad flow \quad speed \times unit \quad interval \quad length} + 0.5\} \qquad (4.2)$$

- <u>*Define connectors between cells*</u>: A connector is defined to indicate the potential traffic flows between two connected segments.

### 4.2.2 Flow Conservation Formulations

Flow conservation equations depict the evolution of the cell status (i.e., the number of vehicles in each cell) over time. With the revised cell transmission formulation, all cells will be updated at every unit time interval $\tau$, regardless of their size. As illustrated in Figure 4.2, Equation 4.3 and Equation 4.4 define the flow conservation relations for different types of cells.

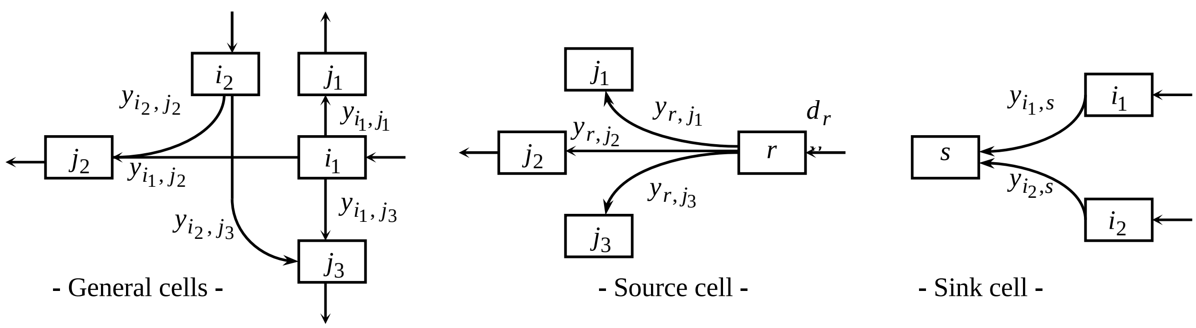


Figure 4-1: Graphical illustration of cell connections

- For general cells (actual highway segments) and sink cells (destinations),

$$x_i^{t+1} = x_i^t + \sum_{k\in\Gamma(i)} y_{ki}^t - \sum_{j\in\Gamma^{-1}(i)} y_{ij}^t \tag{4.3}$$

- For source cells (origins),

$$x_r^{t+1} = x_r^t + d_r^t - \sum_{j\in\Gamma^{-1}(r)} y_{rj}^t \tag{4.4}$$

where $x_i^t$ is the number of vehicles in cell $i$ at the beginning of interval $t$; $y_{ij}^t$ is connector flows from cell $i$ to cell $j$ during $t$; $d_r^t$ is evacuation demand from origin $r$ during interval $t$, which is also called dynamic loading pattern and defined with response curves in practice; $\Gamma^{-1}(i)$ is the set of downstream cells to cell $i$; $\Gamma(i)$ is the set of upstream cells to cell $i$; The subscript $r$ is the index of source cells; and $i, j, k$ is the index of other cells.

### 4.2.3 Revised Flow Propagation Formulations

The flow propagation relations decide the connecting flows between cells during each time interval, which are presented with the following expressions:

$$\sum_{k\in\Gamma(i)} y_{ki}^t \le R_i^t \tag{4.5}$$

$$\sum_{j\in\Gamma^{-1}(i)} y_{ij}^t \le S_i^t \tag{4.6}$$

Equation 4.5 is to model flow propagation relations considering the traffic conditions in a downstream cell, whereas Equation 4.6 is for the traffic conditions in an upstream cell. $R_i^t$ is the receiving capacity of downstream cell $i$ during interval $t$ (veh), and $S_i^t$ is the sending capability of upstream cell $i$ during interval $t$ (veh);

Equation 4.7 defines the receiving capacity of cell $i$, which is proposed after considering the initial cell status $x_i^t$ as well as its potential *internal* evolution during interval $t$.

$$R_i^t = \min\{Q_i^t, N_i^t / l_i, N_i^t - x_i^t\} \tag{4.7}$$

where $Q_i^t$ is the number of vehicles that can flow into/out of cell $i$ during $t$; $N_i^t$ is the number of vehicles that can be accommodated in cell $i$ during $t$; and $l_i$ is the size of cell $i$. Note that if the cell length $l_i$ is equal to 1, Equation 4.7 will converge to the equation for equal-sized cells in the classic cell transmission formulation. The mathematical proof of Equation 4.7 is shown in Appendix A.

Equation 4.8 defines the sending capacity of cell $i$. Note that if $l_i$ is equal to 1, Equation 4.8 is also equivalent to the equation for equal-sized cells (Daganzo 1994).

$$S_i^t = \min\{Q_i^t,\ \ N_i^t / l_i,\ \ x_i^{t-l_i+1} - \sum_{j \in \Gamma^{-1}(i)} \sum_{m=t-l_i+1}^{t-1} y_{ij}^m\} \tag{4.8}$$

Here the first two terms are direct presentation of the maximal flow that can leave cell $i$ during a unit time interval. The third term can be explained as follows: according to the definition of cell size, $l_i$ unit intervals are required to traverse cell $i$ at the free-flow speed. Thus, the total flows that should have left cell $i$ are $\sum_{k \in \Gamma(i)} \sum_{m=1}^{t-li} y_{ki}^m$, while the total flows that have actually left cell $i$ are $\sum_{j \in \Gamma^{-1}(i)} \sum_{m=1}^{t-1} y_{ij}^m$. The sending capacity cannot exceed their difference, i.e.,

$$\begin{aligned} S_i^t &\le \sum_{k \in \Gamma(i)} \sum_{m=1}^{t-li} y_{ki}^m - \sum_{j \in \Gamma^{-1}(i)} \sum_{m=1}^{t-1} y_{ij}^m \\ &= x_i^{t-li+1} - \sum_{j \in \Gamma^{-1}(i)} \sum_{m=t-li+1}^{t-1} y_{ij}^m \end{aligned} \tag{4.9}$$

A numerical test is given in Appendix B to demonstrate the effectiveness of the revised cell transmission formulation.

### 4.3 Base Model: Traffic Routing in Concurrent Evacuation

Applying the revised cell transmission concept as the underlying network flow model, this section will detail the formulations of the base model, which addresses the design of traffic routing strategies under the operation of concurrent evacuation without contraflow options. The optimized control plan mainly includes two types of information, namely, 1) the percentage of demand to be diverted to links immediately downstream of the origins, and 2) the target turning fractions to be controlled at each diverging point during each time interval.

#### 4.3.1 Objective Functions

In response to the unique operational constraints during emergency evacuation, the proposed formulation features a two-level optimization scheme.

The high-level optimization aims to maximize the total throughput within the specified evacuation duration *T*. Since the throughput can be represented with the total number of vehicles entering all destinations over the study period, one can formulate the objective function as follows:

$$\max \quad \sum_{i\in S_S}\sum_{k\in\Gamma(i)}\sum_{t=1}^{T} y_{ki}^{t} = \sum_{i\in S_S} x_i^{T+1} \tag{4.10}$$

where $S_S$ is the set of sink cells (destinations); and $\Gamma(i)$ is the set of upstream cells to cell *i*.

The low-level optimization model intends to minimize the total trip time (including the waiting time in origins) if the specified duration *T* is sufficient for evacuating all demands. The special structure of the underlying network flow model implies that a vehicle in a cell will either wait for one interval without move or take one interval to reach the downstream cell. Thus, the objective function has the following expression:

$$\min \quad \sum_{i \in S \cup S_r} \sum_{t=1}^{T} x_i^t \tag{4.11}$$

where $S$ is the set of general cells (roadway segments); and $S_r$ is the set of source cells (origins).

### 4.3.2 Operational Constraints

- Network Flow Constraints

Although Cell Transmission concept was originally proposed for simulation-based operations, it was later transformed and utilized in various optimization contexts. Some early studies (Li, et al. 1999; Ziliaskopoulos, 2000) have applied Cell Transmission concept to formulate dynamic traffic assignment as an LP model, which uses a set of less-than constraints to relax the minimal-value in flow propagation relations and thus allow vehicle holding (i.e., traffic will not necessarily exit a cell even if it can do so under the prevailing network situation). Note that vehicle holding may be undesirable since no individual driver would wait when perceiving the sufficient capacity ahead. However, holding vehicles in evacuation implies that responsible agencies can improve the overall operation efficiency by delaying certain groups of travelers.

Thus, this study will follow these practices when applying the revised cell transmission concept to formulate the underlying network flow constraints. Note that these constraints, as shown in Equations 4.12-4.19, are the same for both levels of optimization formulations.

$$x_i^{t+1} = x_i^t + \sum_{k \in \Gamma(i)} y_{ki}^t - \sum_{j \in \Gamma^{-1}(i)} y_{ij}^t, \qquad i \in S \cup S_s \tag{4.12}$$

$$x_r^{t+1} = x_r^t + d_r^t - \sum_{j \in \Gamma^{-1}(r)} y_{rj}^t, \qquad r \in S_r \tag{4.13}$$

$$\sum_{k \in \Gamma(i)} y_{ki}^t \le Q_i^t, \qquad i \in S \cup S_s \tag{4.14}$$

$$\sum_{k \in \Gamma(i)} y_{ki}^t \le N_i^t / l_i, \qquad i \in S \cup S_s \tag{4.15}$$

$$\sum_{k\in\Gamma(i)} y_{ki}^t \le N_i^t - x_i^t, \qquad i \in S \cup S_s \tag{4.16}$$

$$\sum_{j\in\Gamma^{-1}(i)} y_{ij}^t \le Q_i^t, \qquad i \in S \cup S_r \tag{4.17}$$

$$\sum_{j\in\Gamma^{-1}(i)} y_{ij}^t \le N_i^t / l_i, \qquad i \in S \cup S_r \tag{4.18}$$

$$\sum_{j\in\Gamma^{-1}(i)} y_{ij}^t \le x_i^{t-l_i+1} - \sum_{j\in\Gamma^{-1}(i)} \sum_{m=t-l_i+1}^{t-1} y_{ij}^m, \ i \in S \cup S_r \tag{4.19}$$

$$y_{ij}^t \le Q_{ij}^t \tag{4.20}$$

Among the above network flow constraints, Equation 4.12 is the flow conservation equation for both general cells and sink cells; Equation 4.13 is the flow conservation equation for source cells; Equations 4.14-4.16 present the relaxed flow propagation constraints related to the receiving capacity of any downstream cells; Equations 4.17-4.19 present the relaxed flow propagation constraints related to the sending capacity of any upstream cells; and Equation 4.20 presents the flow capacity constraints for connectors, which can model the reduced capacity of ramps or the right/left turning movements at the intersections.

Note that Equation 4.20) only defines the restriction on a single connector flow. The modeling for intersections is more complex because different connector flows may conflict with each other and need to share the intersection capacity. Since signal design is not the focus of the network level control, a set of simplified relations as shown in Equation 4.21 is employed here. The equation implies that if one selects a movement arbitrarily from each conflicting phase at an intersection, the sum of the v/c ratios on these movements will not exceed one (i.e., the intersection capacity is satisfied during each interval).

$$\sum_{p\in Ph_I} \{ y_{ij}^t / Q_{ij}^t : \ \ ij \in p \} \le 1 \tag{4.21}$$

where $I$ is the index of intersections; $Ph_I$ is the set of conflict phases at intersection $I$; and $p$ is the index of each conflict phase at intersection $I$, $p \in ph_I$.

- Demand related constraints

The high level optimization enforces no additional constraints on the evacuation demand. For the low level optimization, since evacuation flows are counted in the objective function only before they have arrived at their destinations, the model tends to push as many vehicles as possible at the fastest pace. Thus, one can expect that all evacuation demands can reach their destinations at the end of the evacuation period. Equation 4.22 is proposed to guarantee such a relation: the left-side term is the total number of vehicles that have arrived at destinations after evacuation duration *T* and the right-side term denotes the total demand.

$$\sum_{i \in S_s} x_i^{T+1} = \sum_{r \in S_r} D_r \qquad (4.22)$$

where $x_i^{T+1}, i \in S_s$ is the number of vehicles that has arrived at the destination *i* after the evacuation time window *T*; and $D_r, r \in S_r$ is the total evacuation demand generated at origin *r*.

- Other general constraints

The general constraints include nonnegative constraints, initial value of cell state variables $x_i^1$, and initial value of connector flows $y_{ij}^0$. In most cases, $x_i^1$ (excluding source cells) and $y_{ij}^0$ are set to zero, although $x_i^1$ can be other values to simulate the background traffic prior to the evacuation. Note that $x_i^1$ can also be used to reflect the actual network condition preceding the onset of an accident during the evacuation, and this enables the model users to adjust the evacuation plans as needed.

Another class of general constraints is for the capacity of destinations. Storage capacity $N_i^t, i \in S_s$ can be restricted if the safety shelter has the space limitation. Flow capacity $Q_i^t, i \in S_s$ may be restricted if the entrance capacity of the safety shelter is lower than the capacity of the upstream routes, or if the destination is not the safety shelter but a dummy node to indicate safe area. In the later case, $Q_i^t, i \in S_s$ is set as the capacity of downstream routes to prevent the queue spillback. As the important evacuation control strategies, both diverging proportions and merging proportions are directly estimable from the optimization results.

- Numerical test of the base model

This numerical test aims to demonstrate the applicability of the proposed Base Model for traffic routing with the Ocean City hurricane evacuation network. Ocean City is a famous tour destination located on a narrow peninsula on Maryland's Eastern Shore. The population in the summer peak season can reach 150,000 ~ 300,000 people, compared with 7,000 to 25,000 people during the off-peak season.  This large size of population in the summer season renders the city especially vulnerable to the threat of hurricanes, which demands the state to design its hurricane evacuation plans.

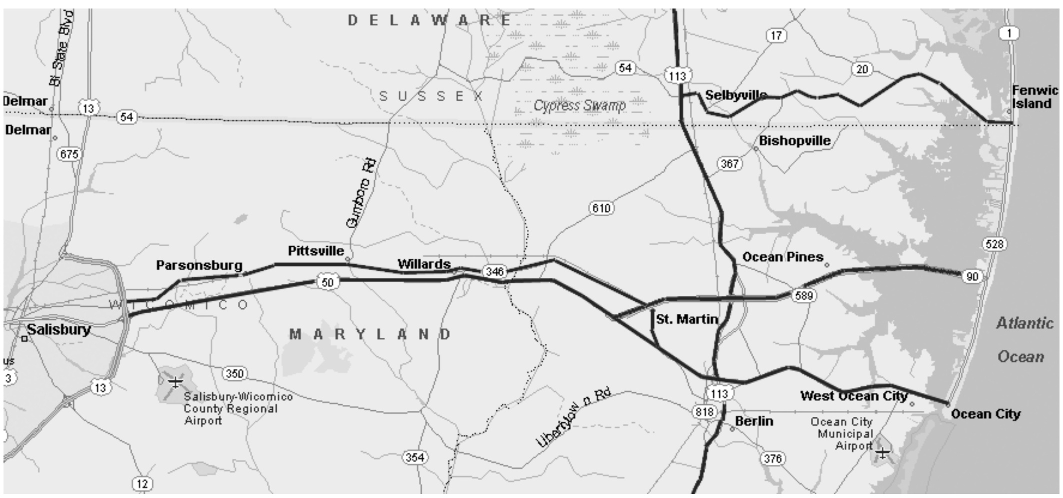


Figure 4-3: Major Evacuation Network for Ocean City

Figure 4.3 presents the major evacuation network for Ocean City. The sole origin is set to be the entire city. Thus, one can divide the city into a number of evacuation zones, based on the optimized demand distribution to the three primary evacuation routes. Among these routes, US50 is an arterial street with two lanes in each direction, MD90 is a freeway with one lane in each direction, and DE20 is an arterial street with one lane in each direction. There are three destinations for evacuation flows. The city of Salisbury is a destination without capacity limit, while US113 north and US113 south are two dummy destinations with a flow capacity of 1800 vehicle per lane per hour.

Following the network conversion procedures in Section 4.2, this numerical test first defines the homogenous segments. Note that all interchanges are modeled with connectors, not cells, to indicate the existence of ramps. The jam density for all cells is set to be 93 vehicles per kilometer per lane, whereas the saturation flow rate is set to be 2160 vehicles per lane per hour for the freeway segment of MD90, and 1800 vehicles per lane per hour for other segments. Based on the actual network geometric data, the length of a unit interval is set to be 20 seconds, which is sufficiently small for evacuation operations. Then, one can convert the network to a cell-connection diagram as illustrated in Figure 4.4. Note that the number in each parenthesis indicates the size of the cell.

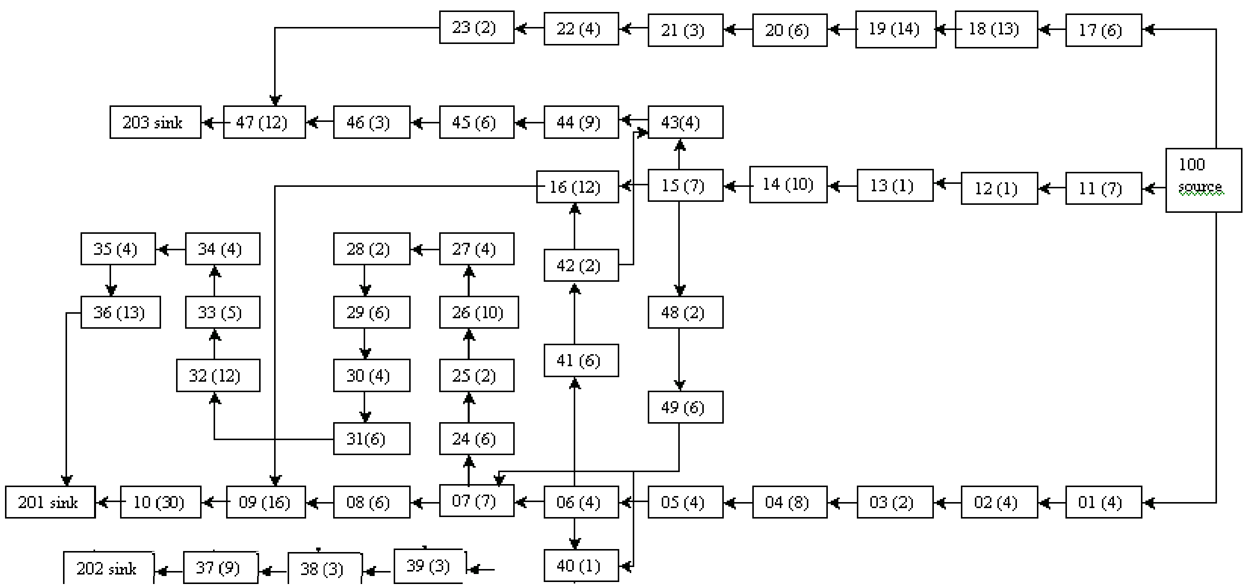

Figure 4-2: Cell Connection Diagram for Ocean City Hurricane Evacuation Network

Note that as indicated in the widely adopted evacuation response curves (Alsnih and Stopher, 2003), the evacuation demand from origin *r* in time interval *t*, $d_r^t$, tends to greatly exceed the evacuation capacity after the inception of evacuation. This surge in evacuation demand may be more apparent for potential hurricane evacuation of Ocean City, since the major evacuation population will be tourists who have limited personal belongings to collect and few local properties to protect. Thus, this numerical test assumes that all traffic demand enters their corresponding source cell at the beginning of the evacuation process.

For the evacuation scenario specified above, the resultant LP formulations contain 720 time intervals, 79,809 variables, and 250,509 constraints. A computer program was created to generate the standard input file for the professional software LINGO 8.0. The global optimal solution for the maximal throughput over 4 hours amounts to 27,268 vehicles to all three destinations. Figure 4.5 presents the cumulative arriving curve for each destination, where most vehicles are directed to Salisbury.

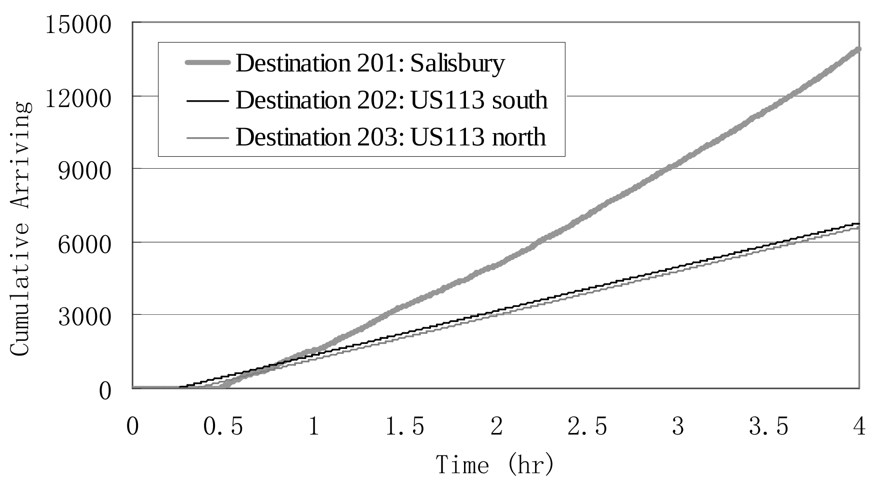


Figure 4-3: Cumulative arriving curves for the high-level optimization

The numerical test then applies the proposed low-level optimization model to obtain the optimal evacuation patterns to minimize the total travel time and waiting time if the allowed time window is sufficiently long for completing the evacuation. The total evacuation demand is set to be 25,000 vehicles in 4 hours. The new LP formulations with the second level optimization contain 80,528 variables and 251,228 constraints for 720 time intervals. Figure 4.6 presents the cumulative arriving curve of each destination based on the global optimal solution.

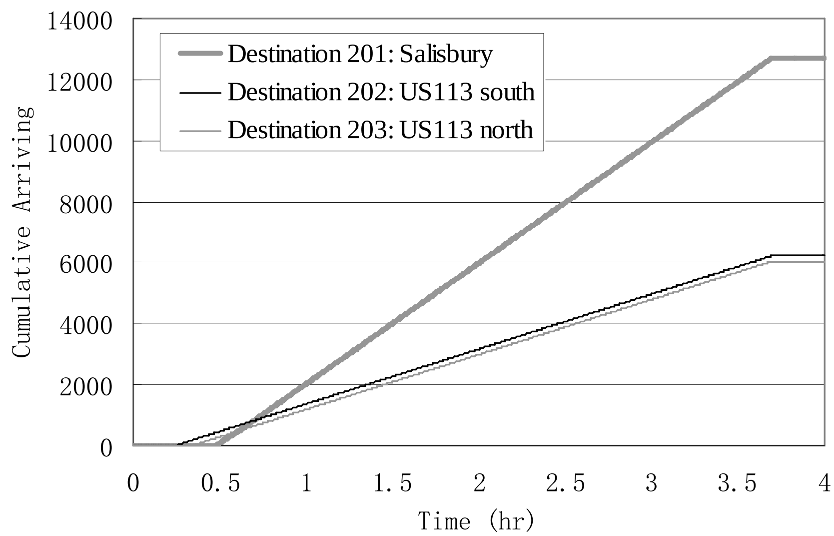


Figure 4-4: Cumulative arriving curves for the low-level optimization

The preliminary results from the low-level model indicate that there is no flow in the south direction of US113 between US50 and MD90, and the capacity usage of the north direction of US113 from US50 to DE54 is very low. Thus, one can exclude these road segments from the major evacuation network in practice. Note that after excluding those low-usage routes, only two diverging cells remain in the network and their diverging patterns are relatively stable (except during the dissipation phase) in the optimal solution.

Thus, the last part of the numerical test will input these diverging rates as the target turning fractions in a CORSIM simulator of the Ocean City hurricane evacuation network, with the objective of evaluating the reliability of the proposed formulations. For this purpose, Figure 4.7 compares the cumulative arriving curve at each destination generated from the model with the same curves generated from the microscopic simulator. The comparison indicates that the time-varying network traffic conditions with two approaches are quite similar, which thus demonstrates the potential of the proposed model in accurately formulating traffic flows for large-scale networks and in efficiently generating the optimal set of evacuation strategies.

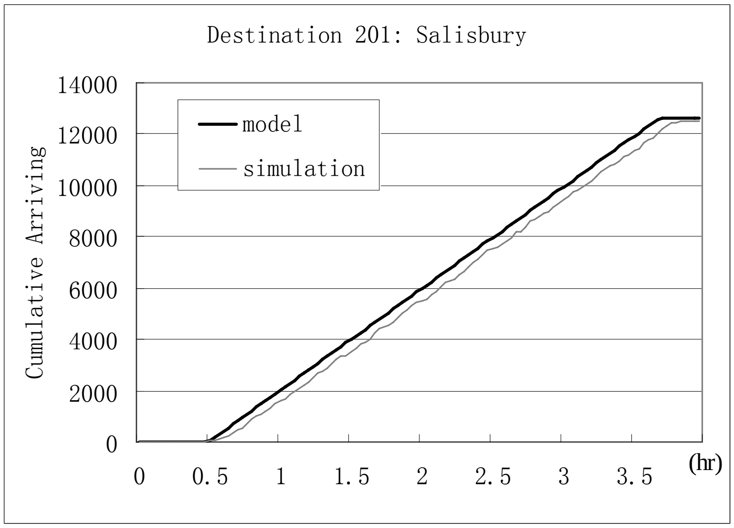


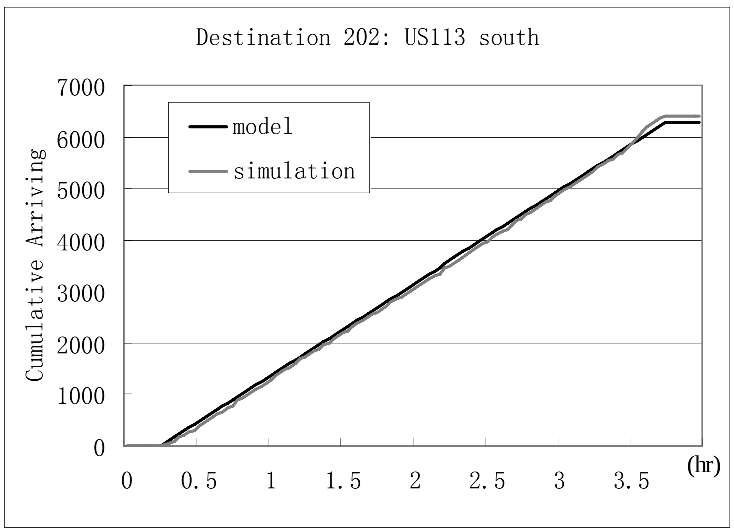


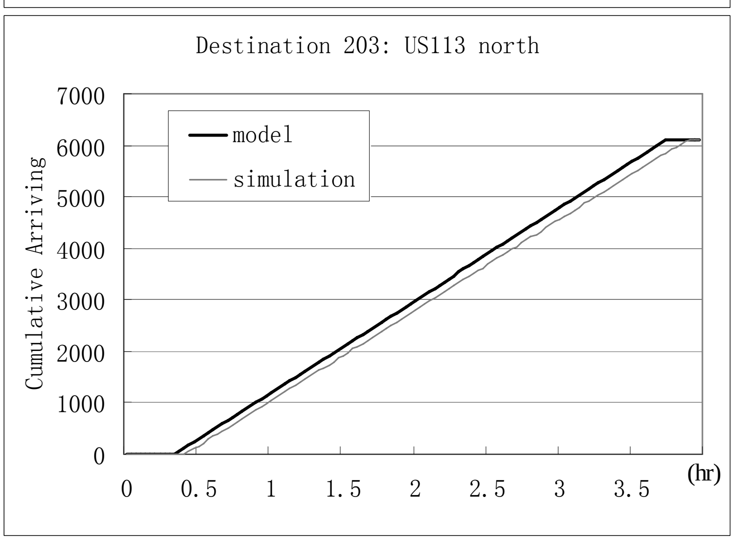


Figure 4-5: Comparison of cumulative arriving curves: model vs. simulator

## 4.4 Extended Model-I: Contraflow Design

The extended model-I aims to incorporate the contraflow decisions into the base model for a concurrent evacuation. The optimized control plan mainly includes three types of information, namely: 1) the segments to implement lane reversal operations under the budget limit; 2) the percentage of demand to be diverted to the links immediately downstream of the origin; and 3) the target turning fractions to be controlled at each diverging point during each time interval. This model is especially essential under the following situations.

- With limited resources: Since contraflow operations requires a large amount of manpower and materials such as barricades or cones, system operators have to decide the reversing priority of candidate segments and assign the available resources to the most critical locations.
- With a complex evacuation network:. For example, when there are many parallel roads connecting the major evacuation corridors, system operators may face the difficulty in deciding whether to reverse some parallel roads and where to enact the reverse-lane operations.

### 4.4.1 Operational Concerns for Contraflow Design

As discussed in the literature review chapter, the key concept of contraflow design is to temporarily reverse some travel lanes for the safety-bound traffic so as to increase the available capacity toward the target evacuation destinations. Although some studies have explored the design of contraflow strategies with optimization models, the following critical modeling issues remain to be investigated.

- Traffic streams on the reversed lanes differ significantly from those on the normal lanes. As noted in some studies, such differences are reflected in the reduced capacity and speed observed on the reversed lanes. Thus, it seems inappropriate to model the reversed and normal lanes on the same segment as one cell or with the identical formulation.

- The reversed lane capacity will not be available at the beginning of the evacuation process, as it needs the law enforcement agency to clear all traffic on the target lanes for reverse-lane operations.
- An increase in the flow capacity due to reverse-lane operations has a non-linear relationship with the number of reversed lanes. For a freeway segment with two lanes in each direction, the data in Table 4.1 clearly indicate this non-linearity nature [Wolshon, 2001].

Table 4.1 Evacuation Traffic Flow Rates

| Contraflow Strategies | Safety-bound Capacity (vph) |
|---|---|
| Normal Two Way Operation (no contraflow) | 3,000 |
| Three Lane (one contraflow lane) | 3,900 |
| One-Way (two contraflow lanes) | 5,000 |

In response to the aforementioned operational concerns, this study proposes the Extended Model-I for contraflow design as the extension of the Base Model. This extended model uses the same two-level optimization objectives as in Equations 4.10 and 4.11. The network flow models are also similar as those in Equations 4.12-4.21, but with a more elaborated network and additional constraints to capture the effects of contraflow decisions on network traffic pattern.

### 4.4.2 Key features of the elaborated network for Extended Model-I

The key features of the elaborated network for applying the extended model for contraflow operations are summarized below.

- To reflect the difference in normal lanes and reversed lanes, the model represents each homogenous road segment $i$ (one direction) with two cells ($i^+$, $i^-$), one in its designed direction and the other in its reversed direction. The length of these two cells may not be equal due to the potential speed differences.
- To reflect the non-linearity in lane capacity the model assigns a binary variable $\delta_{\text{ln}}$ to each lane, $ln$, on a segment for indicating its direction. In addition, each lane will have two flow capacity indices ($Q_{\text{ln}}^+(t)$, $Q_{\text{ln}}^-(t)$), one for each direction. Thus, the flow capacity for each cell ($Q_{i^+}^t$, $Q_{i^-}^t$) will depend on the reversing decisions of each lane on the target segment $i$.

Fig. 4.8 illustrates application of the above concept on a highway of two lanes in each direction. There are two segments for use in operations, one for each direction. Such two segments are named as a pair of segments, and operators will not reverse them concurrently. Note that there are five possible operational plans in this case:

- No lanes are reversed, and thus both reversed cells will have a zero capacity.
- One lane in Segment I (or II) is reversed, and thus both normal cells and the corresponding reversed cell will have a positive capacity.
- Both lanes in Segment I (or II) are reversed, and thus only one normal cell and one reversed cell will have a positive capacity.

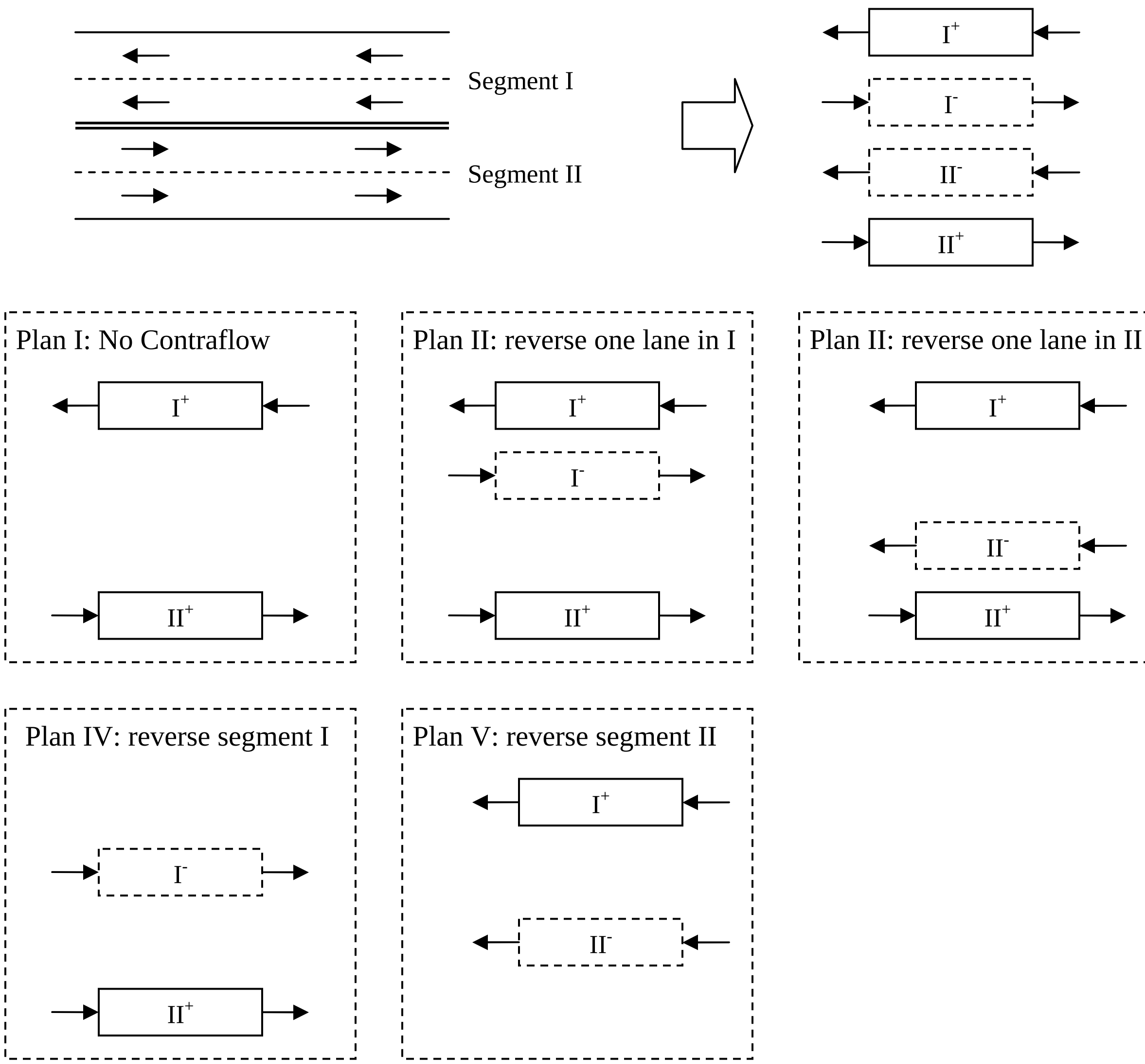


Figure 4-6: Illustration of the network transformation in the Extended Model-I

When applying the extended model-I to design contraflow strategies in emergency evacuation scenarios, system users can easily exclude some of the above five alternatives and thus reduce the size of the elaborated network. For example, safe-bound lanes on those major evacuation corridors will not be reversed.

Additional Constraints in the Extended Model-I

Based on the illustration in Figure 4.8, one can formulate the flow capacity of each cell in the Extended Model-I with Equations 4.23-4.24. The storage capacity of each cell can be formulated in a similar manner. These capacity parameters will be substituted into the network flow constraints 4.13-4.19 of the Base Model, instead of those fixed capacities.

$$Q_{i^+}^t = \sum_{\ln \in LN(i)} Q_{\ln}^+(t) \cdot (1-\delta_{\ln}) \tag{4.23}$$

$$Q_{i^-}^t = \sum_{\ln \in LN(i)} Q_{\ln}^-(t) \cdot \delta_{\ln} \tag{4.24}$$

where $i^+$, $i^-$ are index of the normal and reversed cell for segment $i$; $Q_{i^+}^t$, $Q_{i^-}^t$ are flow capacity (the number of vehicles that can flow in/out) of cell $i^+$, $i^-$ during time interval *t*; $Q_{\ln}^+(t)$, $Q_{\ln}^-(t)$ are capacity of lane $ln$ at time *t* if the lane is in normal direction or reversed; $\ln : \ln \in LN(i)$ is the index of lanes on segment $i$ (ranked from the left most lane); $\delta_{\ln}$ is a binary variable, which equals one if lane $ln$ is reversed and equals zero otherwise.

In addition, Equations 4.25 and 4.26 defines two types of logical relations for lane-reversal decisions.

$$\delta_{\ln} \geq \delta_{\ln'} : \quad \ln \leq \ln', \quad \ln, \ln' \in LN(i) \tag{4.25}$$

$$\delta_{\ln} + \delta_{\ln'} \leq 1 : \quad \ln = 1 \in LN(i), \quad \ln' = 1 \in LN(j) \tag{4.26}$$

where Equation 4.25 defines the logical relations for reversing different lanes in the same segment. In other words, if a segment has multiple lanes traveling in the same direction, operators always have to reverse those lanes on the left first. This equation requires the index of lanes on a segment starting with 1 from the leftmost lane. Equation 4.26 defines the logical relations for reversing lanes in the paired segments $i$ and $j$, i.e., paired segments cannot be reversed concurrently.

Note that if system operators have specified the time $CI_i$ for clearing a reversed segment $i$, the model will change the reversed lane capacity $Q_{\text{ln}}^{-}(t)$ to zero before interval $CI_i$ for any lane on the segment. The model can also include additional constraints on the contraflow plans, such as keeping certain lanes in the danger-bound direction, which is essential for some traffic to get back to the evacuation zone if needed (e.g., for public transit vehicles to pick up non-motorized populations or for emergency response personnel to enforce the operations).

### 4.4.4 Numerical Test of the Extended Model-I

The numerical test in this section is designed mainly for two purposes: 1) to demonstrate the applicability of Extended Model-I for identifying appropriate contraflow strategies in a real-world evacuation network, and 2) to evaluate the effectiveness of the optimization model by comparing the optimal control plan with current plans developed by the responsible agency.

The study network is also the Ocean City hurricane evacuation network as given in Section 4.3. In design of the contraflow strategy, the right lane on US50 eastbound has to remain in its normal direction for potential traffic heading to Ocean City for some justifiable reasons. As mainly for illustration, the results for this numerical test are grounded on the following assumptions.

- It takes 30 minutes to clear the normal traffic on travel lanes before they could be reversed for evacuation flows. Thus, the capacity of reversed lanes is set as zero within 30 minutes of the evacuation start time.
- Resource limit is represented with constraints on the total length of reversed segments.
- Vehicle speed under free flow conditions is equal to the speed limit on reversed lanes.

For the constraints of different reversed lengths, Table 4.2 shows the contraflow plan, the maximal throughput over a 4-hour period generated from the high-level optimization process (without demand constraints), and the clearance time for a total demand of 25,000 vehicles from the low-level optimization results.

Table 4-2: Contraflow Plans under Both Levels of Optimization

| Total length of reversed segments allowed (km) | Reversed segments | High Level: Maximal throughput over 4 hours | Low Level: Evacuation clearance time for 25,000 vehicles |
|---|---|---|---|
| 0 | - | 27,268 | 3.70 |
| 32 | MD90 until US50 | 31,436 | 3.29 |
| 40 | MD90 until US113; US50 between US113 and MD346; US50 after MD90 | 33,672 | 3.11 |
| 48 | MD90 until US50; US50 after MD90 | 33,780 | 3.10 |
| 52 | MD90 until US50; US50 before US113; US50 after MD90; | 36,900 | 2.90 |

Note that extending the currently reversed lane may not always be the best alternative for the entire operations if the resources for such operations have been increased. Instead, one shall redesign the location and length for reverse-lane operations under the available resources so as to maximize its incremental benefits. For example, if the resources allow the length of reversed segments to be 40km instead of 32km, the previously selected segment between US113 and US50 for reverse-lane operation shall be replaced with two other segments (US50 between US113 and MD346, and US50 after MD90) in the new contraflow plan.

The numerical test then compares the following two evacuation control plans with a microscopic CORSIM simulator. The major control strategies of each plan are listed in Tables 4.3 and 4.4, whereas the performance measurements are shown in Table 4.5.

- Plan 1: the final evacuation plan generated with Extended Model-I where MD90 eastbound lane has been reversed
- Plan 2: the evacuation plan from a previous simulation-based project where MD90 eastbound lane has been reversed

Table 4-3: Diverging Rate for Contraflow Plans 1 and 2

| Candidate Evacuation Routes | | Plan 1 | Plan 2 |
|---|---|---|---|
| Ocean City | To DE54 | 17.22 % | 16.5% |
| | To MD90 | 47.10 % | 41.8% |
| | To US50 | 35.67 % | 41.7% |

Table 4-4: Turning Fractions for Contraflow Plans 1 and 2

| Critical Control Points | | Plan 1 | Plan 2 |
|---|---|---|---|
| From MD90 | To US113N | 0.05 (0-180min)<br>0 (181-240min) | 0.075 |
| | To US113S | 0.20 (0-60min)<br>0.15 (61-180min)<br>1 (181-240min) | 0.425 |
| From US50 | To US113N | 0 | 0.1 |
| | To US113S | 0.50 (first 180min)<br>1 (last 60min) | 0.2 |
| | To MD346 | 0.65 | 0.2 |
| From US113N | To MD90 | 0 | 0 |
| From US113S | To US50 | 0.6 | 0.1 |

Table 4-5:Performance Measures for Contraflow Plans 1 and 2

| | Plan 1 | | | Plan 2 | | |
|---|---|---|---|---|---|---|
| Throughput over Time (vehicles) | To Salisbury | To US113 N | To US113 S | To Salisbury | To US113 N | To US113 S |
| By 0.5 hr | 19 | 139 | 394 | 13 | 166 | 330 |
| By 1 hr | 1800 | 1122 | 1586 | 1722 | 1359 | 1434 |
| By 1.5 hr | 4653 | 2191 | 2823 | 4074 | 2652 | 2542 |
| By 2 hr | 7536 | 3117 | 3880 | 6450 | 3875 | 3614 |
| By 2.5 hr | 10393 | 4111 | 5036 | 8846 | 5070 | 4685 |
| By 3 hr | 13287 | 4890 | 5182 | 11197 | 5909 | 5550 |
| By 3.5 hr | 14860 | 4923 | 5216 | 13482 | 5916 | 5550 |
| Clearance Time | 3.50 hr | | | 3.53 hr | | |
| Average Speed | 59.2 km/hr | | | 53.6 km/hr | | |

Comparison of these two plans with the same contraflow designs indicates that the plan generated with the Extended Model-I outperforms the simulation-based plan, which are designed by the collective efforts of local experts through a large number of try-and-error experimental simulation runs. Hence, the proposed model can substantially reduce the required knowledge and efforts at the planning stage.

# Chapter 5

# Signal Optimization for Evacuation Corridors

## 5.1. Introduction

This chapter presents the formulations for design of signal control strategies for designated evacuation corridors. As identified in Chapter 2, existing studies on this regard are quite limited and mostly along the following two lines: a simplified preset control system regardless of the actual demand, or a standardized signal practice with a pre-specified high demand to represent the actual evacuation volumes. Unfortunately, neither approach can adequately address the various operational complexities associated with emergency evacuations. For instance,

- Arterial evacuation operations usually aim at maximizing the throughput, which justifies the use of a limited number of access points to reduce the disturbance of side street traffic to the arterial progression.
- The selected access points should provide a protected green phase to the minor street traffic so as to avoid gap-acceptance based turnings, which is especially dangerous under the oversaturated and stressful evacuation scenarios.
- Since vehicles from minor streets are supposed to enter arterials at selected access points, it is imperative to provide effective routing strategies to guide evacuees from each evacuation origin to those access points via proper local streets.

In response to the aforementioned challenges during emergency evacuations, this chapter proposes two sets of formulations for design of signal control strategies. The base model, presented in Section 5.2, is for an individually operated corridor that typically consists of one major arterial along the evacuation direction. Such an arterial receives evacuation traffic directly from nearby original nodes via local networks, while vehicles after moving onto the arterial will proceed along the arterial until reaching the safe zone. Section 5.3, as an extension, presents the model for more complex situations with several corridors operated integrally. These corridors, as major arterials heading to safe destinations, may exchange traffic flows via connectors so as to avoid local bottlenecks. Note that the grouping of corridors is available from the traffic routing plan at the network level.

Both signal optimization models proposed in this chapter features the use of critical intersection concept, that is, only key intersections will offer protective phases for vehicles from minor streets to turn onto arterials. The proposed core concept intends to reduce the disturbance of side street traffic to the arterial flow progression. With an effective signal control system, the main evacuation arterial should be capable of progressively moving its assigned traffic flows without incurring excessive delay on those waiting at minor streets for joining the evacuation.

Both Sections 5.2 and 5.3 will start with a presentation of model formulations in detail with emphases on the selection of control objectives and identification of various operational constraints, followed by a numerical study to demonstrate the overall effectiveness. The last section summarizes the research efforts in this chapter.

## 5.2. Signal Optimization for a Corridor Operated independently

This section proposes a signal optimization model for individual corridor evacuation using the concept of critical intersections. Such a corridor is typically one major arterial along the evacuation direction, with its side streets connecting to some original nodes. Vehicles, after traveling from their origins to the accessible side street(s) at critical intersections, will turn onto the arterial and proceed until reaching the safe zone. The proposed model is expected to help users concurrently perform the following tasks:

- Select a set of critical intersections;
- Assign demand to critical intersections based on the network topology; and
- Design signal timing plans at critical intersections.

### 5.2.1 Model formulations

To facilitate the presentation of model formulations, Table 5.1 summarizes the notations of major parameters and decision variables used in this section.

Table 5-1: Notations of Parameters and Decision Variables for Signal Optimization on an Independently Operated Corridor

| Parameters | |
|---|---|
| $\Delta t$ | Update interval of system status |
| $T$ | Time horizon of the study (unit: no. of $\Delta t$) |
| $CT$ | Evacuation clearance time (unit: no. of $\Delta t$) |
| $s$ | The evacuation destination at the end of the evacuation corridor |
| $S_r$ | Set of origins |
| $S_I$ , $S_w$ | Set of arterial links and set of side streets |
| $S_m$ | Set of intersections |
| $d_r^t, r \in S_r$ | Demand generated at origin *r* during interval *t* |
| $S_w^r, r \in S_r$ | Set of side streets for traffic from origin *r* to enter the major arterial |
| $\Omega_r, r \in S_r$ | Max no. of alternative side streets evacuees from origin *r* can choose |
| $l_i, i \in S_I$ | Length of link *i*, *l*=physical length/speed (unit: no. of $\Delta t$); |
| $N_i, i \in S_I$ | Storage capacity of link *i*, *N*=jam density$\times$no. of lanes$\times$physical length (unit: veh); |
| $Q_i, i \in S_I \cup S_w$ | Flow capacity of link *i*, *Q*=saturation flow rate$\times$no. of lanes$\times \Delta t$ (unit: veh) |
| $AD_{rw}, w \in S_w^r$ | Delay for traveling from origin *r* to side street *w* (unit: no. of $\Delta t$); |

| | |
|---|---|
| $ST_m, m \in S_m$ | Set of side streets at intersection *m* |
| $u_m, m \in S_m$ | Index of the upstream arterial link of intersection $m$; |
| $g_m^{\min}, m \in S_m$ | Preset minimal green time for arterial green phase at intersection *m* |
| $\hat{g}_m^{\min}, m \in S_m$ | Preset minimal green time for side street green phase at intersection *m* if it is a critical intersection |
| $rd_m, m \in S_m$ | Preset all-red time for intersection *m* if it is a critical intersection |
| $\gamma_m^t, m \in S_m$ | Binary variable. $\gamma_m^t = 1$ if interval *t* is arterial green phase at intersection *m*; |
| $\hat{\gamma}_m^t, m \in S_m$ | Binary variable. $\hat{\gamma}_m^t = 1$ if interval *t* is side street green phase at intersection *m* |
| $\infty$ | A large positive number |
| $x_i^t$ | No. of vehicles on link *i* at the beginning of interval *t*; |
| $y_{ij}^t$ | No. of vehicles traveling from link *i* to link *j* during interval *t*; |
| Decision Variables | |
| $\delta_m, m \in S_m$ | Binary variables. $\delta_m = 1$ if intersection *m* is critical intersection |
| $C$ | Cycle length on the major arterial (unit: no. of $\Delta t$); |
| $g_m, m \in S_m$ | Arterial green time of intersection *m* (unit: no. of $\Delta t$). |
| $\Delta_m, m \in S_m$ | Offset of intersection *m* (Unit: no. of $\Delta t$); |
| $\theta_{rw}, w \in S_w^r$ | Binary variable. $\theta_{rw} = 1$ if some demand from origin *r* go to side street $w$. |

Objective Functions

Given the time window $T$ during an emergency evacuation, the primary objective of traffic operators shall be to maximize the total throughput, i.e., the total number of evacuees that can get out of the hazardous area via the evacuation arterial. Since this throughput is equal to the total number of vehicles entering the target destination, it can be formulated as Equation 5.1.

$$\max \qquad x_s^{T+1} = \sum_{t=1}^{T} y_{\Gamma(s),s}^{t} \tag{5.1}$$

Where $\Gamma(s)$ is the upstream link of the destination $s$.

However, if the evacuation time window $T$ is sufficiently long for all evacuees to get out of the hazardous area, control objective shall be set to minimize the evacuation clearance time, and be formulated as follows.

$$\begin{aligned} &\min \qquad CT \\ &s.t. \qquad x_s^{CT+1} = \sum_{r \in S_r} \sum_{t=1}^{T} d_r(t), \qquad CT \le T \end{aligned} \tag{5.2}$$

Note that as reported in the literature, maximizing throughput on the main evacuation arterial can cause long queue and delay for side street traffic, and thus may result in some evacuees' inobservance of the intersection control. In view of such a concern, the proposed model consists of a supplemental objective, which is to optimally control the difference in the service level among different locations in the evacuation network.

At the most upstream intersection, one can simply compare the average delay on all approaching links. For each of the other critical intersection $m$, this section proposes to compare the average delay for side street(s) at intersection $m$ with the average delay for all traffic from its upstream intersections. This intends to capture the fact that upstream intersections are closer to the incident site and thus evacuees are more likely to panic and thus have lower tolerance to a long delay. Accordingly, one can formulate the supplemental objective as Equation 5.3.

$$\min \quad \sum_{m=1}\delta_m \sum_{w,w' \in ST_m}\left[\frac{\sum_{t=1}^{T}(x_w^t - \sum_{r\in S_r} y_{rw}^t t)}{\sum_{t=1}^{T}\sum_{r\in S_r} y_{rw}^t} - \frac{\sum_{t=1}^{T}(x_{w'}^t - \sum_{r\in S_r} y_{rw'}^t t)}{\sum_{t=1}^{T}\sum_{r\in S_r} y_{rw'}^t}\right]^2$$

$$+\sum_{m=2}^{M}\delta_m\left[\frac{\sum_{w\in ST_m}\sum_{t=1}^{T}(x_w^t - \sum_{r\in S_r} y_{rw}^t t)}{\sum_{w\in ST_m}\sum_{t=1}^{T}\sum_{r\in S_r} y_{rw}^t}\right.$$

$$\left.-\frac{\sum_{m'=1}^{m-1}\sum_{w\in ST_{m'}}\sum_{t=1}^{T}(x_w^t - \sum_{r\in S_r} y_{rw}^t t)+\sum_{i=1}^{u_m}\sum_{t=1}^{T} x_i^t}{\sum_{m'=1}^{m-1}\sum_{w\in ST_{m'}}\sum_{t=1}^{T}\sum_{r\in S_r} y_{rw}^t}\right]^2 \tag{5.3}$$

where the first term indicates the sum of difference in average delays between each pair of side streets at the most upstream intersection if it is a critical intersection. The second term sums over all other critical intersections the difference in average delays for traffic from side streets and from the arterial to traverse each intersection.

To efficiently contend with the proposed multiple objectives for optimizing arterial control, this study employs the popular Hierarchical Optimization Method (HOM) that allows users to rank the selected objectives in a descending order of importance. Each objective function is then minimized sequentially subject to a constraint that does not allow the minimum for the new function to exceed a prescribed fraction of the minimum of the previous function (Eschenauer et al., 1986; Homburg, 1998).

Network Flow Constraints

The network flow constraints define the temporal and spatial interactions among vehicle flows, including the following dynamic processes.

- Vehicles are generated from and sent out of evacuation origins;

- Vehicles travel via local streets to side streets at critical intersections, and then to downstream evacuation arterial; and
- Vehicles traverse the evacuation arterial to target safety destinations.

This study applies the revised cell transmission concept proposed in Chapter 4 to represent these three processes with three sets of formulations.

- Network flow constraints at origins: Equations 5.4-5.9 summarize the constraints to realistically represent the evacuation flows at all possible origins.

$$\sum_{w \in S_w^r} \theta_{rw} \geq 1, \qquad r \in S_r \tag{5.4}$$

$$\sum_{w \in S_w^r} \theta_{rw} \leq \Omega_r, \qquad r \in S_r \tag{5.5}$$

$$y_{rw}^t \leq \theta_{rw} \times \infty, \qquad w \in S_w^r, \ \ r \in S_r, \ \ t = 1,...,T \tag{5.6}$$

$$\theta_{rw} / \infty \leq \sum_t y_{rw}^t, \qquad w \in S_w^r, \ \ r \in S_r, \ \ t = 1,...,T \tag{5.7}$$

$$\sum_{w \in S_w^r} y_{rw}^t \leq x_r^t, \qquad r \in S_r, \ \ t = 1,...,T \tag{5.8}$$

$$x_r^{t+1} = x_r^t + d_r^t - \sum_{w \in S_w^r} y_{rw}^t, \qquad r \in S_r, \ \ t = 1,...,T \tag{5.9}$$

Here Equations 5.4 and 5.5 indicate that each origin should connect to at least one and at most $\Omega_r$ of its neighboring side streets for dissipating its demand, where the latter constraint is often desirable so as to make the evacuation plan convenient to follow. Equations 5.6-5.8 restrict that there exist some flows between origin $r$ and side street $w$ only if they are connected, and the total outflow from origin $r$ cannot exceed the number of vehicles currently in the origin. Finally, Equation 5.9 defines the flow conservation law at origin $r$, namely, the number of vehicles at the beginning of interval $t+1$ should be equal to the number of vehicles at the beginning of interval $t$ plus demand generated during $t$ and minus the total outgoing flows during $t$.

- Network flow constraints at side streets: Equations 5.10-5.13 summarize the constraints to realistically model the arrivals of vehicles from origins and their departures to downstream links, based on the side street traffic conditions.

$$x_w^{t+1} = x_w^t - \sum_{j\in\Gamma^{-1}(w)} y_{wj}^t, \qquad w \in S_w, \quad t = 1,\ldots, AD_{rw} \tag{5.10}$$

$$x_w^{t+1} = x_w^t + \sum_{r:w\in S_w^r} y_{rw}^{t-AD_{rw}} - \sum_{j\in\Gamma^{-1}(w)} y_{wj}^t, \qquad w \in S_w, \quad t = AD_{rw}+1,\ldots,T \tag{5.11}$$

$$\sum_{r:w\in S_w^r} y_{rw}^t \le Q_w, \qquad w \in S_w, \quad t = 1,\ldots,T \tag{5.12}$$

$$\sum_{j\in\Gamma^{-1}(w)} y_{wj}^t \le \min\{Q_w \hat{\gamma}_{m:w\in ST_m}^t, x_w^t\}, \qquad w \in S_w, t = 1,\ldots,T \tag{5.13}$$

Here the flow conservation equations 5.10-5.11 introduce preset delay $AD_{rw}$ to represent the duration for vehicles to travel from an origin *r* to its neighboring side street $w: w \in S_w^r$. Equation 5.12 states that the total number of vehicles that can enter a side street during each interval cannot exceed the flow capacity of the side street. Note that this study enforces no storage capacity constraints at the side streets so as to model the potentially long queue. Equation 5.13 describes the restriction of side street traffic conditions on the departure of vehicles from a side street to its downstream links, i.e., the total number of vehicles exiting a side street cannot exceed its flow capacity or the number of vehicles currently on the side street.

- Network flow constraints at arterial links as in Equations 5.14-5.16, which intend to capture the movement of vehicles along the arterial links.

$$x_i^{t+1} = x_i^t + \sum_{k\in\Gamma(i)} y_{ki}^t - \sum_{j\in\Gamma^{-1}(i)} y_{ij}^t, \; i \in S_I, t = 1,\ldots,T \tag{5.14}$$

$$\sum_{k\in\Gamma(i)} y_{ki}^t \le \min\{Q_i, N_i / l_i, N_i - x_i^t\}, \; i \in S_I, t = 1,\ldots,T \tag{5.15}$$

$$\sum_{j\in\Gamma^{-1}(i)} y_{ij}^t \le \min\{Q_i \gamma_m^t, N_i / l_i, x_i^{t-l_i+1} - \sum_{j\in\Gamma^{-1}(i)} \sum_{k=t-l_i+1}^{t-1} y_{ij}^k\}, \quad i \in S_I, t = 1,\ldots,T \tag{5.16}$$

Here Equation 5.14 represents the flow conservation law, whereas Equations 5.15-5.16 define the number of vehicles that can enter or exit a link based on its traffic conditions. Note that this study views evacuation destinations as a special type of links on evacuation corridors, which has no outgoing links and has a length of one unit. Thus, Equations 5.14-5.16 can also apply to formulate those vehicles moving into the destination.

Routing to Critical Intersections

This category of constraints defines the sufficient and necessary conditions for an intersection to be defined as a critical intersection. More specifically,

- As the sufficient conditions, Equation 5.17 states that an intersection $m$ is critical ($\delta_m = 1$) if some evacuation traffic has used any side street at the intersection ($\exists w \in ST_m : \theta_{rw} = 1$).

$$\delta_m \geq \theta_{rw:w \in ST_m}, \qquad m \in S_m \tag{5.17}$$

- As the necessary condition, Equation 5.18 requires any critical intersection $m{:}\,\delta_m = 1$ to have at least one side street that has been used by evacuation traffic.

$$\sum_{w \in ST_m} \sum_{r:w \in S_w^r} \theta_{rw} \geq \delta_m, \qquad m \in S_m \tag{5.18}$$

Interrelations between Traffic Control Parameters

Constraints 5.19-5.21 define the following relations between signal timing and control type at each intersection: for a non-critical intersection $m{:}\,\delta_m = 0$, its arterial green time $g_m$ will equal the cycle length $C$, whereas the green time for a critical intersection $m{:}\,\delta_m = 1$ shall always lie between the preset minimal green time $g_m^{\min}$ and the cycle length.

$$g_m \geq g_m^{\min}, \qquad m \in S_m \tag{5.19}$$

$$g_m \geq C - \infty \times \delta_m, \qquad m \in S_m \tag{5.20}$$

$$g_m \leq C - (\hat{g}_m^{\min} + 2 \times rd_m)\delta_m, \qquad m \in S_m \tag{5.21}$$

Besides, Equation 5.22 constrains any offset value to be between zero and the cycle length.

$$\Delta_m \geq 0, \quad \Delta_m < C, \qquad m \in S_m \tag{5.22}$$

Signal Status at Intersection $m$

This set of constraints intends to capture the signal status of intersection $m$ during time interval *t*, which shall include the following relations corresponding to Equations 5.23-5.32:

- The non-critical intersections $m\!:\delta_m = 0$ will always have arterial green phase, or in other words, the binary variable $\gamma_m^t$ will always equal 1 and $\hat{\gamma}_m^t$ will always equal 0.
- For critical intersections $m\!:\delta_m = 1$, the value of $\gamma_m^t$ and $\hat{\gamma}_m^t$ depends on the cycle time *C*, green time $g_m$, offset $\Delta_m$, and all-red time $rd_m$.

$$\gamma_m^t \geq 1 - \delta_m, \qquad m \in S_m \tag{5.23}$$

$$\hat{\gamma}_m^t \leq \delta_m, \qquad m \in S_m \tag{5.24}$$

$$\infty \times \gamma_m^t \geq g_m - \text{mod}(t - \Delta_m - 1, C), \qquad m \in S_m \tag{5.25}$$

$$-\infty \times (1 - \gamma_m^t) < g_m - \text{mod}(t - \Delta_m - 1, C), \qquad m \in S_m \tag{5.26}$$

$$\infty \times \beta_m^t > \text{mod}(t - \Delta_m - 1, C) - g_m - rd_m, \qquad m \in S_m \tag{5.27}$$

$$-\infty \times (1 - \beta_m^t) \leq \text{mod}(t - \Delta_m - 1, C) - g_m - rd_m, \qquad m \in S_m \tag{5.28}$$

$$\infty \times \hat{\beta}_m^t \geq C - rd_m - \text{mod}(t - \Delta_m - 1, C), \qquad m \in S_m \tag{5.29}$$

$$-\infty \times (1-\hat{\beta}_m^t) < C - rd_m - \text{mod}(t - \Delta_m - 1, C), \qquad m \in S_m \tag{5.30}$$

$$\hat{\gamma}_m^t > \beta_m^t + \hat{\beta}_m^t - 2, \qquad m \in S_m \tag{5.31}$$

$$-\infty \times (1-\hat{\gamma}_m^t) \le \beta_m^t + \hat{\beta}_m^t - 2, \qquad m \in S_m \tag{5.32}$$

Note that there are two all-red periods in one cycle. One is between arterial green phase and side street green phase, and the other lies after the side street green phase. Thus this study uses two auxiliary binary variables in Equations 5.27-5.32, where $\beta_m^t = 1$ if interval *t* is after the first all red time and intersection *m* is a critical intersection, and $\hat{\beta}_m^t = 1$ if interval *t* is before the second all red time. Besides, the above formulations use the function $\text{mod}(a,b)$ to return the remainder after dividing $a$ with $b$, which can be replaced with a set of additional constraints.

Other Constraints

To provide a realistic range for the optimized solution, the proposed model also includes nonnegative constraints, initial value of link state variables $x_i^1$, and initial value of flows between links $y_{ij}^0$. In most cases, $x_i^1$ and $y_{ij}^0$ are set to zero for all arterial links and side street links, although $x_i^1$ can be other values to represent the background traffic prior to the evacuation.

### 5.2.2 The Solution Algorithm

The proposed optimization model consists of complex formulations, including binary decision variables as well as nonlinear system constraints. It will generally take a long time to find the global optimal solution. Due to the emergency nature, this study employs a Genetic Algorithm-based heuristic to yield efficient solutions in a relatively short time window for selection of critical intersections and their signal settings.

Note that Genetic Algorithm is a search technique widely used to find near optimal solutions to a variety of real-world large-scale optimization issues. Inspired by evolutionary biology, Genetic Algorithms are typically implemented as a computer simulation in which a population of abstract representations (chromosomes) of candidate solutions (individuals) to an optimization problem evolves toward better solutions. The evolution starts from a population of completely random individuals and proceeds in iterations (generations). In each generation, the fitness of the whole population is evaluated, while multiple individuals are stochastically selected from the current population based on their fitness and modified with mutation or crossover to form a new population for the next generation. (Goldberg, 1988; Ladd, 1996)

Based on the GA method, this study has developed the solution algorithm with Visual C++ language, and encoded the solutions to the proposed MIP model with binary strings of 0s and 1s to capture the selection of critical intersections, demand routing, and signal timing parameters. A step-by-step description of the solution procedures is presented below:

Step 1: Network Data Initialization

Read the following data from a GIS database: 1) timing varying demand for each origin, 2) cell and connector information that defines link properties and the network topology, and 3) intersection information that defines the allowed movements and preset signal control parameters for each signal phase.

Step 2: Initial Solution Generation:

Set the iteration index as 1 and then randomly generate the first population of candidate solutions with binary representations (chromosomes). To improve the computation efficiency, this study has always preset the minimal green plan as one of the initial solutions

Step 3:Fitness Function Evaluation (for each candidate solution)

Step3-1: *Chromosome Decoding*: decode the corresponding chromosome to obtain the real-valued control parameters. The model proposed in this section consists of the following four types of controls: 1) selection of critical intersections and traffic routing decisions from each origin to side streets at critical intersections; 2) the cycle length for intersections along the arterial; 3) arterial green time at each intersection, and 4) offset at each intersection.

It is noticeable that these four control strategies have a special hierarchical relation. The selection of critical intersections affects the signal timings at intersections, i.e., the non-critical intersections always give the green phase to arterial traffic. Thus, the program introduces a gene-activation mechanism in the decoding procedure, which decodes all the high-level controls first and then only decodes those low-level strategies that get activated by the corresponding high-level strategies. Note that all those inactive controls will remain in the chromosome structure and are carried invisibly to the subsequent generations.

Step3-2: *Fitness Computation*: execute a macroscopic simulator based on the revised cell transmission relations after obtaining the real-valued control parameters. During each time interval,

- The simulator will first update each cell status with the connector flows from the previous interval, based on the flow conservation law.
- Based on the updated cell status, the simulator will compute the flows that can move out of each cell.
- The final connector flows between cells are then obtained by taking into account the preset diverging/merging behaviors, the congestion in downstream cells, and the signal phase at intersections.

Note that the fitness function for each candidate solution is first set to maximize the total throughput. Once the algorithm detects the throughput of the solution is equal to the total evacuation demand, the fitness function will automatically change to the minimization of evacuation clearance time. After the optimized throughput or clearance time is found, users can specify the percentage of acceptable loss in these system measurements in order to minimize the difference in the service levels between different locations in the evacuation network. Then, the algorithm will proceed to minimize the third objective function with this additional constraint on the system measurement.

Step 4: Stop Criteria Testing

Exit the algorithm if the number of iterations has reached the preset maximal value, or the best objective function remains unchanged for a preset number of iterations. Otherwise, the algorithm will increase the iteration index by 1 and go to Step 5.

Step 5: Genetic Operators

Run the general genetic operators (selection, crossover and mutation) to generate a new population of candidate solutions based on solutions from the old population. Then the algorithm will turn to Step 3.

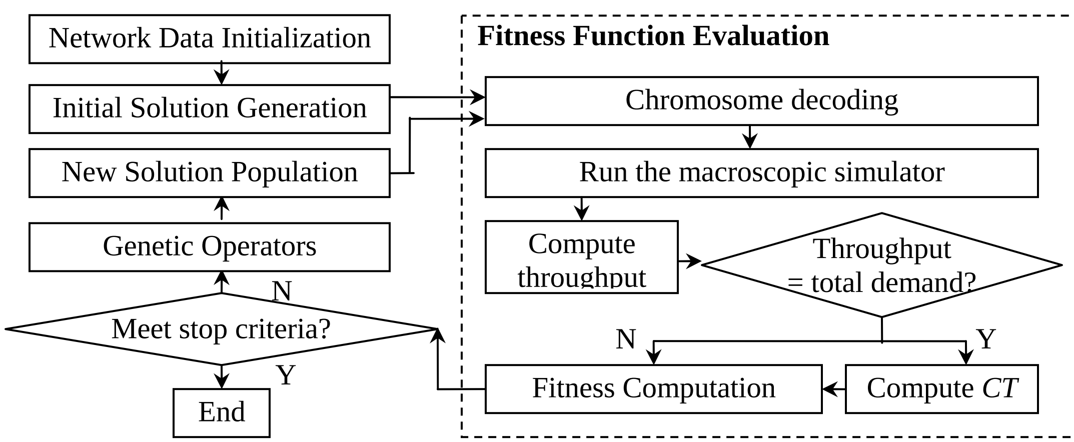


Figure 5-1: Flowchart of the Solution Algorithm for Signal Optimization at the Corridor Level

### 5.2.3 Case Study

Experimental Design

Figure 5.2 presents a target area for numerical experiments, which covers the entire Connecticut Avenue from Washington D.C. to the Capital Beltway. The entire evacuation route starts from the intersection at K Street and ends at the intersection at Chevy Chase Cir. The length of the evacuation corridor is 8km (5 miles), containing a total of 90 origin nodes, 38 signalized intersections, and 24 intersections with stop/yield sign.

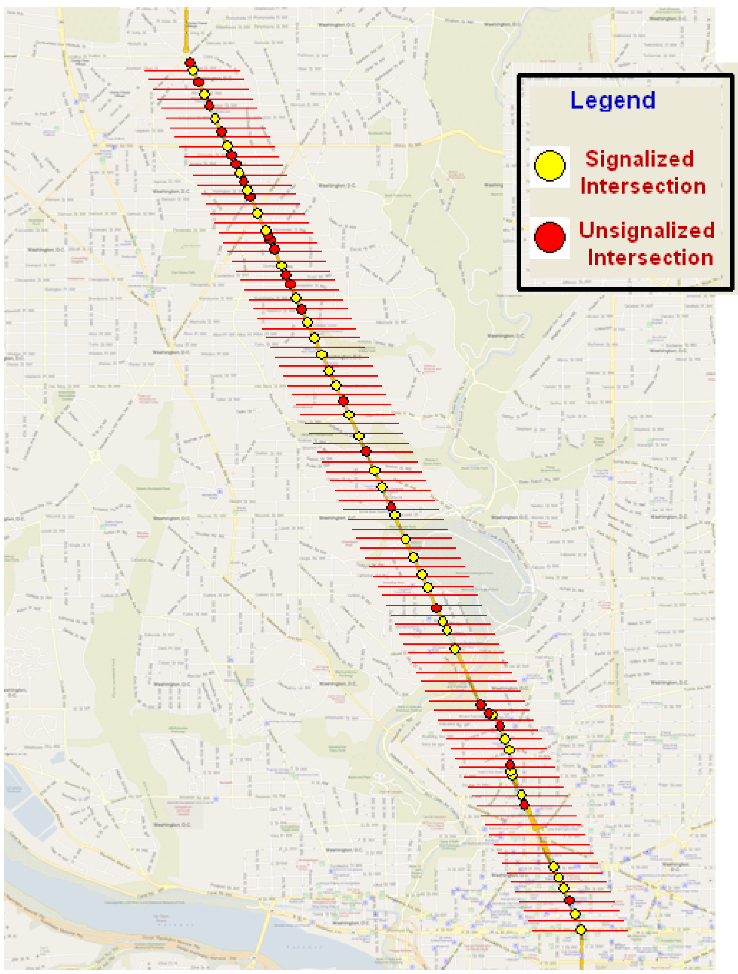


Figure 5-2: An example evacuation eorridor –Connecticut Avenue in Washington, D.C.

To reflect the operational constraints, the application of the signal optimization model is subjected to the following constraints:

- Non-signalized intersections cannot be critical intersections.

- Cycle time will be within a range of 60 to 300 seconds

- Evacuation demand can be directed to any of its downstream critical intersections.

To test the effectiveness of the proposed model with respect to total throughput and the evacuation clearance time, this study has designed different demand scenarios for experimental analysis.

- Scenarios I-1 and I-2 intend to represent the relatively heavy demand condition under which population cannot be evacuated within the period of 2 hours, where Scenario I-1 has more demand concentrated at the arterial upstream than Scenario I-2.

- Scenarios II-1 and II-2 present those arterials with moderate evacuation demand, which can be cleared within 2 hours of operations. Similarly, Scenario II-1 has more demand concentrated at the arterial upstream than Scenario II-2.

. Experimental Results

To show the effectiveness of the proposed model in design of arterial control strategies during emergency evacuations, this paper employs a pre-calibrated CORSIM simulator to compare the control strategies generated from the model with two state-of-art traffic signal plans for evacuation, which are:

- Yellow-Flash Plan: All signalized intersections will give the arterial traffic a yellow-flash phase and the side streets a red-flash phase.

- Minimal-Green Plan: All signalized intersections will have a cycle time of 300 seconds while side street traffic only receive the minimal green time of 10 seconds.

The evaluation results with simulation experiments are organized as follows, where all the indices for comparison are directly extracted from the CORSIM simulation output files:

- Comparing the throughput and/or evacuation clearance time of Yellow Flash Plan and Minimal Green Plan with those of the optimized control strategy that does not restrict the difference in the service level (i.e. have no delay balance considerations) under each demand scenario;

- Presenting throughput and/or evacuation clearance time of the optimized control strategy that intends to restrict the difference in the service level for balanced delay under each demand scenario;

- Comparing the average delay and maximal delay of the Yellow-Flash Plan and Minimal-Green Plan with those two different optimized control strategies.

Table 5.2 and Table 5.3 show the comparison results under Demand Scenarios I and II, whereas the optimized control strategy does not account for the delay balance consideration. These tables have clearly indicated that the optimized arterial control plans outperform those two widely used signal plans in all demand scenarios, and the effectiveness varies with the demand distribution

Table 5-2: Throughput comparison under Demand Scenario I without the secondary objective of delay balance

| Throughput (no. of Vehicles) | Yellow Flash Plan | Min-Green Plan | Optimized Plan |
|---|---|---|---|
| Demand Scenario I-1 | 9102 | 9494 | 9624 |
| Demand Scenario I-2 | 8618 | 9304 | 10624 |

Table 5-3: Throughput Comparison under Demand Scenario II
Without the Secondary Objective of Delay Balance

| Clearance Time (min) | Yellow Flash Plan | Min-Green Plan | Optimized Plan |
|---|---|---|---|
| Demand Scenario I-1 | 120 | 100 | 94 |
| Demand Scenario I-2 | 133 | 120 | 100 |

Table 5.4 presents the simulated throughput and/or evacuation clearance time for the optimized control strategy that takes into account Objective 5.3 with a ten percent of acceptable loss in the optimized throughput or clearance time (as in Table 5.2 and Table 5.3) under the two different demand scenarios.

Table 5-4: Simulated throughput of the optimized plan
with the secondary objective of delay balance

| Demand Scenario | Scenario I-1 | Scenario II-1 |
|---|---|---|
| Throughput in 2hr (no. of Vehicles) | 9378 | 8880 |
| Clearance Time (min) | N/A | 98 |

Comparing Table 5.4 with Table 5.2 and Table 5.3, one can identify that the optimized plan with delay balance consideration may lead to a lower throughput or a longer clearance time. However, the power of these optimized plans is clearly indicated in Table 5.5 and Table 5.6. Table 5.5 presents the averaged delay of the four control plans under Demand Scenario II, whereas Table 5.6 presents the maximal delay among all side streets at critical intersections for those two optimized control plans with or without delay balance consideration under both demand scenarios.

Table 5-5: Average Delay under Demand Scenario II-1

| Control Plan | Yell Flash Plan | Min-Green Plan | Optimized without the Secondary Objective of Delay Balance | Optimized with the Secondary Objective of Delay Balance |
|---|---|---|---|---|
| Average Delay (min) | 20.8 | 19.0 | 17.0 | 14.2 |

Table 5-6: Maximal Delay at Side Streets (Unit: min)

| Control Plan | Demand Scenario I-1 | Demand Scenario II-2 |
|---|---|---|
| Optimized without Secondary Objective of Delay Balance | 61.6 | 40.9 |
| Optimized with Secondary Objective of Delay Balance | 49.2 | 36.0 |
| Improvement with Secondary Objective of Delay Balance | 20.1% | 12.0% |

Table 5.5 and Table 5.6 have indicated that the optimized control plans with delay balance consideration did help the side street traffic but at the price of reduced system throughput or increased evacuation clearance time.

## 5.3 Signal Optimization for Corridors Operated as an Integrated Network

As an extension of Section 5.2, this section proposes a signal optimization model for more complex evacuation networks with multiple corridors operated as an integrated network. Such networks typically contain the following four types of roads: 1) major arterials as the evacuation corridors heading to the safe destinations; 2) connectors that link neighboring corridors; 3) side streets that receive evacuation traffic from original nodes and send them to corridors/connectors; and 4) local streets connecting the original nodes and the side streets. The proposed model is expected to help users concurrently perform the following tasks:

- Select a set of critical intersections;

- Assign demand to critical intersections based on the network topology;

- Design the signal timing plans at critical intersections; and

- Route traffic between corridors via connectors, if necessary, to balance traffic volumes between different corridors.

### 5.3.1 Model formulations

To facilitate the presentation of model formulations, Table 5.7 summarizes the notations of major parameters and decision variables used in this section.

Table 5-7: Notations of parameters and decision variables: signal optimization for corridors operated integrally

| | |
|---|---|
| $\Delta t$ | Update interval of system status |
| $T$ | Time horizon of the study (unit: no. of $\Delta t$) |
| $CT$ | Evacuation clearance time (unit: no. of $\Delta t$) |
| $S_r$, $S_s$ | Set of original nodes and evacuation destinations |
| $S_a$ | Set of corridors/connection streets |
| $S_m$ | Set of intersections |
| $S_m^a, a \in S_a$ | Set of intersections on corridor/ connector *a*. The sets are mutually exclusive, and an intersection where connectors meet corridors is defined belong to the corridor. |

| | |
|---|---|
| $S_I$ | Set of links on corridors/connectors |
| $S_w$ | Set of side streets |
| $S_w^r, r \in S_r$ | Set of side streets for traffic from origin *r* to enter a corridor or a connector |
| $d_r^t, r \in S_r$ | Demand generated at origin *r* during interval *t* |
| $\Omega_r, r \in S_r$ | The maximal no. of alternative side streets that evacuees from origin *r* can choose |
| $U_m, m \in S_m$ | Set of upstream links on major roads at intersection *m* |
| $UT_m, m \in S_m$ | Set of side streets and/or upstream links on minor roads at intersection *m* |
| $g_m^{\min}, m \in S_m$ | Preset minimal green time for major-road green phase at intersection *m* |
| $\hat{g}_m^{\min}, m \in S_m$ | Preset minimal green time for minor-road green phase at intersection *m* if the intersection is a critical intersection |
| $rd_m, m \in S_m$ | Preset all-red time for intersection *m* if the intersection is a critical intersection |
| $\gamma_m^t, m \in S_m$ | Binary variable. $\gamma_m^t = 1$ if interval *t* is major-road green phase at intersection *m* |
| $\hat{\gamma}_m^t, m \in S_m$ | Binary variable. $\hat{\gamma}_m^t = 1$ if interval *t* is minor-road green phase at intersection *m* |
| $l_i, i \in S_I$ | Length of link *i*, *l*=physical length/speed (unit: no. of $\Delta t$); |
| $N_i, i \in S_I$ | Storage capacity of link *i*, *N*=jam density$\times$no. of lanes$\times$physical length (unit: vehicles); |
| $Q_i, i \in S_I \cup S_w$ | Flow capacity of link *i*, *Q*=saturation flow rate$\times$no. of lanes$\times \Delta t$ (unit: vehicles) |
| $\eta_i, i \in S_I \cup S_w$ | Binary variable. $\eta_i = 1$ if link *i* has been used by any evacuation traffic |

| | |
|---|---|
| $AD_{rw}, w \in S_w^r$ | Delay for traveling from origin *r* to side street *w* (unit: no. of $\Delta t$); |
| $\infty$ | A very large positive number |
| $x_i^t$ | No. of vehicles on link *i* at the beginning of interval *t*; |
| $y_{ij}^t$ | No. of vehicles traveling from link *i* to link *j* during interval *t*; |
| Decision Variables | |
| $\delta_m, m \in S_m$ | Binary variables. $\delta_m = 1$ if intersection *m* is critical intersection |
| $C_a, a \in S_a$ | Cycle length on corridor/connector *a* (unit: no. of $\Delta t$); |
| $g_m, m \in S_m$ | Main-road green time of intersection *m* (unit: no. of $\Delta t$). |
| $\Delta_m, m \in S_m$ | Offset of intersection *m* (Unit: no. of $\Delta t$); |
| $\theta_{rw}, w \in S_w^r$ | Binary variable. $\theta_{rw} = 1$ if some demand from origin *r* is diverted to side street *w*. |

Note that this section assumes the use of a two-phase signal control at critical intersections, which include a green phase for major road and a green phase for minor road. Here major road and minor road are defined as below:

- At an intersection where an evacuation corridor meets connectors and/or side streets, main road refers to the evacuation corridor and minor road refers to connectors and/or side streets
- At an intersection where a connector meets side streets, main road refers to the connector and minor road refers to side streets.

Objective Functions

This study is focused mainly on improving the efficiency of the entire evacuation process, which may vary with the selected control objectives such as maximization of throughput, minimization of clearance time, minimization of average trip time, and minimization of fatality. The proposed model in this section suggests the use of the clearance time minimization or throughput maximization as the control objective, depending on the length of the safety time window. More specifically,

- If the time window is sufficiently long for all evacuees to reach the safety destinations, the control objective shall be to minimize the evacuation clearance time, $CT$ , as in Equation 5.33.

$$\begin{aligned} &\min \quad CT \\ &s.t. \quad \sum_{i \in S_s} x_i^{CT+1} = \sum_{r \in S_r} \sum_{t=1}^{T} d_r^t, \qquad CT \le T \end{aligned} \tag{5.33}$$

- If the evacuation process cannot be completed within the given time window, the control objective would be to maximize the total throughput $\sum_{i \in S_s} x_i^{T+1}$ , where $x_i^{T+1}, i \in S_s$ is the total number of evacuees that have arrived at destination *i* by time *T*.

$$\max \quad \sum_{i \in S_s} x_i^{T+1} \tag{5.34}$$

To realistically capture the complex interrelations among network flows so as to design critical intersections and signal timing plans, the proposed model in this section formulates the following six major categories of constraints.

Network Flow Constraints

The network flow constraints define the temporal and spatial interactions among vehicle flows, including the following dynamic process:

- Vehicles are generated from and sent out of the evacuation origins;

- Vehicles travel via local streets to the side streets at critical intersections, and then to the downstream evacuation corridors or connectors; and

- Vehicles traverse connectors and evacuation corridors to target safety destinations.

Accordingly, this section applies the generalized cell transmission concept to generate the following three groups of constraints.

- The constraints to represent the evacuation flows at all possible origins are the same as Equations 5.4-5.9 proposed for signal optimization for a corridor operated individually.

- The constraints to capture the network flow evolution at side streets are similar to Equations 5.10-5.13, except that the flow conservation equation 5.13 is modified as in Equation 5.35. The binary variable $\hat{\gamma}_m^t, m \in S_m$ is removed from the equation, and its impact on side street flows will be defined separately to account for the more complex network with connectors.

$$\sum_{j \in \Gamma^{-1}(w)} y_{wj}^t \le \min\{Q_w, x_w^t\}, \qquad w \in S_w, t = 1,...,T \tag{5.35}$$

- The constraints to capture the movement of vehicles along the corridor or connectors are also similar to Equations 5.14-5.16, except that the flow conservation equation 5.16 is modified as in Equation 5.36. The binary variable $\gamma_m^t, m \in S_m$ is removed from the equation, and its impact on traffic flows from the upstream arterial links will be defined separately to account for the more complex network with connectors.

$$\sum_{j \in \Gamma^{-1}(i)} y_{ij}^t \le \min\{Q_i, N_i / l_i, x_i^{t-l_i+1} - \sum_{j \in \Gamma^{-1}(i)} \sum_{k=t-l_i+1}^{t-1} y_{ij}^k\} \qquad i \in S_I, t = 1,...,T \tag{5.36}$$

Definition of Critical Intersections

This category of constraints defines the sufficient and necessary conditions for a critical intersection. Since the evacuation network now involves intersections between arterials and connectors, the decision of critical intersections will depend not only on the side street traffic conditions as in Equations 5.17 and 5.18, but also on traffic flows from connectors. Thus, a link usage parameter $\eta_i$ is introduced to indicate if a connector link has been used by evacuation traffic or not, as shown in the following Equations 5.37-5.38.

$$x_i^t \leq \infty \times \eta_i, \qquad i \in S_I \cap UT_m, m \in S_m \tag{5.37}$$

$$\eta_i / \infty \leq \sum_t x_i^t, \qquad i \in S_I \cap UT_m, m \in S_m \tag{5.38}$$

With help of this link usage parameter, Equations 5.39-5.40 state that an intersection is operated as critical intersection if some evacuation traffic has used any minor roads upstream to the intersection, which could be either side streets or links on connectors.

$$\delta_m \geq \theta_{rw}, \qquad \forall r, w : w \in S_w \cap UT_m, m \in S_m \tag{5.39}$$

$$\delta_m \geq \eta_i, \qquad \forall i : i \in S_I \cap UT_m, m \in S_m \tag{5.40}$$

Besides, Equation 5.41 requires any critical intersection to have at least one minor road at its upstream that has been used by evacuation traffic.

$$\sum_{w \in S_w \cap UT_m} \sum_{r : w \in S_w^r} \theta_{rw} + \sum_{i \in S_I \cap UT_m} \eta_i \geq \delta_m, m \in S_m \tag{5.41}$$

Consistency between Intersection Type and Signal Timing

With enhanced formulations to address the cycle length difference on different arterials, Equations 5.42-5.45 define the following relations between signal timing and control type at each intersection: the arterial green time at a non-critical intersection ($\delta_m = 0$) will equal its cycle length, whereas a critical intersection ($\delta_m = 1$) shall give its side street(s) a green time at least equal to the preset minimal value. Besides, any offset value will lie between zero and the cycle length.

$$g_m \geq g_m^{\min}, \qquad m \in S_m \tag{5.42}$$

$$g_m \geq C_{a:m \in S_m^a} - \infty \times \delta_m, \qquad m \in S_m \tag{5.43}$$

$$g_m \leq C_{a:m \in S_m^a} - (\hat{g}_m^{\min} + 2 \times rd_m)\delta_m, \qquad m \in S_m \tag{5.44}$$

$$\Delta_m \geq 0, \quad \Delta_m < C_{a:m \in S_m^a}, \qquad m \in S_m \tag{5.45}$$

### 5.3.1.5 Consistency between Signal Timing and Signal Phase at Intersections

Similarly modified to address the difference in cycle length on different arterials, Equations 5.46-5.55 extend the formulations in Section 5.2.1.5 and determine the signal phase of an intersection for any time interval *t* based on its control type and signal timing parameters:

$$\gamma_m^t \geq 1 - \delta_m, \qquad m \in S_m \tag{5.46}$$

$$\hat{\gamma}_m^t \leq \delta_m, \qquad m \in S_m \tag{5.47}$$

$$\infty \times \gamma_m^t \geq g_m - \text{mod}(t - \Delta_m - 1, C_{a:m \in S_m^a}), \qquad m \in S_m \tag{5.48}$$

$$-\infty \times (1 - \gamma_m^t) < g_m - \text{mod}(t - \Delta_m - 1, C_{a:m \in S_m^a}), \qquad m \in S_m \tag{5.49}$$

$$\infty \times \beta_m^t > \text{mod}(t - \Delta_m - 1, C_{a:m \in S_m^a}) - g_m - rd_m, \qquad m \in S_m \tag{5.50}$$

$$-\infty \times (1 - \beta_m^t) \leq \text{mod}(t - \Delta_m - 1, C_{a:m \in S_m^a}) - g_m - rd_m, \quad m \in S_m \tag{5.51}$$

$$\infty \times \hat{\beta}_m^t \geq C_{a:m \in S_m^a} - rd_m - \text{mod}(t - \Delta_m - 1, C_{a:m \in S_m^a}), m \in S_m \tag{5.52}$$

$$-\infty \times (1 - \hat{\beta}_m^t) < C_{a:m \in S_m^a} - rd_m - \text{mod}(t - \Delta_m - 1, C_{a:m \in S_m^a}), m \in S_m \tag{5.53}$$

$$\hat{\gamma}_m^t > \beta_m^t + \hat{\beta}_m^t - 2, \qquad m \in S_m \tag{5.54}$$

$$-\infty \times (1 - \hat{\gamma}_m^t) \le \beta_m^t + \hat{\beta}_m^t - 2, \qquad m \in S_m \tag{5.55}$$

Consistency between Signal Phase and Traffic Flow at Intersections

Equations 5.56-5.57 have constrained the evacuation flows traversing an intersection by the signal phase at the intersection. More specifically, vehicles can exit major roads only during the major road green phases ($\gamma_m^t$ =1). Likewise, vehicles can exit minor roads only during minor road green phases ($\hat{\gamma}_m^t$ =1).

$$\sum_{k \in U_m} \sum_{j \in \Gamma^{-1}(k)} y_{kj}^t \le \infty \times \gamma_m^t, \qquad m \in S_m \tag{5.56}$$

$$\sum_{k \in UT_m} \sum_{j \in \Gamma^{-1}(k)} y_{kj}^t \le \infty \times \hat{\gamma}_m^t, \qquad m \in S_m \tag{5.57}$$

Except for the aforementioned six groups of operational constraints, the proposed model also includes nonnegative constraints, initial value of link state variables $x_i^1$, and initial value of flows between links $y_{ij}^0$ to provide a realistic range for the optimal solution.

### 5.3.2 Case Study

#### 5.3.2.1. Study Network

This section intends to demonstrate the effectiveness of the proposed model by comparing different control plans in a real-world evacuation network as shown in Figure 5.3.

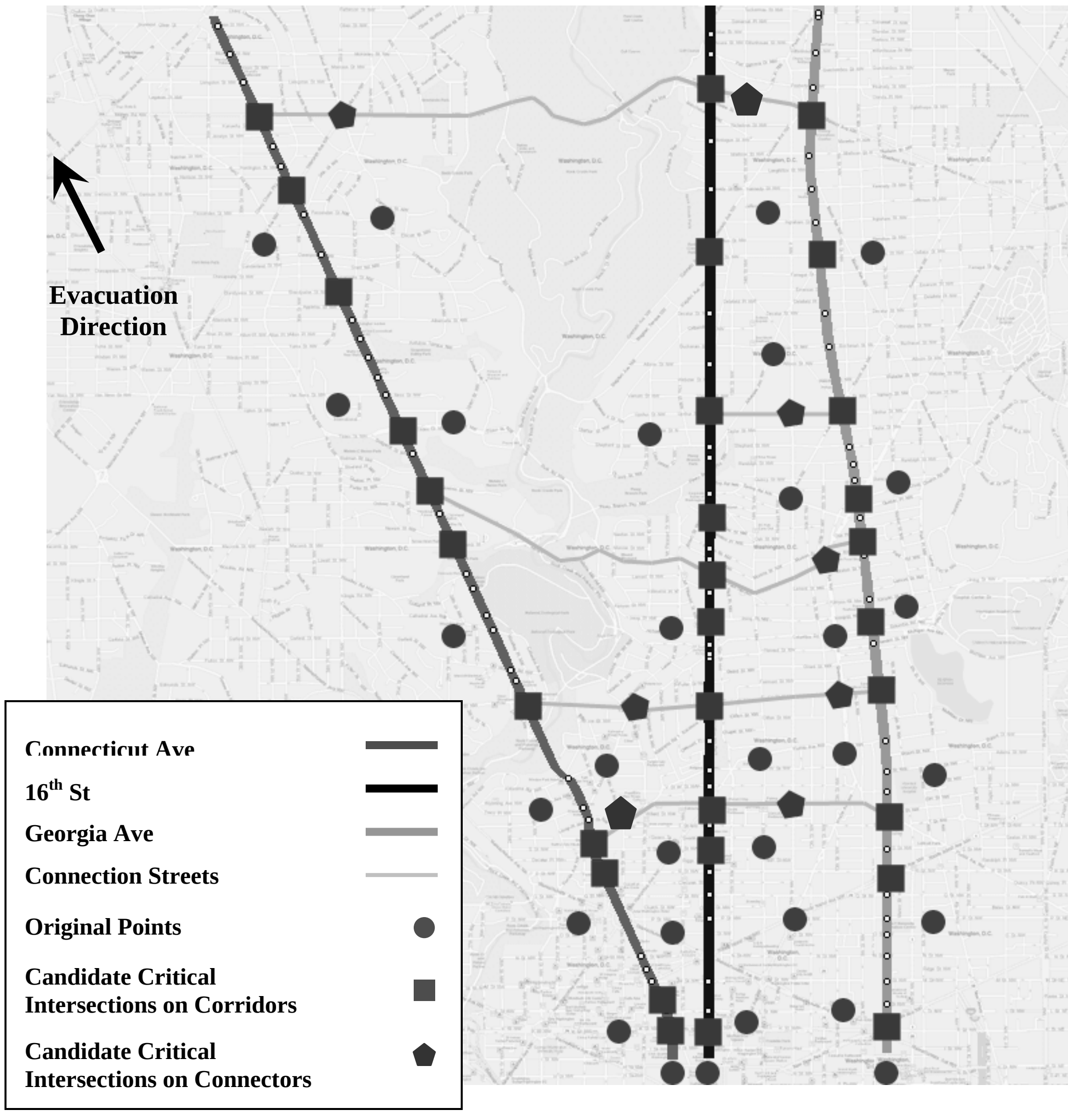


Figure 5-3: Illustration of the study network of multiple corridors

The study network includes three neighboring corridors from the Washington D.C. evacuation network:

- Connecticut Ave from K St. to Chevy Chase Circle. Its number of lanes varies from two to four in the outbound direction. Eleven of its 38 signalized intersections are selected as candidates for critical intersections.

- 16th Street from K St. to Eastern Ave. Its number of lanes varies from two to four in the outbound direction. Ten of its 43 signalized intersections are pre-selected as candidates for critical intersections.

- Georgia Ave from Mt Vernon Pl. to Eastern Ave. Most of its links have only two lanes in the outbound direction. Ten of its 48 signalized intersections are pre-selected as candidates for critical intersections.

The evacuation network also includes five major streets between these corridors as the connectors, on which there are eight intersections that can be chosen as critical intersections. The intersections connecting evacuation corridors and connectors are set as default critical intersections. Besides, the target network includes 31 predefined origins, which connect to nearby candidate critical intersections.

Based on the generalized cell transmission concept, Figure 5.4 has depicted all the origins, side streets at intersections, links in the corridors, and links on the connectors with cells. The arrows between cells represent the actual connections between all these geometric objects. Note that the cells in Figure 5.4 do not necessarily have the same size. Cells for origins and side streets always have the size of one. However, cells for links in the corridors and connectors may have different sizes, which are decided by the physical length of the corresponding link and the travel speed.

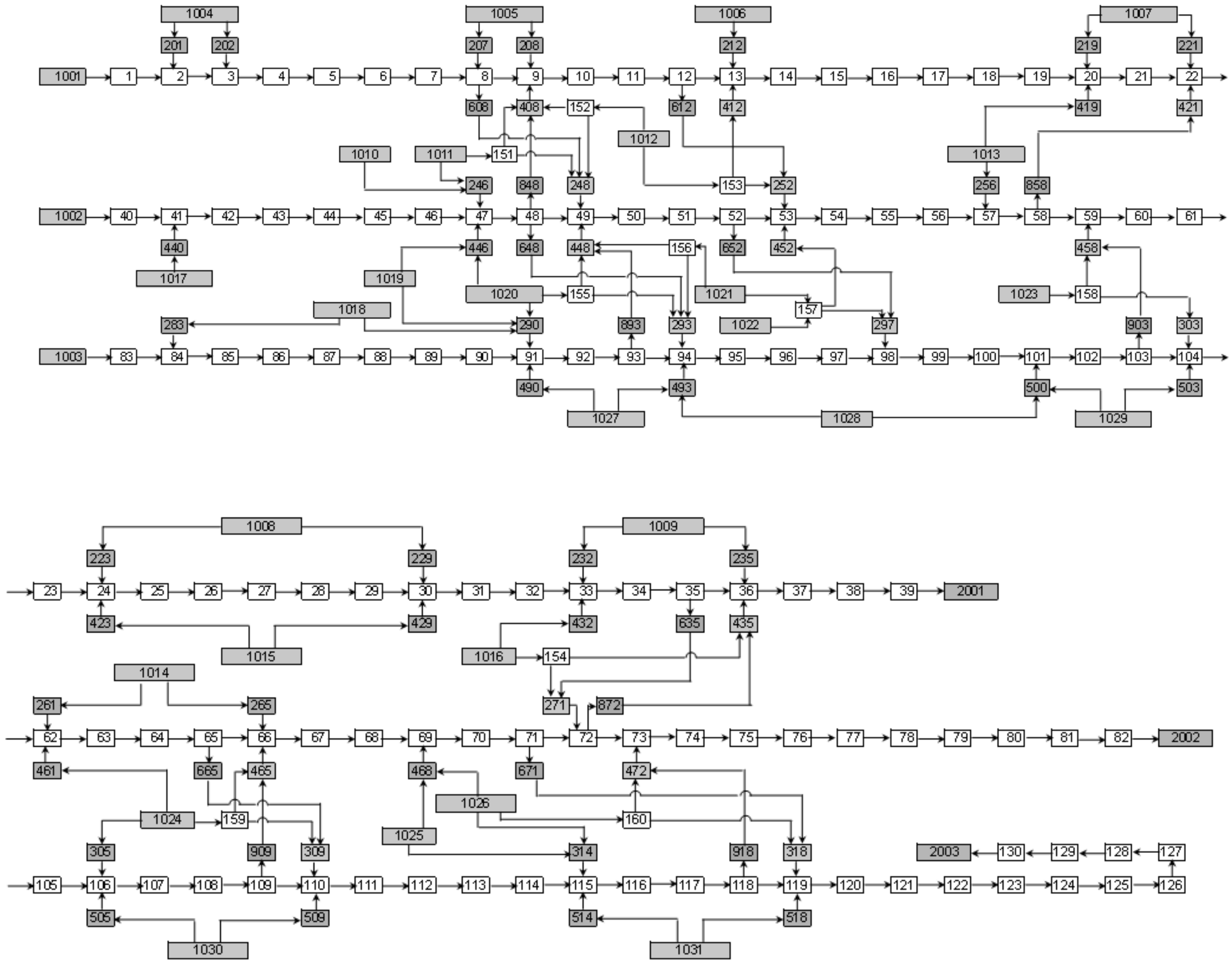


Figure 5.4: A graphical illustration of the cell-transmission network

Control Plans for Comparison

With the example network, this section compares the effectiveness of three plans, which combines different control strategies as shown in Table 5.8. Note that under Plan I and Plan II, each corridor is operated independently. Thus, no movement is allowed to turn from evacuation corridors to connectors, which leads to no through traffic at intersections on the connectors. Plan III offers integrated operations for the three parallel evacuation corridors, allowing traffic to travel between corridors via the connectors.

Table 5-8: Three Control Plans for Multi-Corridor Evacuation

| Control Strategies | | Control Plan I (Minimal Green) | Control Plan II (Individually Operated) | Control Plan III (Integrally Operated) |
|---|---|---|---|---|
| Selection of critical intersections and demand routing from origins | | Optimized | Optimized | Optimized |
| Intersection on corridors | Cycle time | 240s | Optimized | Optimized |
| | Green time for main road (corridor) | 220s | Optimized | Optimized |
| | Green time for minor road (side/connectors) | 10s | Optimized | Optimized |
| Intersection on connectors | Cycle time | 240s | 240s | Optimized |
| | Green time for main road (connectors) | 0s | 0s | Optimized |

| | | | | |
|---|---|---|---|---|
| | Green time for minor road (side streets) | 240s | 240s | Optimized |
| Diverge from corridors to connectors | | N/A | N/A | Optimized |
| Demand from side streets to connectors | | Optimized | Optimized | Optimized |

Those control parameters in each different plan are generated with a Genetic Algorithm based heuristic similar to the one proposed in Section 5.2.2, with the assumptions that each origin can only go to one of its connected critical intersections and the cycle time varies between 100 and 240 seconds. Note that to eliminate impact due to the random nature of the GA heuristic, this study executes the algorithm ten times and pick up the best set of parameters for design of each control plan.

Comparison Results

This section first compares the performance of those three control plans under Demand Scenarios 1-6, as shown in Table 5.9, where the total evacuation demand (17600 vehicles) shifts gradually from the three origins at the upstream of the evacuation corridors to the 28 original nodes specified over the entire network. All these demands will be loaded onto the network during the interval of 30 minutes, based on a logit function.

Table 5.9: Demand Scenarios 1-6 for Multi-Corridor Evacuation

| Scenario / Total Demand from Each Origin (unit: veh) | 1 | 2 | 3 | 4 | 5 | 6 |
|---|---|---|---|---|---|---|
| Origin at the upstream of each evacuation corridor | 5400 | 5120 | 4840 | 4560 | 4280 | 4000 |
| Other minor origin | 50 | 80 | 110 | 140 | 170 | 200 |

With properly designed control parameters, all three plans can help to complete the evacuation process within a three-hour time window under all six demand scenarios. Table 5.10 shows the total evacuation clearance time under different control plans.

Table 5-10: Evacuation Clearance Time under Demand Scenarios 1-6
for Multi-Corridor Evacuation (Unit: seconds)

| Clearance Time | Demand scenario 1 | Demand scenario 2 | Demand scenario 3 | Demand scenario 4 | Demand scenario 5 | Demand scenario 6 |
|---|---|---|---|---|---|---|
| Plan I | 7135 | 7085 | 7025 | 7705 | 9145 | 10585 |
| Plan II | 7135 | 7085 | 7025 | 7105 | 7105 | 7025 |
| PlanIII | 7090 | 7085 | 7025 | 7090 | 7070 | 7025 |

The results reported in Table 5.10 reveal the following information:

- When the evacuation demand concentrates at the upstream segment of the evacuation corridors (Demand Scenario 1-3), the Minimal Green Plan (Plan I) shows the comparable performance as under Plan II and Plan III. This is due to the fact that traffic from minor origins can be accommodated with even the minimal green time and, thus adjusting the corridor signals will not make any significant contribution to the operations.

- When evacuation demand distributes more evenly over the network (Demand Scenario 4-6), Control Plans II and III clearly outperform Plan I, the Minimal Green Plan.

- Traffic diverging between corridors in Plan III does help to reduce the evacuation clearance time, compared to Plan II. However the improvement is not significant under these six demand scenarios. This is due to the fact that the traffic demand has a relatively balanced distribution among the three evacuation corridors.

Next, this section compares the performance of the three control plans under two more demand Scenarios, as shown in Table 5.11, where more evacuation demands are generated at the upstream of Connecticut Ave and less demands at the upstream of the $16^{th}$ St. All the demands will be loaded onto the network during the interval of 30 minutes based on the same distribution pattern.

Table 5-11:Demand Scenarios 7-8 for Multi-Corridor Evacuation

| Demand Scenario / Total Demand from Each Origin (unit: veh) | 7 | 8 |
|---|---|---|
| Cell 1001: Origin at the upstream of Connecticut Ave. | 7840 | 7280 |
| Cell 1002: Origin at the upstream of 16th St. | 1840 | 1280 |
| Cell 1003: Origin at the upstream of Georgia Ave. | 4840 | 4280 |
| Other minor origins | 110 | 170 |

With properly designed control parameters, all three plans can help to complete the evacuation process within a three-hour time window for the Demand Scenario 7 and Scenario 8. Table 5.12 shows the total evacuation clearance time. The table also compares the evacuation clearance time between Scenario 7 and Scenario 3, and between Scenario 8 and Scenario 5, since each pair of scenarios has the same demand from minor origins.

Table 5-12: Evacuation Clearance Time under the Demand Scenario 7 and Scenario 8 for Multi-Corridor Evacuation (unit: seconds**)**

| Clearance Time | Demand scenario 3 | Demand scenario 7 | Demand scenario 5 | Demand scenario 8 |
|---|---|---|---|---|
| Plan I | 7025 | 8935 | 9145 | 9145 |
| Plan II | 7025 | 8935 | 7105 | 8525 |
| Plan III | 7025 | 8470 | 7070 | 7945 |

Results in Table 5.12 have revealed the following information:

- When traffic from minor origins can be accommodated with the minimal green time (Scenarios 3 and 7), Control Plan II provides the same level of evacuation efficiency under Plan I, regardless of the demand distributions among the origins at the upstream of evacuation corridors. But Plan III does reduce the evacuation clearance time by around

10 minutes when the demand is more unbalanced among corridors (i.e., Demand Scenario 7).

- When the minimal green time cannot accommodate traffic from minor origins (Scenarios 5 and 8), Control Plan II has helped to reduce the evacuation clearance time under both demand scenarios. However, by allowing the traffic to redistribute among corridors using connection streets, Plan III has further improved the evacuation clearance time by 10 minutes compared to Plan II, and 20 minutes compared to Plan I, when the demand is more unbalanced among corridors (Demand Scenario 8).

In summary, the numerical results have demonstrated that demand distribution can significantly influence the effects of different control strategies on evacuation clearance time, and thus will affect the control plan selection. More specifically,

- Minimal-Green Plan or Yellow-Flash Plan is preferred when the evacuation demand mainly concentrates at the upstream of evacuation corridors and minor origins only have very light demand. Otherwise, optimizing the corridor signal timings to effectively contend with the arriving evacuation flows from the minor origins will be essential.

- When the evacuation demand distributes approximately balanced among different evacuation corridors, traffic rerouting between corridors will be unnecessary. This implies that the evacuation corridors can be operated individually. Note that whether a demand distribution is balanced or not depends on a variety of factors, such as the demand level, the number of lanes, and the roadway capacity.

### 5.4. Closure

In summary, Chapter 5 has presented the formulations for design of signal control strategies for designated evacuation corridors. The base model, presented in Section 5.2, is focused on an individually operated corridor typically consisting of one major safety-bound arterial connected with original nodes via side streets. As an extension, Section 5.3 has presented the generalized formulations for an integrated network of multiple corridors, which may balance evacuation traffic flows via connectors so as to improve the overall evacuation efficiency. Despite the difference in the formulations, these two models share the following two key features:

- Critical Intersection concept: i.e., only key intersections will offer protective phases for vehicles from minor roads to turn onto major roads (e.g., from side streets to arterials or from connectors to arterials). This core concept intends to reduce the disturbance of minor road traffic to the flow progression on main roads. With an effective signal control system, the evacuation arterial should be capable of progressively moving its assigned traffic flows without incurring excessive delay for those waiting on the minor roads.

- Two-phase control: to maximize the operational efficiency and to reduce the implementation complexity, the proposed model will operate all critical intersections with a two-phase signal control to account for the fact that evacuation flows travel in the same safety-bound direction along the evacuation corridors. For example, critical intersections on the evacuation corridors allow vehicles to exit the upstream link of the arterial during the arterial green phase, and allow traffic from the side street/connectors to turn on the arterial during the side street green phase. All non-critical intersections will not provide a protective green phase for traffic from side streets.

- The numerical tests in this chapter have demonstrated the potential of the proposed models for use in design of signal control strategies. Both models have proved to generate better control strategies than the Minimal Green plan, which is one widely-suggested evacuation signal control strategy. The improvement depends on the demand pattern and is more significant when demands distribute along the corridor instead of concentrating in the upstream segment. In general, a balanced demand distribution along the neighboring evacuation corridors may allow these corridors to operate independently. Otherwise, the integrated multi-corridor control will result in higher operational efficiency. Such balance is defined by a variety of factors, including the demand pattern and the roadway capacity.

# Chapter 6
# Conclusions

## 6.1 Closure

This study has produced a traffic management system for the Eastern Shore region that enables responsible agencies to design the optimal routing plan and monitor traffic conditions under different safe time windows during emergency evacuation. The entire system consists of the following principal components:

- A microscopic network traffic simulator for evaluating the impacts of any potentially implemented plans;
- A set of algorithms for planning of network wide evacuation strategies under different types of emergencies and available time windows for operations;
- A set of control models for design of signal control strategies during evacuation and for assessing the needs of implementing reversed lane operations; and
- A specially designed website (http://oceancity.umd.edu) that allows designated users to execute on-line operations of the developed emergency evacuation system and the regional traffic simulator.

With such a system and the estimated time window for safe evacuation, agencies responsible for Eastern Shore emergency evacuation, if needed, can plan the number of evacuees to be guided to each primary evacuation route on an hourly basis, determine the time-varying turning percentage of traffic volume at each control junction, estimate the number of arrivals to each designated safe destination over time, and assess the total required evacuation time for the given demand level. To evaluate the resulting traffic conditions under the candidate evaluation plan and to identify potential bottlenecks, the responsible users can execute the Eastern Shore network simulator to view the evolution of the projected travel speed, queue, and volume on all evacuation routes during the proposed period of evacuation. Based on the results of simulation, one can assess if the estimated time window for evacuation is sufficient or not, and whether other more resource-demanding strategies such as the reversed-lane operations should be implemented.

The report has documented mainly the theoretical aspects of all models embedded in the developed traffic management system, including the evacuation routing plans from the planning perspective, and corresponding control strategies at both the network and route levels based on the operational needs. The primary methodology employed by each model along with its basic assumptions, operational constraints, detailed formulations, and solution algorithms are all illustrated in the report. To facilitate the application, this study has also developed a customized website that serves not only as the warehouse to keep all computer programs developed for those mathematical models, but also the on-line mechanism to execute the entire system in real time when connected with network traffic sensors. An intelligent user interface is also available on the website for guiding the efficient use of all available system functions. Figures 6-1 to 6-5 illustrate the example interface functions on the customized website.

Note that to best use the developed system during non-emergency periods (e.g., during the summer months) the research team at the University of Maryland has extended its functions to link with traffic detectors in the Eastern Shore region, and to provide real-time monitoring of traffic volume, speed, and estimated travel time for any origin-destination trip in the primary evacuation routes. The on-line operational mechanism and user-guidance modules are available in the same customized website.

## 6.2 Recommendations

Although the study has produced a system that offers quite comprehensive functions for emergency evacuation planning and monitoring of the field operations of implemented strategies, the effectiveness and reliability of such operations can be assured only if a well-functioned traffic detection system has been deployed. By integrating traffic detectors with the emergency evacuation system, one can monitor traffic conditions in real time, estimate the compliance rate of evacuees during the evacuation period, and assess the effectiveness of any implemented strategies.

Also, it is likely that some unexpected incidents may incur during the evacuation process and cause traffic blockages on some primary routes. Hence, the emergency response center shall have the ability to immediately assess the traffic impacts due to detected incidents, and re-design and implement detour plans to guide the large volume of evacuees in a timely manner.

More specifically, grounded on the results and products of this study it is essential for agencies responsible for emergency response in the Eastern Shore region to further enhance the traffic management system on the following critical issues:

- Deploy detectors at critical locations on both freeways and arterials to effectively monitor network traffic conditions in real time;
- Develop an effective incident detection algorithm to take best advantage of available detectors and to minimize the incident response time;
- Design a set of heuristic algorithms to efficiently detour traffic volumes blocked and/or impacted by a detected incident to different evacuation routes in a timely manner;
- Implement an effective information distribution system prior to and during the evacuation period to ensure the best compliance of evacuees during the entire operation period;
- Construct an off-line database with the system developed in this study that shall contain comprehensive possible emergency scenarios, proposed implemented strategies, necessary equipment for operations and communications, and potential interaction issues with evacuees and between different agencies.;
- Periodically hold workshops to train potential users in best use the developed system, to exchange valuable coordination experience, and to provide feedbacks for the research team to incorporate the input of first-line users in the system revision work.

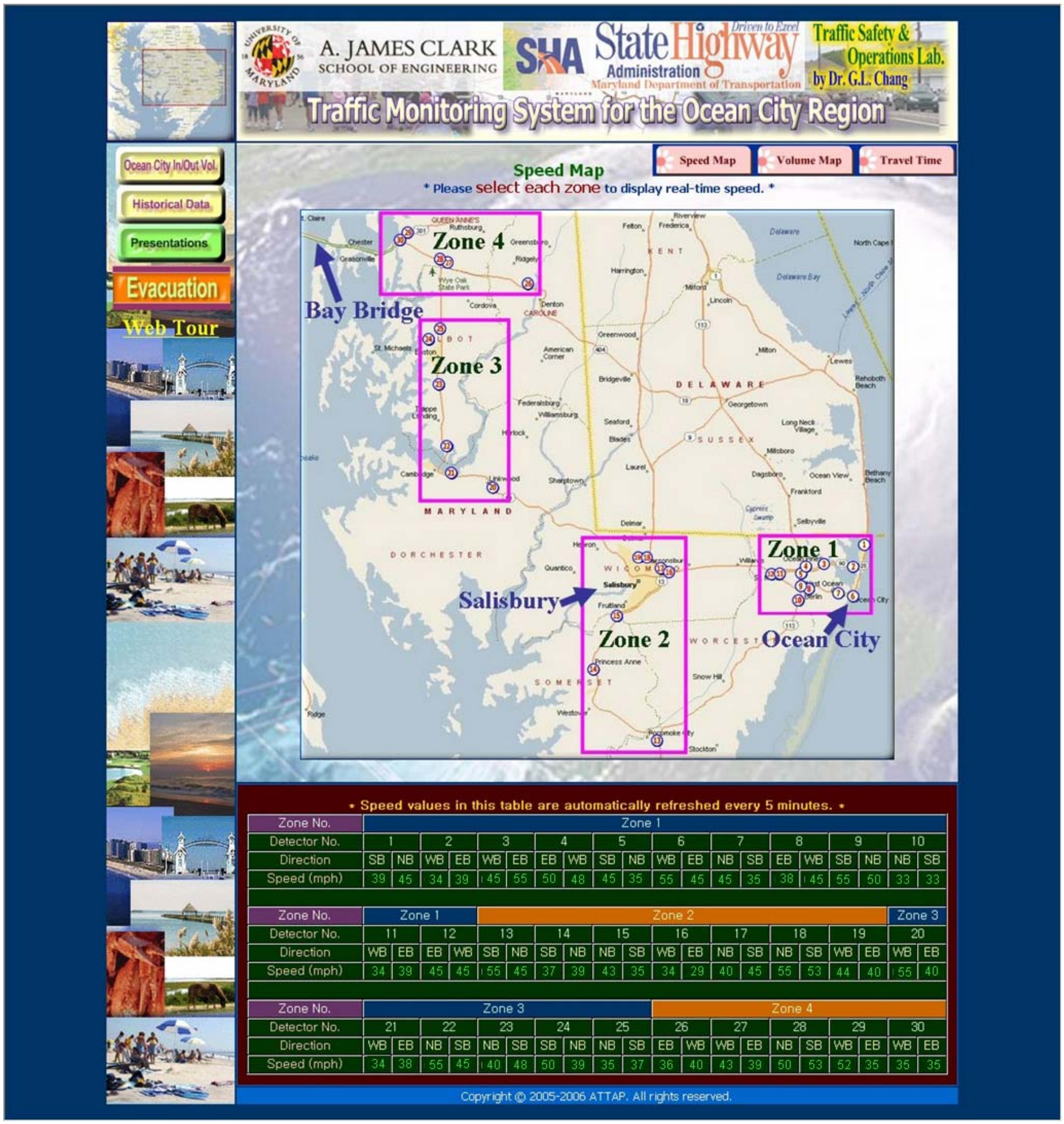


Figure 6.1 Speed Table for Maryland Eastern Shore

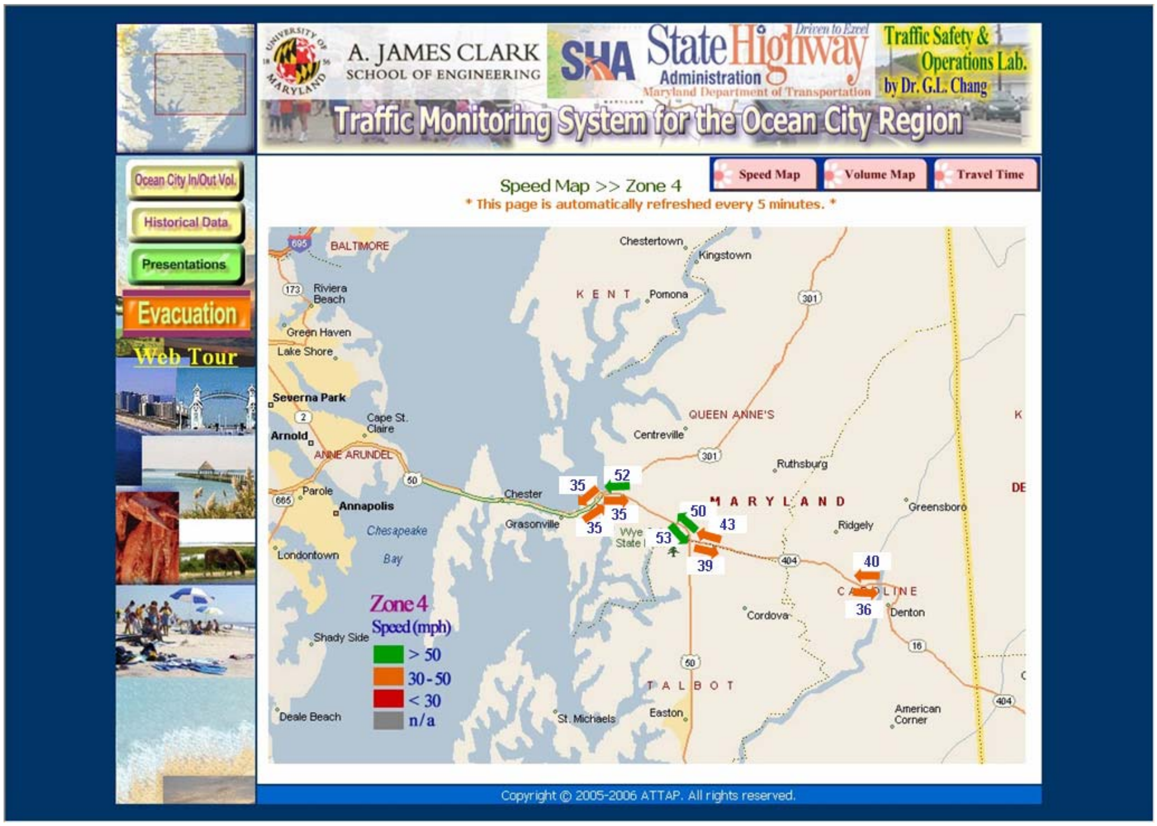


Figure 6.2 Speed Map for Zone 4


Figure 6.3 Prediction of Travel Time between Bay Bridge and Ocean City

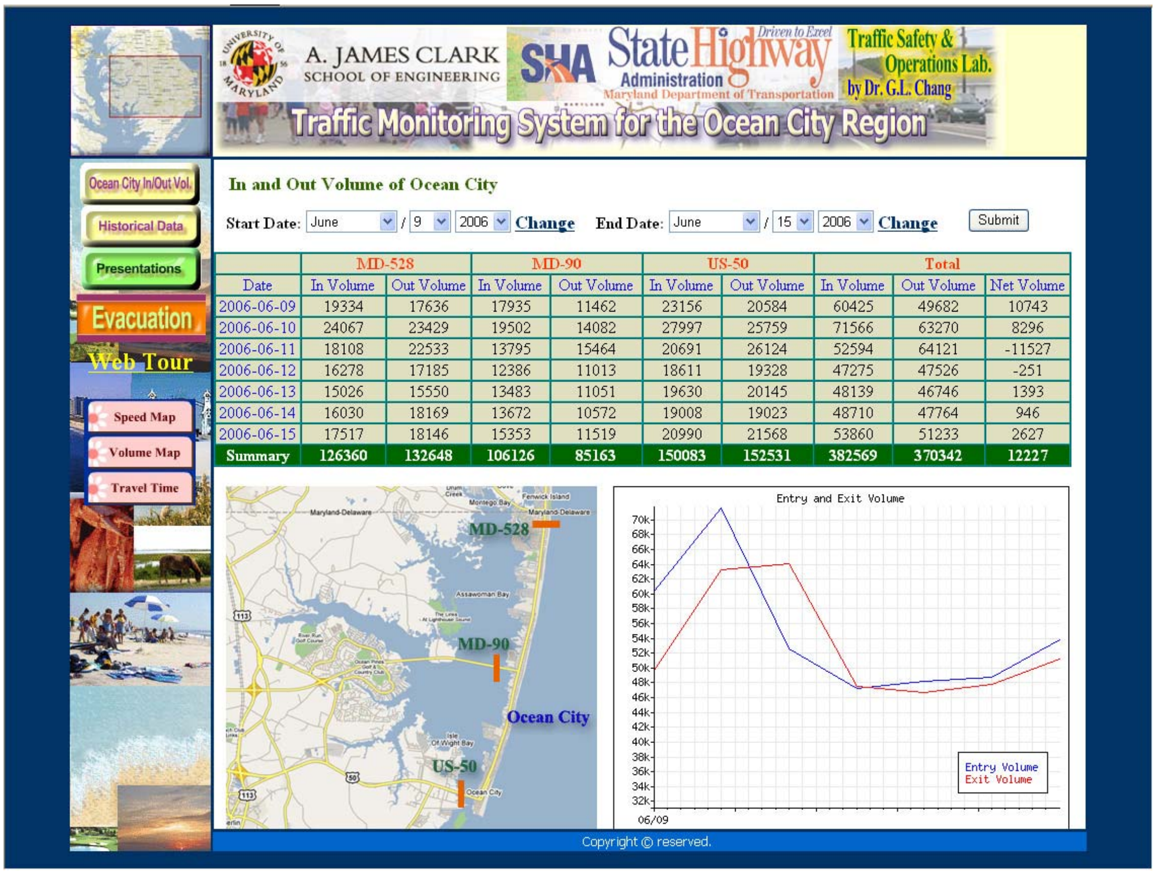


| Date | MD-528 In Volume | MD-528 Out Volume | MD-90 In Volume | MD-90 Out Volume | US-50 In Volume | US-50 Out Volume | Total In Volume | Total Out Volume | Total Net Volume |
|---|---|---|---|---|---|---|---|---|---|
| 2006-06-09 | 19334 | 17636 | 17935 | 11462 | 23156 | 20584 | 60425 | 49682 | 10743 |
| 2006-06-10 | 24067 | 23429 | 19502 | 14082 | 27997 | 25759 | 71566 | 63270 | 8296 |
| 2006-06-11 | 18108 | 22533 | 13795 | 15464 | 20691 | 26124 | 52594 | 64121 | -11527 |
| 2006-06-12 | 16278 | 17185 | 12386 | 11013 | 18611 | 19328 | 47275 | 47526 | -251 |
| 2006-06-13 | 15026 | 15550 | 13483 | 11051 | 19630 | 20145 | 48139 | 46746 | 1393 |
| 2006-06-14 | 16030 | 18169 | 13672 | 10572 | 19008 | 19023 | 48710 | 47764 | 946 |
| 2006-06-15 | 17517 | 18146 | 15353 | 11519 | 20990 | 21568 | 53860 | 51233 | 2627 |
| Summary | 126360 | 132648 | 106126 | 85163 | 150083 | 152531 | 382569 | 370342 | 12227 |

Figure 6.4 In and Out Volume of Ocean City

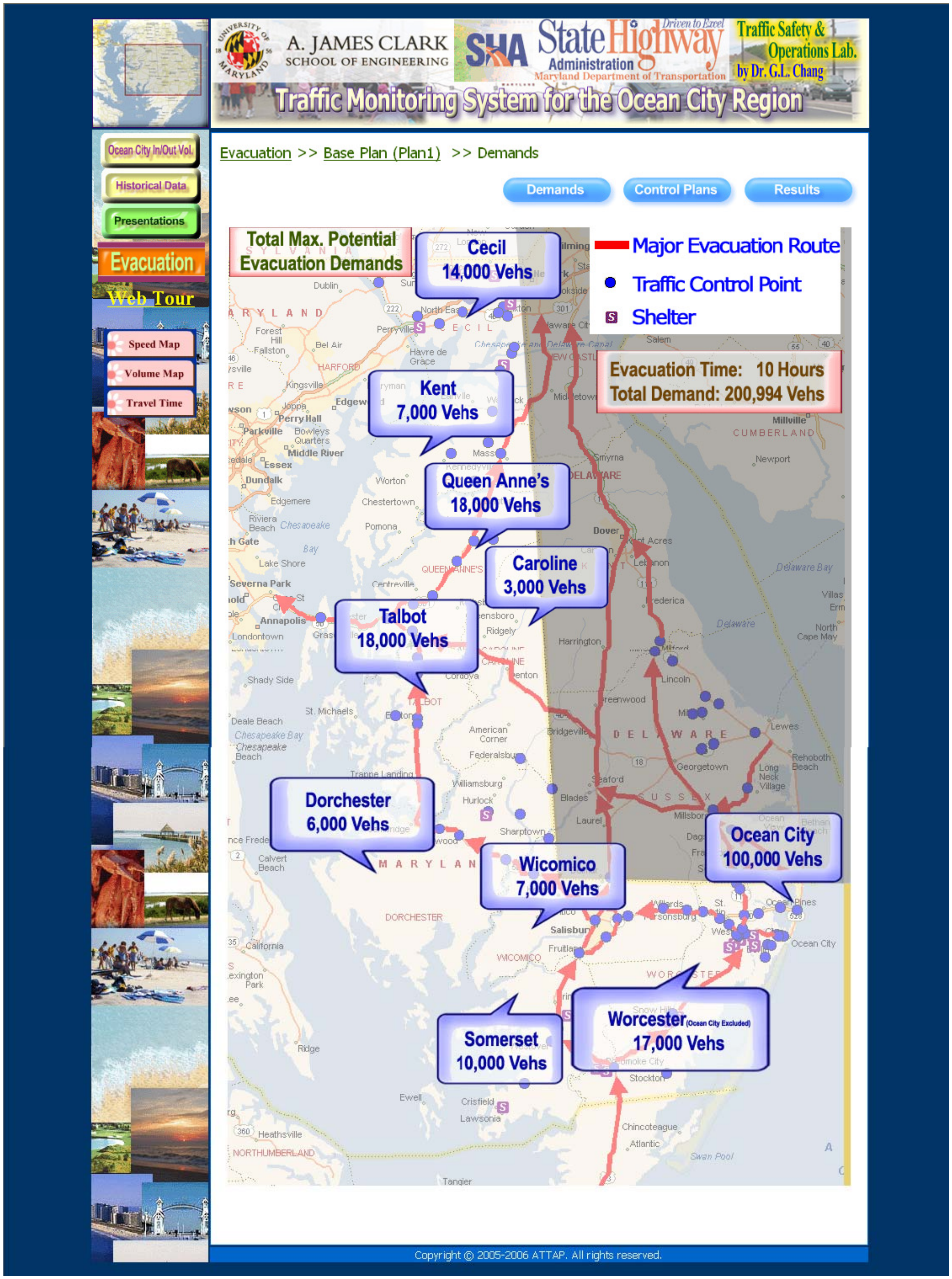


Figure 6.5 Evacuation Plan for Maryland Eastern Shore

# RFERENCES


Alam, S.B., Goulias, K.G., “Dynamic emergency evacuation management system using geographic information system and Spatiotemporal models of behavior,” Transportation Research Record, n. 1660, pp. 92-99, 1999

Alsnih, R., and Stopher, P.R. (2003). “Review of the Procedures Associated with Devising Emergency Evacuation Plans.” Transportation Research Record 1865, Transportation Research Board, Washington D.C., 89-97.

Ballard, A.J., and Borchardt, D.W., “Recommended Practices For Hurricane Evacuation Traffic Operations,” Technical report, FHWA/TX-06/0-4962-P2, 2005

Bullock D., Morales J. and Sanderson B., “Evaluation of Emergency Vehicle Signal Preemption on the Route 7, Virginia, Corridor,” Technical Report, FHWA-RD-99-070, 1999

Campos, V.B.G., de Silva, P.A.L., and Netto, P.O.B., ”Evacuation transportation planning: A method of identify optimal independent routes,” Urban Transport and the Environment for the 21st Century, pp.555-564, 2000

Chalmet, L., Francis, R., Saunders, P., “Network Models for Building Evacuation,” Management Science, vol.28, 1982, pp.86-105.

Chen, M., “Traffic Signal Timing For Urban Evacuation,” Thesis for the University of Maryland, 2005

Chen, X., Zhan, F.B., “Agent-Based Modeling and Simulation of Urban Evacuation: Relative Effectiveness of Simultaneous and Staged Evacuation Strategies,” Presented at the 83rd annual conference of Transportation Research Board, 2004

Chiu, Y.C., “Traffic Scheduling Simulation and Assignment for Area-Wide Evacuation,” 2004 IEEE Intelligent Transportation Systems Conference, Washington, D.C., October, 2004

Chiu, Y.C., Villalobos, J., Gautam, B., and Zheng, H., “Optimal Scheduling of Evacuation Operations,” presented at the 85th annual meeting of transportation research board, 2006

Choi, W., Hamacher, H. W., and Tufekci, S., “Modeling of Building Evacuation Problems by Network Flows with Side Constraints,” European Journal of Operational Research, vol.35, 1988, pp.98-110.

Cova, T.J., Johnson, J.P., “Microsimulation of neighborhood evacuations in the urban-wildland interface,” Environment and Planning A, vol.34, pp. 2211-2229, 2002

Cova, T.J., Johnson, J.P., "A network flow model for lane-based evacuation routing," Transportation Research A, vol.37, pp.579-604, 2003

Daganzo, F.C., "The Cell Transmission Model: A Dynamic Representation of Highway Traffic Consistent with the Hydrodynamic Theory," Transportation Research. Part B, Vol. 28B, No. 4, pp. 269-287, 1994.

Daganzo, F.C., "The Cell Transmission Model. II. Network Traffic," Transportation Research. Part B, Vol. 29B, pp. 79-93, 1995.

de Silva, F., Eglese, R, "Integrating simulation modeling and GIS: spatial decision support systems for evacuation planning," Journal of the Operational Research Society, vol. 51, pp. 423-430, 2000

Dotson, L.J., Jones, J., Schneck, D., and Sullivan, R., "Development of evacuation time estimate studies for nuclear power plants," Technical Report, NUREG/CR-6863 (SAND2004-5900), 2005

Dunn C.E., Newton, D., "Optimal routes in GIS and emergency planning applications," Area, vol.24, n.3, pp.259-267, 1992

Eschenauer, H.A., Koski, J., and Osyczka, A., "Multicriteria Design Optimization : Procedures and Applications," Springer-Verlag, New York, 1986

Farrell, J., "Alternatives to Road Building to Improve Hurricane Evacuation in Coastal South Carolina," Presented at Environmental Advocacy Seminar, April, 2005

FEMA, "Southeast United States Hurricane Evacuation Traffic Study-Executive Summary," Final Report for Southeast United States Hurricane Evacuation Traffic Study, 2000

Goldberg D., "Genetic Algorithms," Addison Wesley, Reading, MA, 1988

Hamacher, H.W., Tufekci, S., "On the Use of Lexicographic Min Cost Flows in Evacuation Modeling," Naval Research Logistics, vol. 34, 1987, pp.487-503.

Harrington, G., "Emergency preparedness: path to safety," Building Operating Management, Apr. 2005

Hobeika, A.G., Kim, S., and Beckwith, R.E., "A decision support system for developing evacuation plans around nuclear power stations," Interfaces, vol.24, n.5, pp.22-35,1994

Hobeika, A., Kim C., "Comparison of traffic assignments in evacuation modeling," IEEE transactions on engineering management, vol.45, n.2, pp.192-198, 1998

Homburg, C., " Hierarchical multi-objective decision making," European Journal of Operational Research, vol.105, n.1, pp. 155-161, 1998

ITE, "Emergency Planning and Preparedness: Guidelines For Transportation Professionals," 2004

Kwon, E., Pitt, S., "Evaluation of emergency evacuation strategies for downtown event traffic using a dynamic network model", Presented at the 84th Annual Meeting of the Transportation Research Board, Washington, D.C., 2005

Ladd, S.R., "Genetic Algorithms in C++," M&T Books, New York, 1996

Li, Y, A.K. Ziliaskopoulos and S. T. Waller, "Linear Programming Formulations for System Optimum Dynamic Traffic Assignment with Arrival Time-based and Departure time-based Demands," Transportation Research Record 1667, TRB, National Research Council, Washington, D.C., pp. 52-59, 1999.

Lim, E., Wolshon, B., "Modeling and performance assessment of contraflow evacuation termination points," Presented at the 84th Annual Meeting of the Transportation Research Board, Washington, D.C., 2005

Liu, H.X., Ban, J.X., Ma, W., Mirchandani, P.B., "Model Reference Adaptive Control Framework for Real Time Traffic Management under Emergency Evacuation," Presented at the 85th Annual Meeting of the Transportation Research Board, Washington, D.C., 2006

Louisell, C., Collura, J. and Tignor, S, "A Proposed Method to Evaluate Emergency Vehicle Preemption and the Impacts on Safety." Presented at the 82nd Annual Meeting of Transportation Research Board, Washington, D.C., 2003

Louisell, C., Collura, J., Teodorovic, D. and Tignor, S., "A Simple Work Sheet Method to Evaluate Emergency Vehicle Preemption and the Impacts on Safety." Presented at the 83rd Annual Meeting of Transportation Research Board, 2004

Louisell, C., Collura J., "A Simple Algorithm to Estimate Emergency Vehicle Travel Time Savings on Preemption Equipped Corridors: A Method Based on a Field Operational Test." Presented at the 84th Annual Meeting of Transportation Research Board, 2005

Mahmassani, H., Sbayti, H., "Optimal Scheduling of Contraflow Operations for Network Evacuation Planning", Presented at the 2005 INFORMS Annual Meeting, San Francisco, 2005

McHale G.M., Collura J., “Improving Emergency Vehicle Traffic Signal Priority System Assessment Methodologies,” presented at the 82nd Annual Meeting of Transportation Research Board, Washington, D.C., 2003

McLoughlin, D., “A Framework for Integrated Emergency Management,” Public Administration Review, vol.45, 1985, pp.165-172

Mei, B., “Development Of Trip Generation Models Of Hurricane Evacuation,” Thesis of Louisiana State University, 2002

Miller-Hooks, E., Patterson, S. S., “On Solving Quickest Time Problems in Time-Dependent, Dynamic Networks,” Journal of Mathematical Modeling and Algorithms, vol.3(1), 2004, pp.39-71.

Mitchell, S.W., Radwan, E., “Heuristic Prioritization of Emergency Evacuation Staging to Reduce Clearance Time,” presented at the 85th annual meeting of transportation research board, 2006

Opasanon, S., “On Finding Paths and Flows in Multicriteria, Stochastic and Time-Varying Networks,” Ph.D. dissertation, University of Maryland, 2004

Pauls, J.L, Jones, B.K, “Building Evacuation: Research Methods and Case Studies,” Fires and Human Behaviour, pp.227-250, John Wiley and Sons, New York, 1980

PBS&J, “Southeast United States Hurricane Evacuation Traffic Study-Technical Memorandum Number 3: Reverse Lane Standards And ITS Strategies,” Final Report for Southeast United States Hurricane Evacuation Traffic Study, 2000

PBS&J, “Florida Department of Transportation Hurricane Response Evaluation and Recommendations,” Technical Memorandum, 2005

Pidd, M., de Silva, F., Eglese, R, “A simulation model for emergency evacuation,” European Journal of Operational Research, vol. 90, n. 3, pp. 413-419, 1996

Rontiris, K., Crous, W., “Emergency evacuation modeling for the Koeberg nuclear power station,” 2nd Asian EMME/2 Users' Meeting, 2000

Sadek, A.W., Chowdhury, M.A., “Fundamentals of Intelligent Transportation Systems Planning,” Artech House, 2003

Sattayhatewa, P., Ran, B., “Developing a dynamic traffic management model for nuclear power plant evacuation,” Presented at the 79th Annual Meeting of the Transportation Research Board, Washington, D.C., 2000

Sbayti, H., Mahmassani, H., “Optimal Scheduling of Evacuation Operations,” presented at the 85th annual meeting of transportation research board, 2006

Sheffi, Y., Mahmassani, H., and Powell, W., "A transportation network evacuation model," Transportation Research A, vol.16, n.3, pp.209-218, 1982

Sheffi, Y., "Urban Transportation Networks," Englewood Cliffs, NJ: Prentice-Hall, 1985.

Sisiopiku, V.P., Jones, S.L., Sullivan, A.J., Patharkar, S.S., Tang, X., "Regional Traffic Simulation for Emergency Preparedness," Technical report, Department of Civil and Environmental Engineering, The University of Alabama, 2004

Smith, J.M., "State-dependent queuing models in emergency evacuation networks," Transportation Research B, vol. 25, pp. 373-389, 1991

Snyder D., "Regional Emergency Evacuation Transportation Coordination Annex of the Regional Emergency Coordination Plan," Presentation to the Metropolitan Washington Council of Governments, 2004

Sorensen, J., Vogt, B.M., Mileti, D.S., "Evacuation: an assessment of planning and research," Technical Report for Oak Ridge National Laboratory, ORNL-6373, 1987

Southworth, F., "Regional evacuation modeling: a state-of-the-art review," Technical Report for Oak Ridge National Laboratory, ORNL/TM-11740, 1991

Talebi, K., Smith, J.M., "Stochastic Network Evacuation Models," Computers & Operations Research, vol.12 (6), 1985, pp.559-577.

Teo, A.P.Y., "Validation of An Evacuation Model Currently under Development," Thesis, University of Canterbury, New Zealand, 2001

Theodoulou, G., Wlshon, B., "Modeling and Analyses of Freeway Contraflow to Improve Future Evacuations," Presented at the 83rd Annual Meeting of the Transportation Research Board, Washington, D.C., 2004

Tuydes, H., Ziliaskopoulos, A., "Network Re-design to Optimize Evacuation Contraflow," presented at the 83rd annual meeting of transportation research board, 2004

Tuydes, H., "Network Traffic Management under Disaster Conditions," Ph.D. Thesis, Northwestern University, 2005.

Tuydes, H., Ziliaskopoulos, A., "The Network Evacuation Problem and Solution Algorithms," Presented at the 2005 INFORMS Annual Meeting, San Francisco, 2005

Tuydes, H., Ziliaskopoulos, A., “A Tabu-based Heuristic Approach for the Optimization of Network Evacuation Contraflow,” presented at the 85th annual meeting of transportation research board, 2006

Tweedie, S., Rowland, J., Walsh, S., Rhoten, R., and Hagle, P., “A methodology for estimating emergency evacuation times,” The Social Science Journal, vol. 23, pp. 189-204, 1986

Urbanik T. II., “Evacuation time estimates for nuclear power plants,” Journal of Hazardous Materials, vol.5, pp.165-180, 2000

Urbina, E.A., “A state-of-the-practice review of hurricane evacuation plans and policies,” Thesis of the Louisiana State University, 2002

Urbina, E., Wolshon, B., “National review of hurricane evacuation plans and policies: a comparison and contrast of state practices,” Transportation Research A, vol.37 (3), pp.257-275, 2003

US Army Corps of Engineers, “South Carolina Hurricane Evacuation Study,” Technical Data Report, Charleston District, December 1986.

US Army Corps of Engineers, “Treasure Coast Region Hurricane Evacuation Study,” Technical Data Report, 1994.

US Army Corps of Engineers, “Rhode Island Hurricane Evacuation Study,” Technical Data Report, May 1995

US Army Corps of Engineers, “Alabama Hurricane Evacuation Study Technical Data Report: Behavioral Analysis”, Final Report, 2000.

Wilmot, C.G., Meduri, N., “A methodology to establish hurricane evacuation zones,” Presented at the 84th Annual Meeting of the Transportation Research Board, Washington, D.C., 2004

Wolshon, B., ““One-way-out”: contraflow freeway operation for hurricane evacuation”, Natural hazards review, August, pp.105-112, 2001

Wolshon, B., “Planning for the evacuation of New Orleans,” ITE Journal, vol.72 (2), pp.44-49, 2002

Yuan, F., Han, L.D., Chin, S.M., Hwang, H., “A Proposed Framework for Simultaneous Optimization of Evacuation Traffic Destination and Route Assignment,” Presented at the 85th Annual Meeting of the Transportation Research Board, Washington, D.C., 2006

Ziliaskopoulos, A., and S. Lee, “A Cell Transmission Based Assignment-Simulation Model for Integrated Freeway/Surface Street Systems,” Presented at the 76th Annual Meeting of the Transportation Research Board, Washington, D.C., 1997

Ziliaskopoulos, A.K., “A Linear Programming Model for the Single Destination System Optimum Dynamic Traffic Assignment Problem,” Transportation Science, Vol. 34, No. 1, pp. 37-49, 2000.

Zou, N., Yeh, S.T., and Chang, G.L., “A simulation-based emergency evacuation system for Ocean City, Maryland under hurricane attacks,” Transportation Research Record 1922, Transportation Research Board, Washington D.C., 138-148, 2005